

Comparison of frequency control concepts in isolated power systems with diesel generators and fully rated wind energy converters

Vom Fachbereich Elektrotechnik und Informationstechnik der Technischen Universität Darmstadt
zur Erlangung des akademischen Grades eines Doktor-Ingenieurs (Dr.-Ing.) genehmigte Dissertation



TECHNISCHE
UNIVERSITÄT
DARMSTADT

von

Dipl.-Ing. Georgia Papaioannou, M. Sc.

Geboren am 05.06.1985 in Athen

Referentin: Prof. Dr.-Ing. Jutta Hanson

Korreferent: Prof. Dr.-Ing. Albert Moser

Tag der Einreichung: 16.05.2017

Tag der mündlichen Prüfung: 22.06.2017

D17

Darmstadt 2017

Anlage 2: Erklärung laut §9 PromO

Erklärung laut §9 PromO

Ich versichere hiermit, dass ich die vorliegende Dissertation allein und nur unter Verwendung der angegebenen Literatur verfasst habe. Die Arbeit hat bisher noch nicht zu Prüfungszwecken gedient.

Datum und Unterschrift

Köln, den 30.04.2017

Georgia Papaioannou

Dedication

To my all beloved brother and my daughter

Preface - Acknowledgements

This Doctorate of Engineering thesis started in February 2012 and was completed in July 2016. It has been conducted in the Department of Electrical Power Supply with Integration of Renewable Energies of Technische Universität Darmstadt.

First of all, I would like to thank a lot my supervisor Prof. Dr.-Ing. Jutta Hanson for her flexibility and the provided freedom, as well as her felicitous remarks that formed the research frame of this thesis and have oriented me during all these years. Additionally, I especially thank her for her understanding, her support and her tolerance over the time I was her research associate. I would like to thank my co-supervisor Prof. Dr.-Ing. Albert Moser of RWTH Aachen University for his engagement and support .

Furthermore, I have to thank very much Mr. Daskalaki, Mr. Safra, Mr. Katsikea, Mrs. Polychronaki and Mr. Koureli active in the Department of Islands of Hellenic Electricity Distribution Network Operator (HEDNO) for providing data regarding the electrical power system of the island of Lesbos. Without their willingness, their support and help it would have been much more difficult to demonstrate a real case study of an isolated power system in this thesis. I also thank Prof. Dr. Kalabokidi from the Department of Geography of the University of the Aegean for providing me with wind speed data of remote autonomous weather stations that enabled a realistic simulation of the power coming from wind energy converters installed in Lesbos.

I couldn't possibly forget my colleagues who have shared my everyday life, my difficulties and my achievements. They have accompanied me during my research and they have integrated me in a new and friendly environment. I thank you all very much: Arnaud Hoffmann, Peter Franz, Ignacio Talavera (Küken), Christina Fuhr, Marco Fleckenstein (Fleckerino), Sebastianako Weck, Henning Zimmer, Damian Batorowicz.

My students Alba Hidalgo Ferreira, Peter Landgraf and Julien Becker as well as the internship student Sotiris Makatsoris have supported under my supervision the execution and implementation of tasks belonging to the realisation and completion of this thesis. Moreover, I could not fail to mention Mr. Fabian Tutschka from the MATLAB Support Team for his help, as well as Mr. Stefan Weigel of DiGSILENT for his support with reference to PowerFactory software.

Mentioning my daughter Theodora Avgousta in acknowledgments is not enough. I am very grateful to my parents and to her, since they have lived with me during the last years of my efforts and have always believed in me. Through their support they have contributed to this work in a significant way. I will always thank them and I will always thank my "Ritter", who came in my life and since then accompanies me with all his strength.

Πρόλογος - Ευχαριστίες

Η διατριβή αυτή ξεκίνησε τον Φεβρουάριο του 2012 και ολοκληρώθηκε τον Ιούλιο του 2016. Εκπονήθηκε στο Τμήμα Παραγωγής Ηλεκτρικής Ενέργειας με ένταξη Ανανεώσιμων Πηγών Ενέργειας του Technische Universität Darmstadt.

Αρχικά θα ήθελα να ευχαριστήσω θερμά την κύρια επιβλέπουσα αυτής της εργασίας Καθηγήτρια Dr.-Ing. Jutta Hanson για την ευελιξία και την παρεχόμενη ελευθερία αλλά και τις πολύ εύστοχες παρατηρήσεις της που οδήγησαν στη διαμόρφωση του πλαισίου εκπόνησης. Επίσης την ευχαριστώ εγκάρδια για την κατανόηση, την υποστήριξη και τη συμπαράστασή της καθ' όλη τη διάρκεια της απασχόλησής μου ως ερευνητική συνεργάτης της. Επίσης ευχαριστώ ιδιαίτερα το συνεπιβλέποντα καθηγητή Dr.-Ing. Albert Moser στο Πανεπιστήμιο RWTH Aachen για την προθυμία και την υποστήριξη του.

Αντίστοιχα ευχαριστώ θερμά τους κ.κ. Δασκαλάκη, Σαφρά, Κατσικέα, Πολυχρονάκη και Κουρέλη της Διεύθυνσης Περιφέρειας Νησιών (ΔΠΝ) του Διαχειριστή Εθνικού Δικτύου Διανομής Ηλεκτρικής Ενέργειας (Δ.Ε.Δ.Δ.Η.Ε.) για την παραχώρηση δεδομένων του ηλεκτρικού συστήματος της νήσου Λέσβου. Χωρίς την προθυμία, τη συμπαράσταση και την βοήθειά τους δεν θα ήταν δυνατή η παρουσίαση μιας πραγματικής περίπτωσης μελέτης στα πλαίσια αυτής της εργασίας. Ευχαριστώ επίσης τον κ. Καθηγητή Δρα Κώστα Καλαμποκίδη του Τμήματος Γεωγραφίας του Πανεπιστημίου Αιγαίου για την παροχή μετεωρολογικών δεδομένων από σταθμούς εγκατεστημένους στη Λέσβο που βοήθησαν στη ρεαλιστική μοντελοποίηση της ισχύος προερχόμενης από αιολικούς σταθμούς.

Δεν θα μπορούσα να παραλείψω όλους τους συναδέλφους μου που καθημερινά κατά τη διάρκεια των τεσσάρων χρόνων εκπόνησης της διατριβής μοιράζονταν την καθημερινότητα, τα ερωτηματικά, τις δυσκολίες και τις επιτυχίες μου. Αυτοί ήταν που με συντρόφευαν στην αναζήτηση απαντήσεων σε ερευνητικό επίπεδο, αλλά και αυτοί που με ενέταξαν σε ένα καινούριο και φιλόξενο περιβάλλον. Σας ευχαριστώ όλους θερμά: Arnaud Hoffmann, Peter Franz, Ignacio Talavera (Küken), Christina Fuhr, Marco Fleckenstein (Fleckerino), Sebastianako Weck, Henning Zimmer, Damian Batorowicz.

Στην πραγματοποίηση αυτής της εργασίας παρείχαν την αμέριστη συνεργασία τους οι σπουδαστές Alba Hidalgo Ferreira, Peter Landgraf και Julien Becker καθώς και ο φοιτητής πρακτικής άσκησης Σωτήρης Μακατσώρης. Επιπλέον δεν θα μπορούσε να παραλειφθεί ο Fabian Tutschka για την υποστήριξη τεχνικών ερωτήσεων στο λογισμικό MATLAB και αντίστοιχα ο Stefan Weigel της DIgSILENT για το λογισμικό PowerFactory.

Η αναφορά στις ευχαριστίες δεν αρκεί να περιγράψει την ευγνωμοσύνη μου για την κόρη μου Θεοδώρα Αυγούστα αλλά και τους γονείς μου, που έζησαν τις προσπάθειές μου όλο αυτό το διάστημα. Αυτή η διατριβή είναι και δικό τους επίτευγμα. Ευχαριστώ ειλικρινά και θα τους ευγνωμονώ παντοτινά για τη στήριξή τους, όπως επίσης και τον «Ritter» που με συντροφεύει με όλη του τη δύναμη.

Eidesstattliche Erklärung

Ich versichere an Eides statt durch meine eigenhändige Unterschrift, dass ich die vorliegende Arbeit selbstständig und ohne fremde Hilfe angefertigt habe. Alle Stellen, die wörtlich oder dem Sinn nach auf Publikationen oder Vorträgen anderer Autoren beruhen, sind als solche kenntlich gemacht. Ich versichere außerdem, dass ich keine andere als die angegebene Literatur verwendet habe. Diese Versicherung bezieht sich auch auf alle in der Arbeit enthaltenen Zeichnungen, Skizzen, bildlichen Darstellungen und dergleichen. Die Arbeit wurde bisher keiner anderen Prüfungsbehörde vorgelegt und auch noch nicht veröffentlicht.

Ort, Datum

Dipl. - Ing. Georgia Papaioannou, M.Sc.

Contents

Dedication	i
Preface - Acknowledgements	ii
Πρόλογος - Ευχαριστίες	iii
Eidesstattliche Erklärung	iv
Contents	v
Abstract	ix
Abstract (deutsch)	x
Acronyms	xii
Nomenclature	xiii
List of Figures	xv
List of Tables	xix
1.....Introduction	1
1.1. Scientific scope	2
1.2. Structure	3
2.....Isolated power systems	5
2.1. Overview of isolated power systems	5
2.2. Characteristics of autonomous isolated power systems	6
2.3. Classification of autonomous isolated power systems according to characteristics	8
2.4. Demarcation of considered isolated power systems	11
3.....Frequency stability of electrical power systems	12
3.1. Definition of frequency stability	12
3.2. Primary control and secondary frequency control in interconnected power systems with conventional power plants	12

<hr/>	
3.2.1. Primary control	15
3.2.2. Secondary control	22
3.3. Primary control and secondary frequency control in isolated power systems	23
3.3.1. Primary control in isolated power systems	23
3.3.2. Secondary control in isolated power systems	23
3.3.3. Overview of existing frequency control concepts for diesel generators in isolated power systems	25
3.4. Challenges regarding frequency stability of isolated power systems based on diesel power generation with high integration of wind power	29
3.4.1. Grid code requirements regarding frequency in isolated power systems	32
3.5. Outlook and Discussion	34
4....Introduction and modelling of speed governors for diesel generators in isolated power systems	35
<hr/>	
4.1. Fundamental components and structure of a control system	35
4.2. Diesel generator's speed governors	37
4.3. Modelling of a diesel engine	37
4.4. Modelling of diesel speed governors	38
4.4.1. Introduction of isochronous speed governor	38
4.4.2. Introduction of droop speed governor	40
4.5. Validation of implemented speed governors	42
4.5.1. Speed governor's validation	43
4.6. Control systems tuning	45
4.6.1. Tuning methods	46
4.6.2. Tuning methods for diesel generator's speed governors in isolated power systems with integrated renewable energy sources	47
4.6.3. Tuning of isochronous and droop speed governors	47
4.7. Outlook and discussion	54
5....Introduction of "DIGLO IPS" for tuning and comparing frequency control concepts	55
<hr/>	
5.1. Model "2 DIGLO IPS"	55
5.1.1. Voltage Levels	56

<hr/>	
5.1.2. Transformers	56
5.1.3. Transmission Line	56
5.1.4. Synchronous Generators	56
5.1.5. Automatic voltage regulators	58
5.1.6. Loads	59
5.2. Load - flow results of “2 DIGLO IPS”	59
5.3. Tuning speed governors of “2 DIGLO IPS”	62
5.4. Dynamic simulations	65
5.5. Conclusion - Discussion	67
6.....Extension of “DIGLO IPS” with more synchronous generators and tuning	68
<hr/>	
6.1. Model “3 – and “4 DIGLO IPS”	68
6.2. Load-flow results of “3 – and “4 DIGLO IPS”	70
6.3. Tuning speed governors of “3 – and “4 DIGLO IPS”	72
6.4. Dynamic simulations	74
6.5. Conclusion - Discussion	81
7.....Extension of “4 DIGLO IPS” model including a fully rated wind energy converter	82
<hr/>	
7.1. Modelling of Fully Rated Wind Energy Converter	82
7.1.1. Load flow	83
7.1.2. Stability Analysis	87
7.2. Model “4 DIGLOW IPS”	89
7.2.1. Load-flow results of “4 DIGLOW IPS”	89
7.2.2. Dynamic simulations	90
7.3. Conclusion and discussion	95
8.....A real isolated power system – Case study of Lesbos IPS	96
<hr/>	
8.1. Lesbos isolated power system topology	96
8.1.1. Power Generation	98
8.1.2. Power Consumption	100

8.2.	Power infeed scenarios of Lesbos IPS	100
8.2.1.	Load - flow results	101
8.3.	Outlook	103
9.....	Frequency stability analysis of Lesbos IPS	104

9.1.	Grid code requirements	104
9.1.1.	Voltage	104
9.1.2.	Frequency	105
9.1.3.	Short - circuit currents	105
9.1.4.	Wind power plants	105
9.2.	Definition and configuration of frequency stability analysis	107
9.2.1.	Generator tripping	108
9.2.2.	Wind power plant tripping	110
9.2.3.	Three - phase short circuit	111
9.3.	Conclusion and Discussion	113
10...Final	conclusion and further works	114

10.1.	Final conclusion	114
10.1.1.	Frequency control	114
10.1.2.	Tuning	114
10.1.3.	Integration of fully rated power energy converters	115
10.2.	Further works	115
References		117
Appendix		xx

Abstract

Isolated power systems are usually small remote electrical power systems facing a range of technical challenges. Without possessing primary conventional energy resources of their own and being often situated long distances away from countries exporting fossil fuels, *isolated power systems* (IPS) depend on expensive imports of primary energy for ensuring power generation. Integration of *renewable energy sources* (RES) would therefore seem to be both a practical and financially beneficial solution.

Frequency stability is a crucial aspect for all electrical power systems. However, interconnected power systems have in comparison to isolated power systems the ability of maintaining frequency stable due to large conventional power plants and to power reserves, as well as mechanisms that prevent a system collapse in case of a sudden severe power loss. The isolated power systems mentioned in this thesis dispose usually an *autonomous power station* (APS) mostly comprised from diesel fired synchronous generators and some kind of renewable energy sources. Since this is the most usual case in this thesis, the challenge of ensuring frequency stability for this kind of IPSs is presented, analysed and further explored by proposing and comparing frequency control concepts improving dynamic system response.

Primary and secondary frequency control in isolated power systems takes place in a different way as in interconnected power systems. Existing frequency control concepts are presented and two of them are selected. Their relation to the two most common used speed governors for diesel fired synchronous generators are implemented and tuned as well. With reference to several dynamic simulation events like load steps and three - phase short circuits, these frequency control concepts are compared before and after tuning, so as to be able to propose a best practice for a network operator of isolated power systems generally.

Moreover, the integration of RES and especially of *fully rated wind energy converters* (FRWEC) is further explored. The aim is to determine if the proposed frequency control concept presented and explored before the integration would have a further positive effect after the integration, or if a new frequency control concept should be considered.

At last, a real case study validates the selected frequency control concept. IPS of Lesbos in Hellas has been modelled in detail and according to real data provided from the *Hellenic electricity distribution network operator* (HEDNO). The generalisation of conclusions enables proposing a frequency control concept for isolated power systems operators improving frequency stability.

Abstract (deutsch)

Inselnetze sind im Allgemeinen kleine in sich geschlossene Energieversorgungssysteme, in denen unterschiedliche – im Vergleich zu Verbundnetzen andere - Herausforderungen zu bewältigen sind. Ohne eigene Ressourcen von Primärenergien und der Tatsache, dass die Entfernung zu Brennstoff liefernden Ländern zu groß ist, stehen Inselnetze in einer Abhängigkeit zu teuren Importen von Primärenergieträgern, um ihre Energieversorgung sicherzustellen. Die Integration von Erneuerbaren Energien (EE) scheint eine Lösung zu sein, die sowohl technisch als auch wirtschaftlich darstellbar ist.

Frequenzstabilität ist ein zentraler Aspekt für die Funktionalität eines jeden Energieversorgungssystems. Große Verbundnetze haben im Gegensatz zu Inselnetzen die Möglichkeit, über konventionelle Großkraftwerke Frequenzstabilität zu gewährleisten. Des Weiteren stehen in Verbundnetzen große Reservekraftwerke und Steuerungsmechanismen zur Verfügung, die einem plötzlichen Spannungseinbruch entgegenwirken können. Inselnetze hingegen müssen aus verschiedensten Gründen auf eine derartige Infrastruktur verzichten. Das in dieser Arbeit betrachtete Inselnetz verfügt über eine gewöhnliche autonome Energieerzeugungsstation, welche mit dieselgespeisten Synchrongeneratoren betrieben wird. Ergänzend dazu ist in dem genannten Inselnetz ein kleiner Anteil an Erneuerbaren Energien installiert. Da dies dem Normalfall entspricht, werden die Herausforderungen zur Sicherstellung der Frequenzstabilität für diese Art von Inselnetzen betrachtet und analysiert. Im Rahmen der Analyse wird das entwickelte Konzept zur Primär- und Sekundärregelung vorgestellt und im Hinblick auf die Verbesserung der dynamischen Systemantwort untersucht.

Die Primär- und Sekundärregelung in Inselnetzen muss im Vergleich zur Primär- und Sekundärregelung in Verbundnetzen differenziert betrachtet werden. Es werden bereits existierende Konzepte zur Primär- und Sekundärregelung vorgestellt und die Analyse der zwei meistverwendeten miteinander verglichen. Die Interaktion dieser meist eingesetzten Konzepte für dieselgespeiste Synchrongeneratoren wird implementiert und ausgewertet. Basierend auf durchgeführten dynamischen Simulationen sowie unterschiedlich angelegten Lastszenarien werden diese beiden Konzepte vor und nach dem Tuning miteinander verglichen. Durch diesen Vergleich lässt sich ein „best practice“-Ansatz ableiten, welcher Verteilnetzbetreibern von Inselnetzen vorgeschlagen werden kann.

Des Weiteren wird die Integration von Erneuerbaren Energien und im Detail die Integration von Vollumrichter-Windenergieanlagen untersucht. Der Fokus liegt hier auf der Beweisführung, ob das entwickelte Konzept zur Primär- und Sekundärregelung auch nach der Integration von Erneuerbaren Energien einen positiven Effekt auf das System hat. Abschließend wird anhand einer realen Fallstudie das gezeigte Konzept zur Primär- und Sekundärregelung validiert. Grundlage hierfür stellt das Inselnetz der griechischen Insel Lesbos dar. Die technischen und topologischen Daten zum betrachteten Energieversorgungssystem wurden vom griechischen Verteilnetzbetreiber (HEDNO) zur Verfügung

gestellt. Durch die Untersuchung des dynamischen Verhaltens dieses realen Inselnetzes lassen sich die Ergebnisse bezüglich der vergleichbaren Konzepte übertragen und validieren. Die Abstraktion dieser ermöglicht es, dass ein verbessertes Konzept zur Primär- und Sekundärregelung für die Gewährleistung der Frequenzstabilität Betreibern von Inselnetzen vorgeschlagen werden kann.

Acronyms

ACE	Area Control Error
AGC	Automatic Generation Control
APS	Autonomous Power Station
AVR	Automatic Voltage Regulators
DG	Diesel Generators
DIGLO	Diesel Generators and LOad
DIGLOW	Diesel Generators LOad and Wind
FRWEC	Fully Rated Wind Energy Converters
HEDNO	Hellenic Electricity Distribution Network Operator
HVDC	High Voltage Direct Current
IPS	Isolated Power System
LFC	Load-Frequency Control
LVRT	Low Voltage Ride Through
PCC	Point of Common Coupling
PID	Proportional Integral Differential
PLL	Phase Locked Loop
RES	Renewable Energy Sources
ROCOF	Rate Of Change Of Frequency
SG	Synchronous Generator
WDHS	Wind Diesel Hybrid System
WPP	Wind Power Plant
WTG	Wind Turbine Generator

Nomenclature

D	Load damping coefficient	p.u./Hz
E_{fd}	Field voltage	p.u.
f_{act}	Actual frequency	Hz
f_n	Nominal frequency	Hz
H	Inertia constant	seconds
I_{fd}	Field current	p.u.
K	Gain	p.u.
P_{rG}	Active power of connected synchronous generator	MW
P_m	Mechanical power output	p.u.
P_N	Rated power of prime mover	MW
P_{turb}	Turbine power	p.u.
R	Resistance	Ω
R_d	Speed droop characteristic	Hz/p.u.
S_{rG}	Rated power of generator	MVA
T_D	Diesel engine time constant	seconds
T_G	Governor time constant	seconds
T_{max}	Actuator maximum output torque	seconds
T_{min}	Actuator minimum output torque	seconds
T_T	Generator-turbine time constant	seconds
V	Terminal voltage magnitude	p.u.
V_{angle}	Voltage angle	deg
V_{base}	Base voltage	Volt

V_{ref}	Regulator reference voltage	p.u.
V_t	Regulator voltage input	p.u.
β	Composite frequency response characteristic	MW/Hz
δ	Power angle	deg
ω	Rotor speed	p.u.
ω_0	Rotor speed corresponding to nominal frequency	p.u.
ΔP	Active power deviation	p.u.
ΔP_L	Load deviation	p.u.
ΔP_m	Mechanical power deviation	p.u.
$\Delta \omega$	Rotor speed deviation	p.u.

List of Figures

Figure 1: Schematic block diagram of a synchronous generator with basic frequency control loops	13
Figure 2: Schematic diagram model of Load Frequency Control loops for one Generator - Load Model	14
Figure 3: Effect of droop characteristic in speed governor control loop	16
Figure 4: Ideal steady-state characteristics of a governor with speed droop	16
Figure 5: Electrical frequency response of one generator having governor with speed-droop characteristic	17
Figure 6: Load sharing by parallel units with droop governor characteristic	18
Figure 7: N - areas power system	19
Figure 8: Schematic diagram of primary control for control area i of an interconnected power system	21
Figure 9: Schematic diagram of complete supplementary control for control area i of an interconnected power system	22
Figure 10: Secondary control concept in selected units on AGC for isolated power systems	24
Figure 11: Response of a generating unit with isochronous governor	25
Figure 12: Operation of Droop/Isochronous load sharing on an isolated bus	27
Figure 13: Isochronous load sharing	28
Figure 14: Droop control characteristic of wind turbines for primary frequency support	31
Figure 15: Open-loop (without feedback) and closed-loop control system with feedback	35
Figure 16: Block diagram of isochronous speed governor	38
Figure 17: Block diagram of isochronous speed governor modelled in MATLAB Simulink	39
Figure 18: Block diagram of droop speed governor	41
Figure 19: Block diagram of droop speed governor modelled in MATLAB Simulink	42
Figure 20: Rotor speed ω of isochronous as well as for droop speed governor for a load step of 0.3 MW	44
Figure 21: Turbine power P_{turb} output of isochronous as well as for droop speed governor for a load step of 0.3 MW	44

Figure 25: Specifications on set-point following based on time response to a unit step in the set-point	46
Figure 23: Applied tuning process	49
Figure 24: Custom target time-domain response to a disturbance used for tuning	52
Figure 25: Overview of “2 DIGLO IPS” model	55
Figure 26: General functional block diagram for synchronous machine excitation control system	58
Figure 27: Load - flow results for Scenario A of “2 DIGLO IPS”	60
Figure 28: Load - flow results for Scenario B of “2 DIGLO IPS”	61
Figure 29: Load - flow results for Scenario C of “2 DIGLO IPS”	61
Figure 30: Block diagram of electric control box and actuator for demonstrating the effect of time constants before and after tuning	63
Figure 31: Output signal x of electric control box before and after tuning for Scenario A, B and C	64
Figure 32: Output signal u of actuator before and after tuning for Scenario A, B and C	64
Figure 33: Electrical frequency before and after tuning in case of 0.3 MW load step for Scenario A	65
Figure 34: Electrical frequency before and after tuning in case of 0.4 MW load step for Scenario B	66
Figure 35: Electrical frequency before and after tuning in case of 0.5 MW load step for Scenario C	66
Figure 36: Overview of “3 DIGLO IPS”	69
Figure 37: Overview of “4 DIGLO IPS”	69
Figure 38: Load - flow results for Scenario A of “3 DIGLO IPS”	71
Figure 39: Load - flow results for Scenario A of “4 DIGLO IPS”	72
Figure 40: Electrical frequency for a load step of 0.63 MW for Scenario A - “3 DIGLO IPS”	74
Figure 41: Electrical frequency for a load step of 1 MW for Scenario B - “3 DIGLO IPS”	75
Figure 42: Electrical frequency for a load step of 1.28 MW for Scenario C - “3 DIGLO IPS”	76
Figure 43: Electrical frequency for a load step of 0.9 MW for Scenario A - “4 DIGLO IPS”	77
Figure 44: Electrical frequency for a load step of 1.5 MW for Scenario B - “4 DIGLO IPS”	77

Figure 45: Electrical frequency for a load step of 1.5 MW for Scenario C - "4 DIGLO IPS"	78
Figure 46: Rotor speed of SG1 in case of a three - phase short circuit for IDD and IDD of Scenario A, B and C - "3 DIGLO IPS"	79
Figure 47: Rotor speed of SG1 in case of a three - phase short circuit for IDDD and IDDI of Scenario A, B and C - "4 DIGLO IPS"	80
Figure 48: Terminal voltage of SG1 in case of a three - phase short circuit for both frequency control concepts of Scenario A, B and C - "3 and 4 DIGLO IPS"	80
Figure 49: FRWEC model including the current controller	82
Figure 50: Options for local controller of FRWEC	84
Figure 51: Voltage Q -Droop control of FRWEC model	84
Figure 52: Voltage I_q -Droop control of FRWEC model	86
Figure 53: Current source model of FRWEC	87
Figure 54: Voltage source model of FRWEC	88
Figure 55: Overview of "4 DIGLOW IPS"	89
Figure 56: Load - flow results for Scenario A_WP30 of "4 DIGLOW IPS"	90
Figure 57: Electrical frequency before and after tuning in case of SG2 and SG3 tripping for Scenario A_WP30 - "4 DIGLOW IPS"	91
Figure 58: Electrical frequency before and after tuning in case of WPP tripping for Scenario A_WP70 - "4 DIGLOW IPS"	92
Figure 59: Electrical frequency before and after tuning in case of SG2 and SG3 tripping for Scenario C_WP30 - "4 DIGLOW IPS"	92
Figure 60: Electrical frequency before and after tuning in case of WPP tripping for Scenario C_WP70 - "4 DIGLOW IPS"	93
Figure 61: Rotor speed of SG1 before and after tuning in case of a three - phase short circuit for Scenario A_WP70 - "4 DIGLOW IPS"	94
Figure 62: Rotor speed of SG1 before and after tuning in case of a three - phase short circuit for Scenario C_WP70 - "4 DIGLOW IPS"	94

Figure 63: Lesbos isolated power system	96
Figure 64: Simplified diagram of Lesbos island power system	97
Figure 65: Detailed structure of APS	99
Figure 66: Voltage requirements for LVRT	106
Figure 67: Electrical frequency of Lesbos IPS in case of SG tripping for Scenario A	109
Figure 68: Electrical frequency of Lesbos IPS in case of SG tripping for Scenario C	109
Figure 69: Electrical frequency of Lesbos IPS in case of WPP tripping - 25 % power loss for Scenario A	110
Figure 70: Electrical frequency of Lesbos IPS in case of WPP tripping - 7 % power loss for Scenario C	111
Figure 71: Electrical frequency of Lesbos IPS in case of a three - phase short circuit at APS busbar for Scenario A	111
Figure 72: Electrical frequency of Lesbos IPS in case of a three - phase short circuit at APS busbar for Scenario C	112
Figure 73: Voltage magnitude in p.u. at the PCC of WPP4 connected in P31KCS of Lesbos IPS	112

List of Tables

Table 1: Hellenic isolated power system categories according to rated power of APS in MW	9
Table 2: Isolated power system categories according to voltage levels in kV	10
Table 3: Frequencies in normal and abnormal conditions for isolated power systems and the European interconnected power system	33
Table 4: Default time constants and gains for isochronous speed governor	43
Table 5: Parameters of SG1 of “2 DIGLO IPS” model	57
Table 6: Parameters of SG2 of “2 DIGLO IPS” model	57
Table 7: Tuned values for time and droop constant of isochronous and droop speed governors - Scenario A, B and C	62
Table 8: Overview of realised speed governors’ combinations	68
Table 9: Tuned droop constants of “3 DIGLO IPS” for Scenario A, B and C	73
Table 10: Tuned droop constants of “4 DIGLO IPS” for Scenario A, B and C	73
Table 11: Load - flow results of Lesbos isolated power system for Scenario A	101
Table 12: Load - flow results of Lesbos isolated power system for Scenario C	102
Table 13: Load - flow results of wind power plants of Lesbos isolated power system	102
Table 14: Overview of synchronous generators in operation and relevant speed governors for each scenario and combination	108

1. Introduction

System frequency provides an instantaneous indication of system operating conditions, as any imbalance between active power generated and consumed manifests itself as a deviation from nominal system frequency. The magnitude of the frequency excursion and the *rate of change of frequency* (ROCOF) are dependent on a number of factors, including the size of the power imbalance and the characteristics of the power system. While small variations in system frequency will not result in a reduction of system's reliability or security, large frequency deviations can have a serious impact on power system components and power quality is degraded. Damage to generators and transformers can result from overheating during times of low frequency or generator damage due to mechanical vibrations can occur if frequency deviations higher than 5 % of nominal frequency occur [1].

As a result, most power system components are equipped with protective relays, which are triggered if system frequency reaches critical conditions. Therefore, control of system frequency is vital for the secure, reliable and stable operation of a power system. The objective of frequency control is to maintain adequate balance between active power consumed and generated on a power system such that frequency remains within acceptable limits around nominal frequency. As power demand is constantly changing, frequency control is continuously called upon to fulfil this objective. To be more precise, a continuous balance between active power generated and active power consumed by loads including losses is required to maintain frequency constant at nominal system frequency. Any imbalance in active power will result in a frequency deviation. While precise instantaneous balancing of active power is not viable, frequency control ensures that the system frequency remains within acceptable frequency limits.

To a large extent, the changing system load is predictable and generators are committed and dispatched based on the forecast load levels [2]. Therefore, under normal operating conditions, the power balance is achieved by adjusting generator active power set-points. Signals to generators for such adjustments are either issued by the system operator or automatically generated and issued by *automatic generation control* (AGC). The functional principles of AGC will be presented in detail in this thesis.

Frequency control can be called upon for a variety of conditions ranging from a gradual change in load levels over time to a sudden loss of generation or step increase in demand. A range of power system characteristics including system size, individual generator and load frequency response characteristics and plant mix on the system influence frequency control. The size and speed of a frequency deviation depends on the magnitude of the power imbalance and the power system size. Power system inertia is the inertia of the individual rotating masses of all generators and load components synchronised to the system to a change in system speed. The higher the inertia of the system, the slower the ROCOF after a power imbalance event is. Large interconnected power systems have high system inertia, due to a large number of synchronous generators operating in this system. As such, large frequency excursions from

nominal are uncommon, and ROCOF is relatively slow due to high inertia. Small IPSs, in contrast, have much lower system inertia. Combined with the fact that a single generator can comprise a sizeable proportion of total generation, large power imbalances relative to the system size are more frequent and frequency changes are faster. Adequate frequency control on such a system is vital to prevent the excursion of system frequency beyond limits where interruption to customer supply through load tripping starts to occur. Therefore, maintaining system frequency at nominal frequency for a small IPS with limited interconnection can be technically challenging. Plant mix is continually evolving, for all power systems, large and small. Traditionally large diesel and oil fuelled thermal plants comprised the majority of the generation mix on the majority of IPSs. However, due to economic and environmental driving forces, increasing power penetration coming from RES in such power systems is desired.

Although there is no doubt about the importance of ensuring the highest technically possible penetration from RES to these weak grids, there are also aspects affecting the stability of the IPSs for the case of none RES penetration. The centralised power production is usually based on *diesel generators* (DG). The efforts of operating the power stations at technical minimum, so as to achieve the minimisation of fuel costs and the continuous variations in loading conditions require for the case of IPS an extremely careful study of their stability margins for all cases including and excluding RES.

1.1. Scientific scope

The objective of this thesis is to examine frequency control on IPSs with evolving plant mix. In particular, the influence of the characteristics of diesel generators and FRWECs on system frequency control will be examined. After developing and implementing generic models, a real case study, the isolated power system of Lesbos is used as an illustration.

For this purpose, two common speed governors used in diesel generators are analysed and their control loops are implemented in MATLAB simulation software. To explore their interaction in an isolated power system where both of them are in operation, a simple model is implemented and both speed governors are validated and tuned.

This system model is subsequently extended with more *synchronous generators* and different combinations of the implemented speed governors. Tuning takes place and loading scenarios enable the comparison of frequency control concepts. Dynamic simulations are performed for all models including load steps of a defined duration and three - phase short circuits.

Moreover, the effect of high wind power penetration is further explored for the model comprising of four synchronous generators. The wind energy converter model is presented in detail for steady-state and dynamic simulations. Afterwards, modelling a real isolated power system and performing similar dynamic simulations validates the results concerning the most appropriate frequency control concept.

To sum up, the scientific scope of this thesis is to provide a “best practice” to network operators of isolated power systems with diesel generators and wind energy converters regarding the interaction of the speed governors, the important variables that could be adapted according to the loading of the generators, or their most usual operating point before and after the integration of wind power.

1.2. Structure

The structure of the presented document is described in the following paragraphs. After a general introduction provided in *Chapter 1*, in *Chapter 2* an overview of IPSs explaining their characteristics is given. According to the discussed features a classification of them is provided.

Chapter 3 focuses on frequency stability of electrical power systems. The definition, the operational principles and the differences between interconnected and IPSs are illustrated. Within Chapter 3 general theoretical aspects and frequency control methods are presented to provide the required information in order to focus in the following chapters on IPSs with conventional power generation based on diesel generators.

Chapter 4 presents digital speed governing of diesel generators operating in IPSs. Already existing control concepts are presented and compared. This chapter describes the implementation process of isochronous and droop speed governor and covers the validation of them in MATLAB Simulink. Chapter 4 is rounded up by an outlook of realising the proposed frequency control concepts. Furthermore, general aspects of tuning and modelling are discussed and the applied tuning process is described.

Chapter 5 implements the self-contained implemented model named *DIGLO* (Diesel Generators and Loads) model with two synchronous generators and denoted as “2 DIGLO IPS”. In section one, all its attributes and components are described in detail. In section two three implemented power infeed scenarios regarding different loading conditions are defined and the load - flow results are presented. Furthermore, simultaneous tuning of speed governors is realised and the results are analysed. Dynamic simulations and before and after tuning demonstrate the tuning effect. The last section sums up the conclusion and continues the discussion.

In *Chapter 6* the introduced model “2 DIGLO IPS” is extended with three and consequently with four synchronous generators, denoted respectively as “3 DIGLO IPS” and “4 DIGLO IPS”. Likewise, in Chapter 6 three power - infeed scenarios as well as two frequency control concepts are implemented with the scope of exploring further model’s dynamic response and tuning results. As a sum up the conclusions of this chapter are discussed in brief at the end of this chapter.

Chapter 7 describes the extension of “4 DIGLO IPS” model’s including a FRWEC. This model is renamed as ‘Diesel Generators and Load and Wind model’, “4 DIGLOW IPS”. Firstly the wind energy converter is presented in detail concerning load flow as well as stability analysis functions. Secondly the

“4 DIGLOW IPS” is configured with reference to power infeed scenarios and dynamic simulations are performed by applying the already introduced frequency control concepts and tuning results from “4 DIGLO IPS”.

Chapter 8 illustrates a real case study concerning the island of Lesbos. The first section describes the topology of power system. The second section presents the results of the considered power infeed scenarios. The scope is to configure the power system at this way so as to perform dynamic simulations corresponding to the frequency control concepts introduced, implemented, compared and validated with the “4 DIGLOW IPS”.

Chapter 9 at the very beginning presents in brief grid code requirements valid in Greece for all IPSs. Moreover, dynamic simulations with this IPS verify the conclusions of former chapters based on “4 DIGLOW IPS” model. Stability of Lesbos IPS is evaluated according to the grid code requirements.

Chapter 10, as the last chapter, summarises important conclusions and gives an outlook of further works.

2. Isolated power systems

In this chapter the general characteristics and aspects of *isolated power systems* (IPS) are introduced as well as a categorisation of them, so as to define these ones, which are subjected to the problematic of this thesis.

An IPS is commonly thought of as a power system with lack of interconnection to a stiff power system, being autonomous and independent without a synchronous connection to other power systems. Islands for example are principally IPSs, since their geographical condition fulfils the requirement of not being a part of an interconnected power system. However, it is also possible that island power systems have interconnections to other electrical grids or to each other. Hence, the criteria of defining and recognising an autonomous IPS cannot be restricted only to the geographical condition, but they have to be extended considering aspects of the power system operation.

In the following section an overview of existing IPSs is given and considers these ones that are characterised as isolated from an electrical operation point of view. Consequently, characteristics of IPSs are presented, so as to underline the common points and similarities of all systems but also to demonstrate the possibility of combinations of these features which make each IPS unique and the drawing of general conclusions for these power systems a challenging task.

2.1. Overview of isolated power systems

In this section an overview of IPS will be given. This categorisation has been result of a literature review and after matching characteristics and information concerning generally any power system operating independently.

1. Islands

The most common IPSs are island power systems. All over the world there are thousands of them operating in isolated modus without having any connection to other electrical grids. In Europe, those systems can be found in the Mediterranean Sea being operated from the Spanish, Portugal, Italian or Hellenic network operator. There are also the examples of Malta or Cyprus, being island-nations and completely power independent. On the other hand, Ireland and Great Britain are also island-nations having however *high voltage direct current* (HVDC) interconnections to each other and to the European electrical grid making them different in comparison to the classical island power systems of the Mediterranean Sea, although this interconnection is asynchronous and can only contribute to a restricted amount of power exchange and not to system inertia. Additionally, a high number of islands in the Pacific Ocean belong to the same category of IPSs without interconnections, operating autonomously.

2. Non-connected regions

Another category of IPSs are the ones being on the mainland without having an interconnection to the mainland electrical grid, either because of long distances or because of political situations. Such an example is the villages of Alaska, or regions which are politically isolated, such as Israel. In these cases the fact that these systems operate independently and completely autonomously again plays the most important role.

3. Isolated on-purpose

Another case of IPS would be islanding of a part of the interconnected power system for security reasons or for ensuring stable operation of a specific part of the grid in case of faults in the rest of power system, or when there are power deficits. These parts of the grid that can be isolated are medium or commonly low-voltage grids and have mostly controllable loads, storage devices and RES connected. The operation principles of the autonomous subsystem after a successful islanding is based most of the time on the appropriate configuration of power converter interfaces, since there is normally no conventional power generation provided. These autonomous power systems operate in this modus for specific time duration and then have to be reconnected to the main power system at their *point of common coupling* (PCC). Therefore, they can be considered autonomous only for the time interval between the islanding and their reconnection [3, 4].

4. Industrial networks

Industrial networks are also a category of a potential IPS. They normally operate under connection, but they could under certain circumstances operate in isolated mode as well. Typically, at normal operation the industrial network and the utility grid are connected in order to benefit from a higher short - circuit power and better primary frequency reserve of the utility grid. When islanding, the industrial power plant should be capable of controlling the voltage and frequency by supplying the island network with the required amount of active and reactive power. The islanding would take place in case of a severe external fault by disconnecting the decoupling device between the utility grid and the industrial power plant and the designated industrial island network. Once the utility grid has recovered, the synchronisation and connection to the utility grid can be restored [5].

2.2. Characteristics of autonomous isolated power systems

In this section the main criteria for characterising a power system as isolated will be summed up. Most of the IPSs present a combination of all these characteristics and only a few of them could possibly simultaneously possess all of these characteristics.

1. Centralised power generation

One (or more) generator serves a composite load and for most of them the sum of all generators are connected in parallel. Usually there is only one conventional power plant, the so called APS, depending strongly on the size of the IPS. By “size” we do not refer only to the geographical extent, but also to the peak load of the system that represents the necessary amount of power generation.

2. Nature of conventional power plants

The generation units of these systems are mostly internal combustion engines and gas turbines. The most common practice is burning diesel, since in the world of rural electrification the alternative way for supplying energy to rural areas is (except for grid extension), the use of DGs [6, 7, 8].

3. Rated power of conventional power generation

The installed power of APS of these power systems can vary between hundreds of kW up to more than 100 MW, dependent again on their size as defined above in the first criterion [6].

4. Lack of “infinite” bus concept

The generators running in parallel are of such total capacity that they cannot compensate their active and reactive power output for all changes in the load, in order to maintain their terminal voltage constant and adapting rotor speed so as to ensure nominal frequency. In an IPS, there is no concept of “infinite” bus with a constant voltage and frequency where the generator connected to it can generate or absorb real power and reactive power for any operational condition [9].

5. Radial network topology

The network topology of classical IPSs can be directly recognised as an open ring network structure or weakly meshed networks with low ratios of $\frac{X}{R}$ [10]. The fact that power generation is centralised requires then a radial topology for power transmission and distribution to the final consumers. As a result, from the central power station depart lines of medium-voltage, essentially providing possible connection points that can be connected in case of faults. Of course, there are often lines dedicated to power transmission of higher voltage levels, but this depends again on the size and extent of the IPS.

6. Load factor

The load factor of IPSs is usually very low (0.25 – 0.4) due to high peaks of short duration occurring during summer (high tourist season) and low values during the rest of the year [6]. This criterion refers mostly to touristic islands. The summer peak load demand may be almost five-times the minimum winter

load demand, while even during the same day one may observe load demand variation between $\pm 60\%$ of the corresponding daily average power required [8].

7. Ratio of peak load to rated power of APS

A consequence of the former point is that the relationship between the peak load of these IPSs and the maximum active power of APS lies for the most of these systems above 70%. This is the case for most of them, since the rated power of APS is planned according to normal operation conditions and a low load factor. Therefore generating units of APS for short-time peak loads could come up to their limits without having any reserves. In several cases there is a very narrow power security margin, hence the local APSs do not guarantee the consumers' safe electricity supply, especially in occasions of serious malfunction of a major unit of the system or in cases of unexpected high-load demand [8].

8. Low inertia and spinning reserves

Overall system inertia is very low due to the reduced number of generators connected to the system. Such power systems are more sensitive to system disturbances, due to less stored energy in generator's and turbine rotors which would be able to cover energy imbalances and to compensate a severe ROCOF [11]. The fact of a low number of conventional generators in operation and the lack of interconnections automatically sets the definition of spinning reserves as a crucial aspect [12].

9. Simple system controllers

Control schemes in IPSs are limited to the speed governors and voltage regulators of conventional generators with a possible supplementation of load-sharing or self-synchronising machines [7].

10. Short - circuit power

Short circuits are also to be considered as a characteristic which differentiate these power systems in comparison to the interconnected ones, since for the most of them short circuits have to be considered as short circuits in generators terminals. For many of them there aren't long transmission lines to apply a short circuit and in case that there is one, the distances are not long enough to be considered far away from the central power generation. In these power systems the main characteristic is a low short - circuit power [10].

2.3. Classification of autonomous isolated power systems according to characteristics

Based on the criteria mentioned in the former section, the autonomous IPSs can be categorised into main groups in order to provide a classification. It is obvious that these classes overlap and that an IPS could belong to more than one, when it fulfils more than one criterion.

a. Rated power of APS

According to this criterion the autonomous IPSs can be categorised in four main classes with regard to the assumptions met in scientific papers published for Hellenic IPSs. Table 1 presents an overview of these classes and is based on the experience of HEDNO and the data provided for IPSs of the Aegean Sea. Of course these classes could differ dependent on the network operator assumptions.

Category	Installed power capacity of APS in MW	Islands
Very small	<1	e.g. Anafi
Small	>1 and <9	e.g. Kithnos
Medium small	>9 and <20	e.g. Milos
Medium	>20 and <50	e.g. Mikonos
Large	>50	e.g. Lesvos

Table 1: Hellenic isolated power system categories according to rated power of APS in MW [8]

Similarly, a categorisation of power systems with reference to installed power capacity is provided in [7]. There is a slight difference in the definition of an IPS typically driven by a large centralised power plant incorporating multiple diesel engines of different sizes. The rated power of the APS is up to 5 MW and systems above this rated power are characterised as large IPSs with multiple integrated power plants and a higher voltage open ring grid. Matching both categorisations the basic difference is that above 5 MW it is assumed that the installed power capacity does not only refer to one APS but to more power stations. However, there are many islands with installed power capacities over 5 MW exclusively installed in one APS.

b. Network Topology

Another possible categorisation of IPSs is based on voltage levels and of course is strongly dependent on the installed capacity. Table 2 is based on the categorisation of Table 1 but extends and classifies IPSs as Low-, Medium- and High-Voltage grids (respectively with acronyms LV, MV and HV grids) [13]. The classification is based on the relevant information provided from grid codes edited from network operators for several IPSs, such as Great Britain, Ireland, Iceland, Madeira, Malta, Hellas, Canary Islands, New Zealand and Tasmania [14–21].

Category	Voltage level in kV
LV	0.4
MV	33/20/15/11
HV	400/275/220/150/132/110/66

Table 2: Isolated power system categories according to voltage levels in kV

The voltage levels listed in Table 2 are combined in each IPS and result in a unique network topology. For example, in Great Britain the HV grid consists of lines of 400 kV, 275 kV and 132 kV, although in Ireland the HV grid consists of lines of 400 kV, 200 kV and 110 kV. The island of Madeira uses HV lines of 60 kV and a MV grid of 30 kV and 6.6 kV and Malta has a HV grid of 132 kV and the MV grid is composed from lines of 33 kV and 11 kV. Obviously all IPSs provide a LV grid serving the final consumers.

c. Power generation mix

A very important classification is based on the so-called plant mix. The fact that each IPS fulfils the characteristics mentioned in 2.2 in a different extent makes each one of them unique. Additionally, the possibility of supplying the required power from conventional and/or renewable power generation and in several combinations and penetration levels for each grid demonstrates the need for classifying them with reference to the plant mix.

A first general categorisation is between the ones with only conventional power generation and the ones which take advantage of RES as well. Possible conventional power sources are e.g. oil, coal, gas, diesel etc. and similarly the commonly known RES such as hydro, wind, geothermal, solar and biomass energy sources. Therefore, the first category relates IPSs combining several types of conventional power generation and constitutes for example a diesel-gas or an oil-coal-diesel power system. The second category, the so called “Hybrid Power Systems”, is the most common and in general, hybrid power systems incorporate at least two types of power sources [20]. Typically, they combine power generation from conventional and non-conventional power sources. For instance, possible configurations for a hybrid IPS would be wind-diesel or wind-solar-diesel-gas power system.

d. Hybrid power systems

As mentioned above hybrid power systems set a separate category concerning plant mix. For example, a *wind diesel hybrid system* (WDHS) is any autonomous IPS using *wind turbine generators* (WTG) with *diesel generators* (DG) to obtain a maximum contribution by the intermittent wind resource to the total power produced, while providing continuous electric power [22]. This type of hybrid autonomous IPS is very promising and reliable because the diesel acts as a cushion to take care of variation in wind speed, and

would always provide power equal to load minus the wind power. However there are many options for the operational configuration of these systems.

Dependent on the operation ability, these hybrid power systems can have several operation modes. If the WDHS is capable of shutting down the DGs during periods of high wind availability, the WDHS is classified as high wind penetration. High penetration WDHS have three modes of operation: Diesel Only (DO), Wind Diesel (WD) and Wind Only (WO). In DO mode the DGs supply the active and reactive power demanded by the consumer load. Load sharing and speed regulators controlling each diesel engine, perform frequency regulation and the synchronous voltage regulators in each generator perform voltage regulation. In WD mode, the WTGs also supply active power and the same regulators as in DO mode are in charge of the control of the frequency and the voltage. In WO mode the DGs are not running, only the wind turbines are supplying active power and therefore auxiliary components are needed to control frequency and voltage [23]. There are also WDHS concluding energy storage systems so as to be able to operate in WO modus safely [24].

Some examples of WDHS that operate with medium or even high wind power penetration are the “Toksook Bay” in Alaska with an average load of 370 kW and 300 kW of total wind power capacity. Furthermore another system thought to operate the most of the time in WO mode is the “St. Paul” in Alaska with an installed wind capacity 225 kW and diesel engine generators power capacity of 300 kW. The case of “Ten Mile Lagoon” in Australia is also such a case with an installed wind capacity of 2.025 MW and covering the rest of power demand from DGs [7, 25].

2.4. Demarcation of considered isolated power systems

After having presented the most common categories of IPSs, the category of interest for this thesis is defined. To be very accurate, it has to be mentioned that from now on and for this thesis, the analysis concerning IPSs refers only to autonomous wind-diesel hybrid IPSs meaning that independent of the geographical/ political or operational condition of them it is always assumed that the plant mix includes power generation from DGs and FRWECs.

3. Frequency stability of electrical power systems

The frequency of a power system is dependent on real power balance. A change in real power demand at one point of a network is reflected throughout the system by a change in frequency. Therefore, system frequency provides a useful index to indicate system generation and load imbalance. Any short - term power imbalance will result in an instantaneous change in system frequency as the disturbance is initially offset by the kinetic energy of rotating machines. Significant loss in generation without an adequate system response can produce extreme frequency excursions outside the working range of the power generating units. The control of frequency and power generation is commonly referred to as *Load-Frequency Control* (LFC) which is a major function of *automatic generation control* (AGC) systems. The primary objective of AGC is to regulate frequency to the specified nominal value and to maintain the interchanged power between areas at the scheduled values by adjusting the output of selected generators. Power system frequency regulation as major function of AGC has been one of the important control problems in electric power system design and operation [26, 27].

3.1. Definition of frequency stability

Frequency stability refers to the ability of power systems to maintain a steady frequency following a severe system disturbance resulting in a significant imbalance between generation and load [28]. Generally, losing frequency stability is associated with poor coordination of control and protection equipment, insufficient generation reserves and inadequacies in equipment responses [27].

3.2. Primary control and secondary frequency control in interconnected power systems with conventional power plants

The principles of frequency stability will be explained in brief in the following sections with the scope to extent the operational concept from one machine to multi-machine interconnected power systems beginning with the primary speed governing and going on with supplementary control concepts. Moreover, the differences between interconnected and isolated power systems regarding frequency control are analysed.

The most basic controller of a synchronous generator is the speed governor. Speed governors define the primary frequency control of synchronous generators [29]. Depending on the type of generation, the real power delivered by a generator is controlled by the mechanical power output of a prime mover such as a steam turbine, gas turbine, hydro-turbine or diesel engine. In the case of a steam-turbine, mechanical power is controlled by the opening or closing of valves regulating the input of steam flow into the turbine. Steam input to turbines must be continuously regulated to match real power demand. Hence, generator's speed has to vary with consequent change in frequency. For satisfactory operation of a power system, the

frequency should remain nearly constant [26]. Figure 1 presents the block diagram of a synchronous generator with basic frequency control loops operating in a conventional steam power plant.

In addition to a primary frequency control, most large synchronous generators are equipped with a supplementary frequency control loop, which is commonly known as secondary control. An extended schematic block diagram of a synchronous generator equipped with supplementary frequency control loops is shown in Figure 2 based on [27].

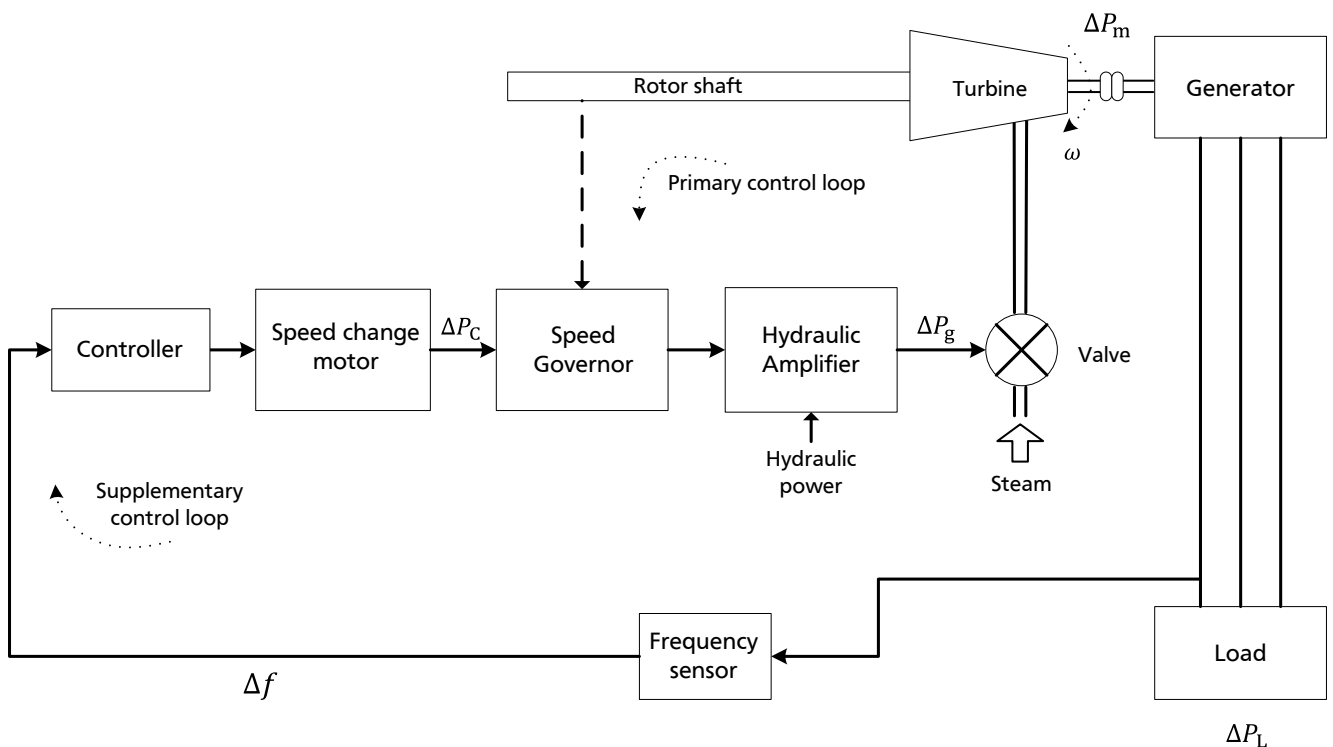


Figure 1: Schematic block diagram of a synchronous generator with basic frequency control loops [27]

In Figure 1, the speed governor senses the change in frequency via the primary and supplementary control loops. The hydraulic amplifier provides the necessary mechanical forces to position the main valve against the high-steam pressure, and the speed changer provides a steady-state power output setting for the turbine.

The speed governor on each generating unit provides the primary speed control function and all generating units contribute to the overall change in generation, irrespective of the location of the load change, using their speed governing. However, primary control action is not usually sufficient to restore the system frequency, especially in an interconnected power system and the supplementary control loop is required to adjust active power set point through the speed-changer motor.

The supplementary loop performs a feedback via the frequency deviation and adds it to the primary control loop through a dynamic controller. The resulting signal ΔP_C expressed in per unit is used to regulate the system frequency. The output signal of speed governor denoted ΔP_g expressed in per unit is used as input for the turbine so as to manage the appropriate mechanical power output. In real-world power systems, the dynamic controller is usually a simple integral or *Proportional Integral* (PI) controller. According to Figure 1 frequency experiences a transient change Δf expressed in per unit following a change in load ΔP_L expressed in per unit as well. Thus, the feedback is activated and generates an appropriate signal for the turbine to make generation ΔP_m expressed in per unit track the load and restore the system frequency [27].

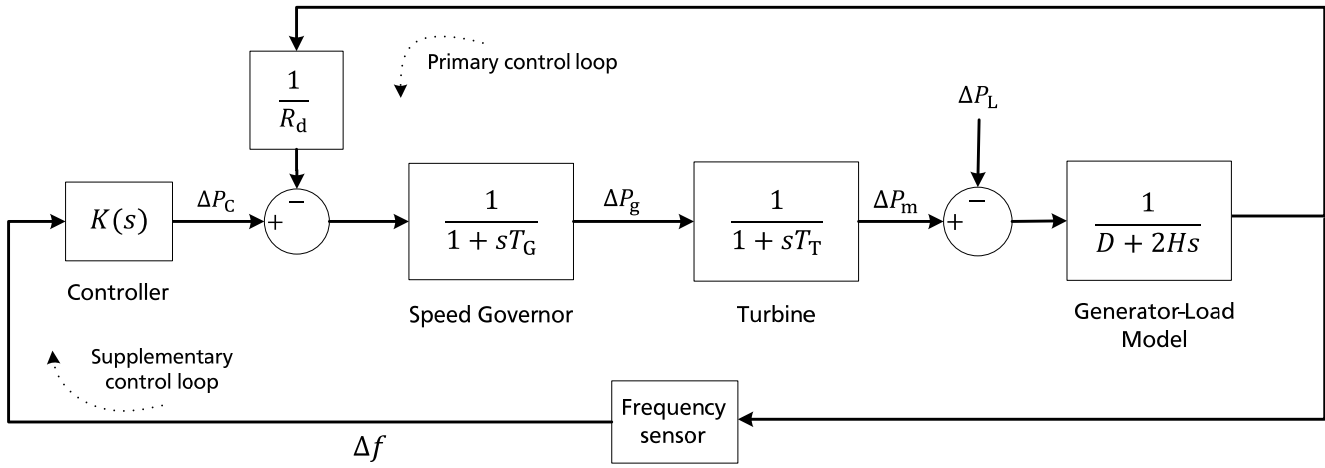


Figure 2: Schematic diagram model of Load Frequency Control loops for one Generator - Load Model [27]

Considering the time-varying characteristics of power systems and the fact that frequency dynamic response corresponds to a range of seconds or minutes enables the simplified analysis of frequency response. Going into detail of this schematic diagram, the overall generator - load dynamic relationship between the incremental mismatch power ($\Delta P_m - \Delta P_L$) and the frequency deviation Δf can be expressed as

$$\Delta P_m(t) - \Delta P_L(t) = 2H \frac{d\Delta f(t)}{dt} + D\Delta f(t) \quad 3.1$$

where ΔP_m is the deviation in mechanical power, ΔP_L is the load power deviation in per unit representing the non - frequency sensitive load deviation, H is the inertia constant of the generator in per unit seconds. The term $D\Delta f(t)$ represents the frequency - sensitive load deviation and is expressed in per unit. Load-damping coefficient D expresses a percent change in load for a 1 % change in frequency. For example, a typical value of 1.5 % for D means that a 1 % change in frequency would cause a 1.5 % change in load [26]. Equation 3.3 can be written as follows using the Laplace transformation

$$\Delta P_m(s) - \Delta P_L(s) = 2Hs\Delta f(s) + D\Delta f(s) \quad 3.2$$

As a result resistive loads, such as lighting and heating loads, are frequency independent and therefore they do not react in frequency deviations. On the contrary, motor loads such as pumps, are frequency dependent because of the direct matching of rotor speed and system frequency [26].

Furthermore, considering now the governor and turbine dynamics there are many low order models that can be used to represent them. Consequently T_G and T_T expressed in seconds are the governor and generator – turbine time constants respectively. The controller is represented as a gain constant. Droop constant is further to be seen and corresponds to the primary control loop, as already presented.

3.2.1. Primary control

The primary control loop is realised as described in 3.2 and is restricted for the speed regulation or droop $R_d \neq 0$. It is very common to express speed regulation in percent as described in equation 3.3

$$\text{Percent } R_d = \frac{\Delta f}{\Delta P} \times 100 = \frac{\Delta \omega}{\Delta P} \times 100 = \frac{\omega_{NL} - \omega_{FL}}{\omega_0} \times 100 \quad 3.3$$

where Δf is the frequency deviation in per unit, $\Delta f = (f_{act} - f_n)$, ΔP the power output deviation in per unit referring whether to the valve / gate position or to the power output but influences in reality the mechanical power output P_m expressed in per unit, ω_{NL} the steady-state speed at no load in rad / second, ω_{FL} the steady-state speed at full load in rad/second and ω_0 the rated speed in rad / second corresponding to the nominal frequency f_n .

With regard to speed governor model, for the steady state it is valid that $\lim_{s \rightarrow 0} G(s) = 1/R_d$ where R_d expressed in per unit. The value R_d is the speed droop characteristic that models the speed regulation due to governor action and determines the steady-state speed versus load characteristic of the generating unit. There are three possible options for the values of this characteristic:

- a. $R_d \neq 0$ and $R_d < \infty$
which implies that the machine regulates the power proportionally to its rated power. The proportional controller has a gain of $1/R_d$
- b. $R_d = 0$
which implies that the speed governor is a pure I-controller meaning an integrator implementing constant frequency control
- c. $R_d \rightarrow \infty$
which implies that constant power control is realised

Figure 3 presents the effect of droop constant relating the rotor speed to the output mechanical power of a generator.

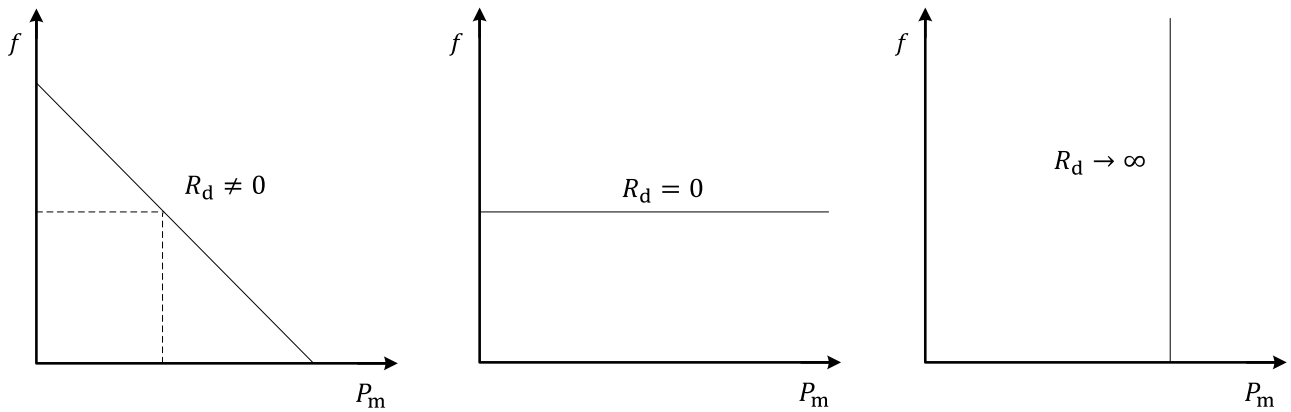


Figure 3: Effect of droop characteristic in speed governor control loop [29]

Typical droop values are between 4 % and 8 % and the physical meaning is that a 4 % frequency deviation will lead to a 100 % change in power output [30]. Figure 4 shows the ideal steady state characteristics of a governor with speed droop based on equation 3.3 [26].

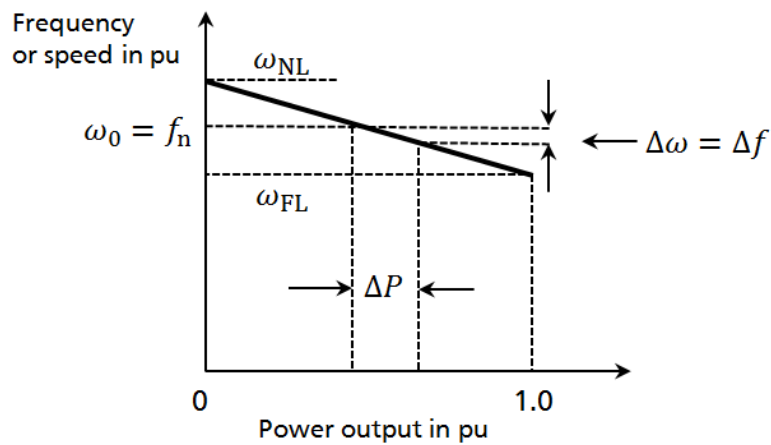


Figure 4: Ideal steady-state characteristics of a governor with speed droop [26]

To be more accurate an increase in load would cause a frequency drop and an increase in power output of a generating unit. The frequency response can be seen in Figure 5.

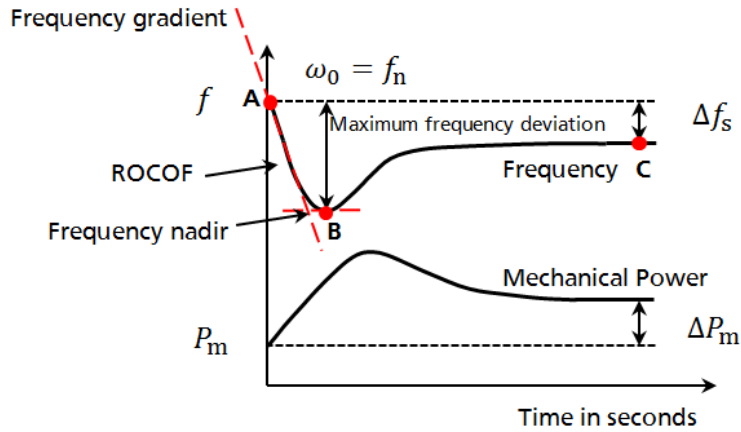


Figure 5: Electrical frequency response of one generator having governor with speed-droop characteristic [26]

A frequency drop event shows three main characteristic parameters: ROCOF or initial frequency gradient, minimum frequency also called frequency nadir and the steady-state frequency deviation Δf_s expressed in Hz. In the first few seconds following the loss of a large power plant, the grid frequency starts to drop. The initial frequency dynamics is dominated by the inertial response of the generators that operate further. So, the initial frequency gradient is determined by the inertia present in the power system and the active power mismatch, as indicated by the swing equation 3.1. IPSs have inherently lower inertia constants, and therefore, the initial ROCOF is usually higher.

The reason frequency stops declining at the minimum frequency (point B in Figure 5) is due to a combination of system inertia, load / frequency, and governor response [31]. Finally, at point C in Figure 5, the system reaches a steady-state, determined by the droop characteristic of the generators, as indicated in equation 3.1. A poor regulation capability in a power system will lead to large steady-state frequency errors [32].

Figure 4 can be expanded for more than one generator with droop governor characteristics which are connected to a power system and share the electrical load as is normally the case. A load change would be compensated from the online generators according to the droop value.

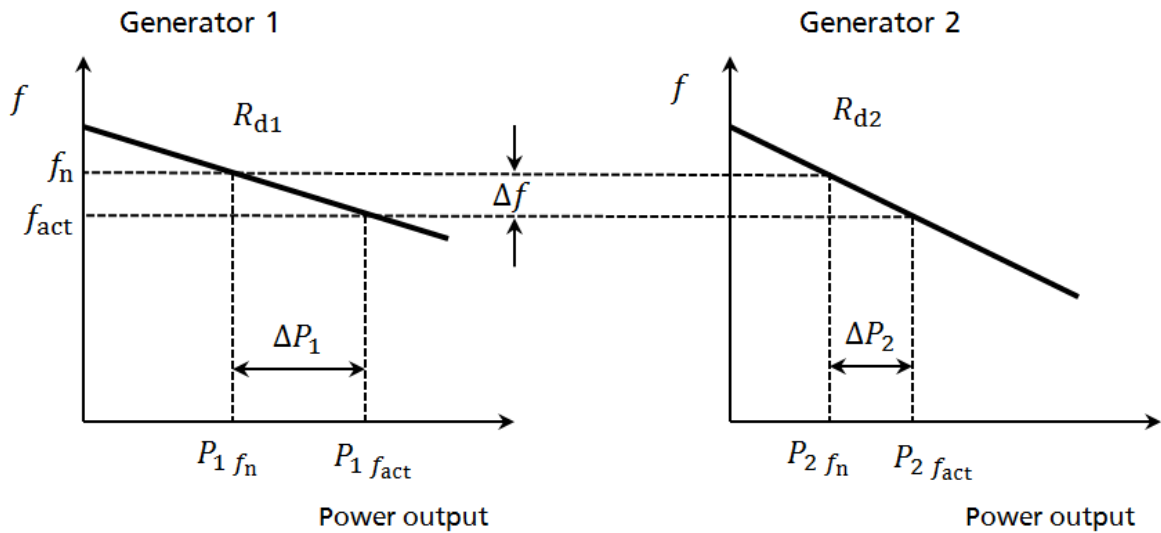


Figure 6: Load sharing by parallel units with droop governor characteristic [26]

Figure 6 presents the sharing of load between two generators with different droop feeding a load. The gradient of the bold line represents the speed regulation, meaning that a generator with a low droop and smooth gradient (Generator 1) will react more intense to a load frequency change in comparison to a generator with a high droop value and larger gradient (Generator 2). It is valid that $R_{d1} < R_{d2}$. In order to be more specific, it is to be seen that both generators run initially at nominal frequency f_n with power outputs $P_{1 f_n}$ and $P_{2 f_n}$ respectively. A load increase would result in a frequency deviation and the actual frequency f_{act} will be lower than the nominal one. This actual frequency is unique for the power system and equal for both of them. Therefore, based on equation 3.3, since the percent of droop is different and the frequency deviation Δf is for both the same, the power output of each one is related to the value of droop and would be for Generator 1, $P_{1 f_{act}}$ and for Generator 2, $P_{2 f_{act}}$ with $\Delta P_1 > \Delta P_2$. Similarly in case of more generators sharing a load, the same principle can be applied according to their droop configuration [26].

The operation principles that have been presented and regard only one generator can be extended for the operation of interconnected power systems. Regulation of interchange power is a control issue and the LFC task is limited to restore system frequency to the nominal value. Frequency control is becoming more significant today due to the increasing size, the changing structure and the complexity of interconnected power systems. Increasing economic pressure for power system efficiency and reliability has led to a requirement for maintaining system frequency and tie-line flows closer to scheduled values as much as possible. Therefore, in a modern power system, LFC plays a fundamental role, as an ancillary service, in supporting power exchanges and providing better conditions for the electricity trading [27].

In order to generalise the described model for interconnected power systems, the control area concept needs to be used, as it is a coherent area consisting of a group of generators and loads, where all the generators respond to changes in load or speed-changer settings. The frequency is assumed to be the

same in all points of a control area. A multi-area power system comprises areas that are interconnected by high-voltage transmission lines or tie-lines. The trend of frequency measured in each control area is an indicator of the trend of the mismatch power in the interconnection and not in the control area alone. The LFC system in each control area of an interconnected (multi-area) power system should control the interchange power with the other control areas as well as its local frequency [27]. Therefore, the described dynamic LFC system model presented in Figure 2 has to be modified including more control areas as presented in Figure 7.

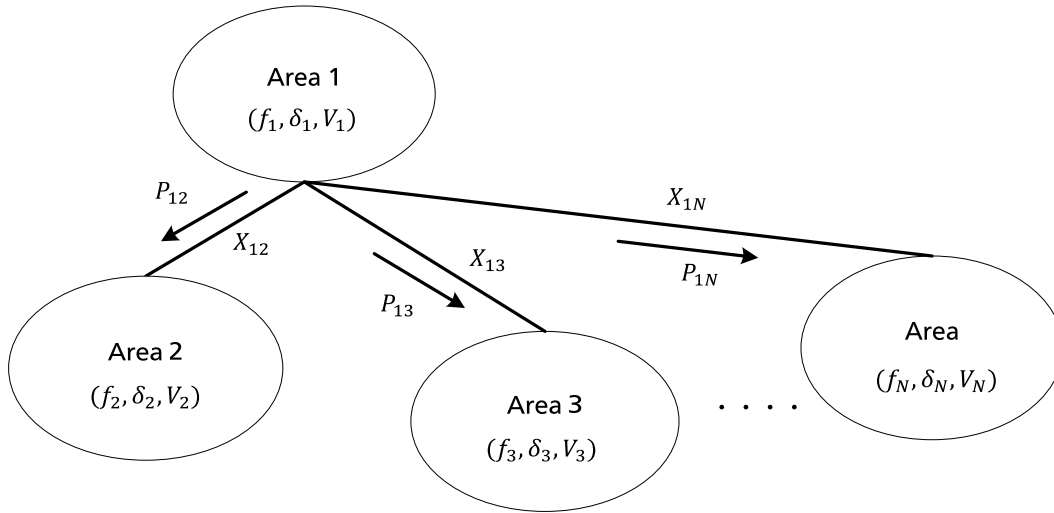


Figure 7: *N*- areas power system [27]

The electrical equivalent of the system is composed of each area represented by a voltage source behind an equivalent reactance as viewed from the tie bus. The power flow for instance between Area 1 and Area 2 would be

$$P_{12} = \frac{V_1 V_2}{X_{12}} \sin(\delta_1 - \delta_2) \quad 3.4$$

where X_{12} is the coupling reactance between areas 1 and 2, δ_1 and δ_2 the power angles of equivalent machines, meaning machines with similar dynamic response that could be represented as one, in areas 1 and 2 and V_1 and V_2 are respectively terminal voltages of machines in areas 1 and 2. By linearizing equation 3.4 about an equilibrium point where $\delta_1 = \delta_1^0$ and $\delta_2 = \delta_2^0$ and by indicating T as the synchronising torque coefficient we have

$$\Delta P_{12} = T_{12}(\Delta \delta_1 - \Delta \delta_2) \quad 3.5$$

$$T_{12} = \frac{|V_1| |V_2|}{X_{12}} \cos(\delta_1^0 - \delta_2^0) \quad 3.6$$

Considering the relationship between area power, angle and frequency equation 3.5 can be written as

$$\Delta P_{12} = T_{12} \left(\int \Delta \omega_1 - \int \Delta \omega_2 \right)$$

$$\Delta P_{12} = 2\pi T_{12} (\int \Delta f_1 - \int \Delta f_2) \quad 3.7$$

where Δf_1 denotes frequency deviation of area 1 and Δf_2 frequency deviation of Area 2 respectively. Using consequently the Laplace transform, equation 3.7 can be written

$$\Delta P_{12}(s) = \frac{2\pi}{s} T_{12} (\Delta f_1(s) - \Delta f_2(s)) \quad 3.8$$

Similarly, for instance, the tie line power exchange between areas 1 and 3 will be

$$\Delta P_{13}(s) = \frac{2\pi}{s} T_{13} (\Delta f_1(s) - \Delta f_3(s)) \quad 3.9$$

Considering both 3.8 and 3.9 tie line power exchange between area 1 and areas 2 and 3 can be calculated as follows

$$\Delta P_1 = \Delta P_{12} + \Delta P_{13} = \frac{2\pi}{s} \left[\sum_{j=2,3} T_{1j} \Delta f_1 - \sum_{j=2,3} T_{1j} \Delta f_j \right] \quad 3.10$$

Generalising equation 3.10 for N control areas power exchange between area 1 and other areas is

$$\Delta P_i = \sum_{\substack{j=1 \\ j \neq i}}^N \Delta P_{ij} = \frac{2\pi}{s} \left[\sum_{\substack{j=1 \\ j \neq i}}^N T_{ij} \Delta f_i - \sum_{\substack{j=1 \\ j \neq i}}^N T_{ij} \Delta f_j \right] \quad 3.11$$

Equation 3.11 is explained with a block diagram in Figure 8 regarding area i of an interconnected power system of N control areas being the extension of the primary control loop presented in Figure 2 which takes only one area into consideration.

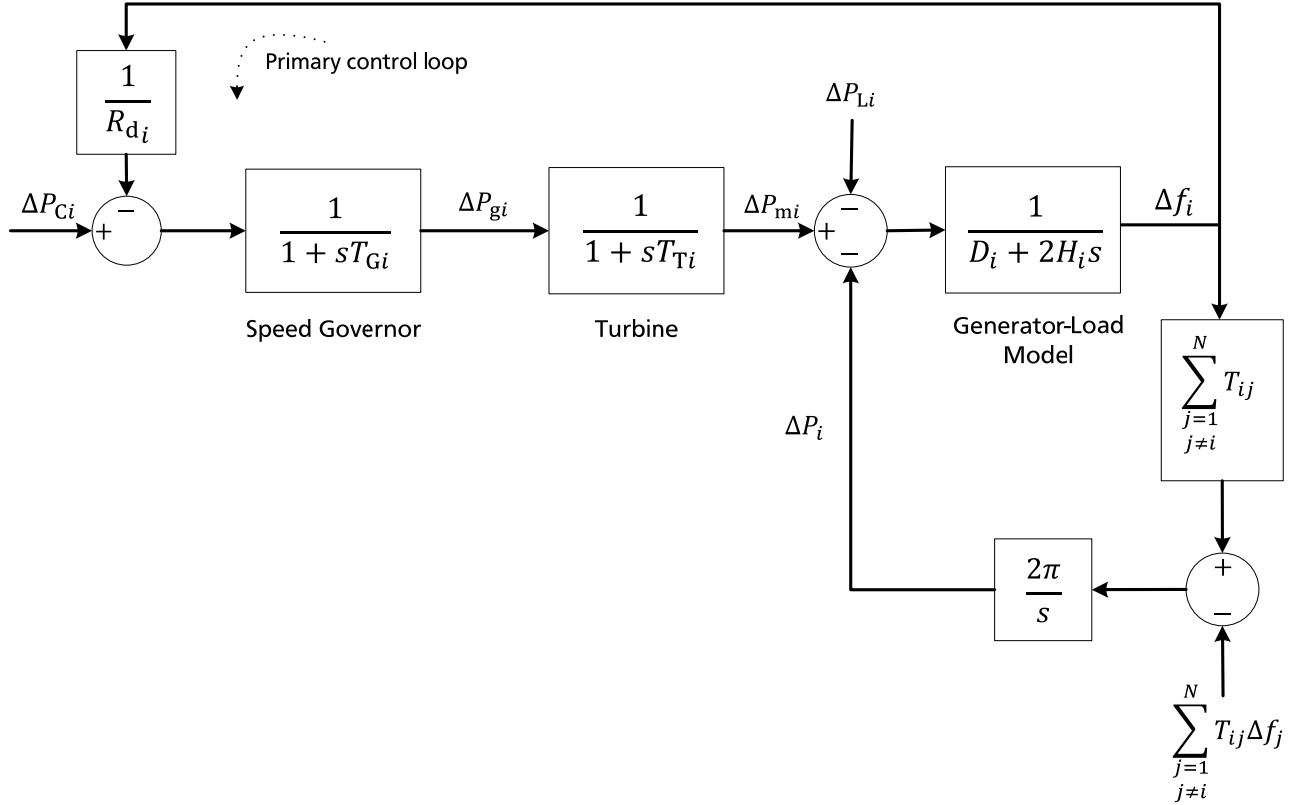


Figure 8: Schematic diagram of primary control for control area i of an interconnected power system [27]

Explaining in brief the schematic diagram of Figure 8, it can be seen that area i is modelled by an equivalent inertia H_i and a corresponding damping constant D_i . It can be also mentioned that the equivalent inertia H_i would result as sum of the inertia constant of each generating unit and each rotor in area i . Respectively, the speed governor and the turbine have time constants corresponding to this area and effective speed droop is adapted to the regarded area R_{d_i} . Tie line between area i and other areas is represented through synchronising torque coefficient T_{ij} and power exchange between area i and other $N - 1$ areas with ΔP_i . The meaning of a positive ΔP_i is that there is an increase in power transfer from area i to area j which is the effect of increasing load of area i and decreasing load of area j [27]. Relating mechanical power to power exchange based on Figure 8 for frequency deviation Δf_i of area i can be written

$$\Delta P_{mi} - \Delta P_i - \Delta P_{Li} = \Delta f_i D_i \quad 3.12$$

Considering the expression of mechanical power deviation for area i in equation 3.12 and considering the negative sign of droop from the control loop we have

$$\Delta f_i \left(\frac{1}{R_{d_i}} + D_i \right) = -\Delta P_i - \Delta P_{Li} \quad 3.13$$

and by assuming that $\left(\frac{1}{R_{di}} + D_i\right) = \beta_i$ which represents the composite frequency response characteristic, caused from loads and generators of area i and is normally expressed in MW / Hz equation 3.13 becomes

$$\Delta f_i = \frac{-\Delta P_i - \Delta P_{Li}}{\beta_i} \quad 3.14$$

3.2.2. Secondary control

The next point to consider is the supplementary control loop in the presence of a tie-line. In a multi-area power system, in addition to regulating area frequency, AGC is realised through a supplementary control that maintains the net interchange power with neighbouring areas at scheduled values. This is generally accomplished by adding a tie-line flow deviation to the frequency deviation in the supplementary feedback loop. A suitable linear combination of frequency and tie-line power changes for area i , is known as the *area control error* (ACE), represents the mismatch between scheduled and actual power within a control area and is described as

$$ACE_i = \Delta P_i + \beta_i \Delta f_i \quad 3.15$$

The schematic diagram of Figure 9 illustrates how supplementary control is applied for an area i of an interconnected power system of N control areas being the extension of the primary control loop presented in Figure 2 and Figure 8 which takes only one area into consideration.

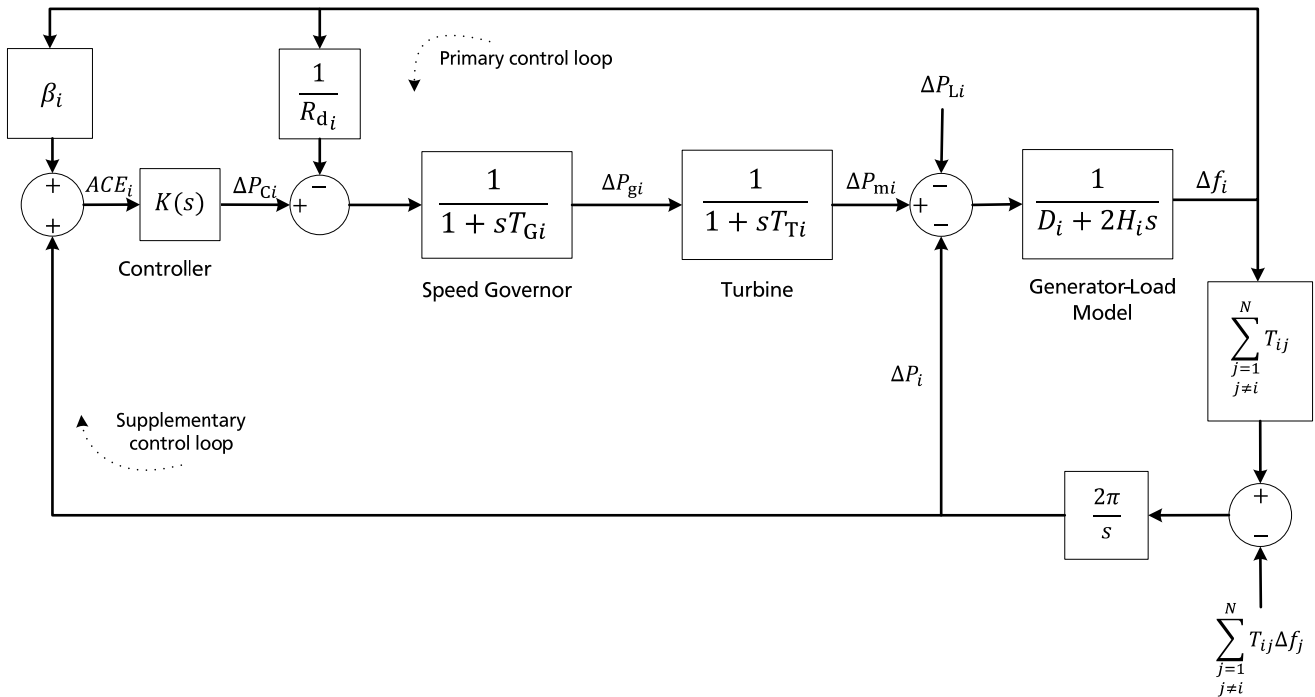


Figure 9: Schematic diagram of complete supplementary control for control area i of an interconnected power system [27]

The ACE signal is computed and allocated to the controller $K(s)$, which is usually a simple integral or PI controller, as mentioned describing Figure 1. Finally, the resulting control action signal is applied to the turbine block. Therefore, it is expected that the supplementary control shown in Figure 9 can ideally meet the basic LFC objectives and maintain area frequency and tie-line interchange at scheduled values. In reality there are many generators in each control area with different governor, turbine and generator type parameters. Furthermore, some of them may participate in the LFC task or not. Therefore the LFC participation factor of a generating unit indicated as α_{ki} meaning that belongs to an area i of an interconnected power system composed of k generating units would vary between zero and one demonstrating a unit participating fully ($\alpha_{ki} = 1$) or not at all ($\alpha_{ki} = 0$) in the LFC process. Following a load disturbance within the control area, the produced appropriate supplementary control signal is distributed among generator units in proportion to their participation, to make generation follow the load [27].

3.3. Primary control and secondary frequency control in isolated power systems

The main challenges faced by IPSs are related to system security, control of frequency and management of system generation reserve. A common aspect to all these problems is the requirement to ensure that sufficient reserve capacity exists within the system to compensate for sudden loss of generation. Thus, mismatches in generation and load and/or unstable system frequency control might lead to system collapse [33]. Frequency control in IPSs is based on the same principles as for the interconnected power systems and consists of the primary and secondary control loop. However, the differences will be described in the following section.

3.3.1. Primary control in isolated power systems

Primary control in isolated power systems is realised at the same way as in interconnected power systems, meaning with speed regulation and droop control. The values for the droop constant R_d depend on the power generation mix, on the installed capacity and vary normally between 3 % and 5 %. However the primary control loop remains the same as presented in Figure 2.

3.3.2. Secondary control in isolated power systems

As far as secondary control in isolated power systems is concerned, there are two main aspects that differ with comparison to the concepts presented in 3.2.2.

Supplementary control could be implemented in two ways:

1. Through AGC with the same operational principle as described in 3.2.2. for interconnected power systems. The main difference is that this control method is dedicated to restore frequency for IPSs to the nominal value, since power exchange is not more an issue and there are no control areas.

An integral control which acts on the load reference settings of the governors' settings of units on AGC ensures zero frequency error in the steady state.

- Through appropriate configuration of speed droop characteristic. As a result, primary and secondary control are implemented without an additional control loop but only by adapting generators speed governor's gain R_d . As appropriate configuration is meant an integrator implementing constant frequency control with value $R_d = 0$. This is the so called isochronous governor.

As referred above there are two main ways of implementing supplementary control (secondary control) in IPSs. These concepts will be explained more in detail.

A. Automatic generation control in isolated power systems

This control method is used in interconnected and isolated power systems. However, there are two important differences regarding the control loops. Firstly, in isolated power systems there is no synchronizing torque coefficient, since there are no interconnected areas. Secondly instead of ΔP_i , used to describe the power transfer between areas, the term ΔP_{mP} is used representing the resulted deviation in mechanical power of the primary control loop. Furthermore, a common option for realising AGC in IPSs is accomplished by adding a reset or integral control acting on the load reference settings of the governors of units participating in AGC [27]. The proposed control concept can be seen in Figure 10.

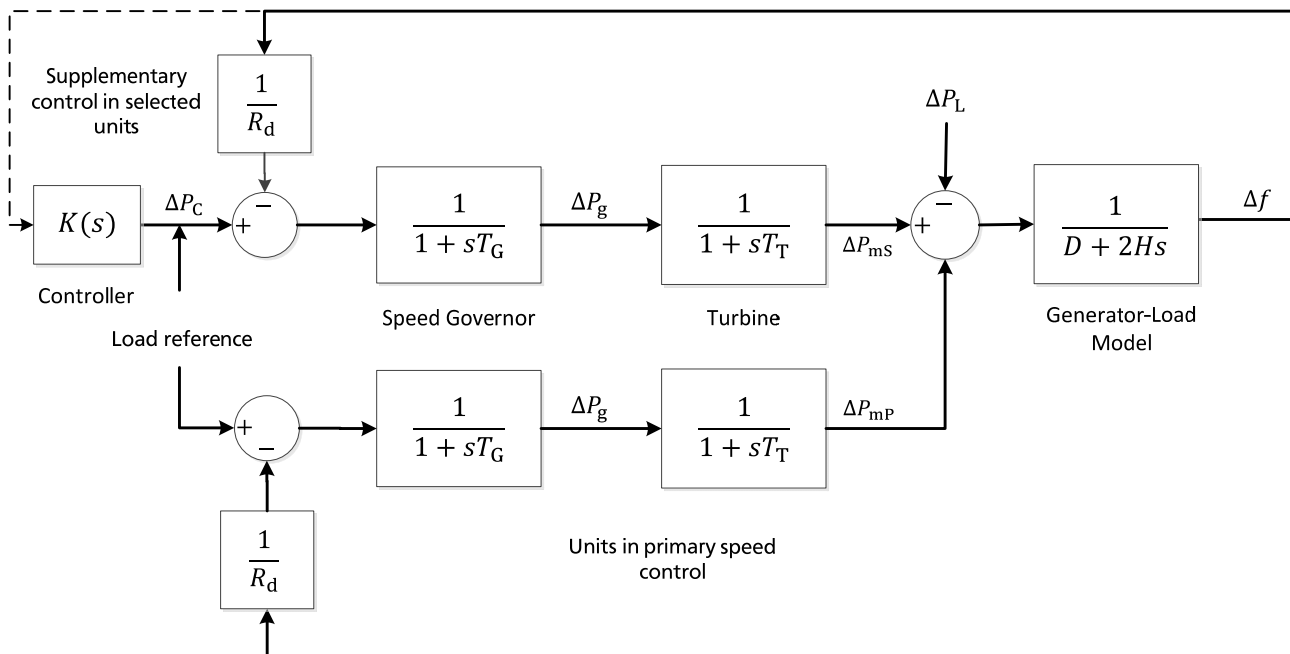


Figure 10: Secondary control concept in selected units on AGC for isolated power systems [27]

To define the input of "Generator-Load Model", ΔP_{mP} is added with the deviation in mechanical power of secondary control loop ΔP_{mS} . The supplementary control action is much slower than the primary speed

control action so as to take effect after the primary speed control which has been activated for all generating units has reached a new steady-state frequency. Hence, AGC adjusts load reference settings of selected units and therefore their output power in order to restore frequency to the nominal value.

B. Isochronous speed governor

This pure integrator brings frequency back to the nominal value and only when frequency deviation equals to zero, steady state can be reached. As a result, frequency deviation resulting from primary control will be compensated from generators having isochronous governors instead of droop regulation. In IPSs, it is required that one generator works with this operational principle; otherwise the frequency deviation could not be compensated [26].

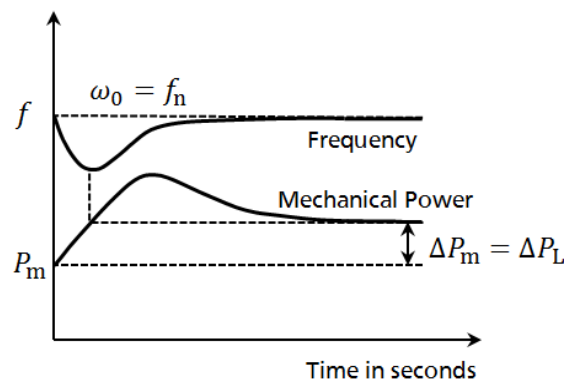


Figure 11: Response of a generating unit with isochronous governor [26]

It is clear that in IPSs with more than one generating unit a very common applied control concept is the use of many governors with speed-droop characteristics adapted to the rated power of each unit in order to react appropriately to load changes, meaning that some of them would participate more intensively than others. The remaining steady-state frequency deviation would be compensated from generating units with an isochronous governor, which usually are DGs with the largest rated power. These DGs implement secondary control and restore frequency to the nominal value [26].

3.3.3. Overview of existing frequency control concepts for diesel generators in isolated power systems

In this chapter several power system frequency control concepts are presented, based on the literature as well as on practical application of speed controllers. The principles of droop and isochronous operation have been explained in 3.2.1 and 3.3.2. The combination and extension of these concepts will be considered in this section. For parallel operation these concepts are mostly used. Additionally the mix of droop/isochronous, isochronous load sharing and base load can be also applied [30].

Paralleling frequency control

The two most applicable modes used for paralleling are droop and isochronous governing. For the first one, rotor speed is adapted according to frequency deviation as introduced in 3.2.1 and in case of isochronous governors, rotor speed remains constant. For parallel generators with different droop constants R_d the load changes will be shared proportionally, as presented in Figure 6.

A generator set operating in isochronous mode would operate at the same frequency regardless of the supply, up to the full load capability of the generator set. This mode can be used on one generator set running by itself in an IPS. The isochronous mode can also be used on a generator set connected in parallel with other generator sets. Unless the governors are configured with load sharing attribute, however, no more than one of the generator sets operating in parallel can be in the isochronous mode. If two generator sets, operating in the isochronous mode without load sharing attribute, are tied together to the same load, one of the units will try to carry the entire load and the other will shed its entire load.

Droop/Isochronous frequency control

Droop/isochronous frequency control is a combination of the first two modes. All generator sets in the system except one are operated in the droop mode. The one unit not in droop is operated in the isochronous mode. It is known as the swing machine. In this mode, the droop machines will run at the frequency of the isochronous unit. The droop and speed settings of each droop unit are adjusted so that each generates a fixed amount of power. The output power of the swing machine will change to follow changes in the load demand. Maximum load for this type of system is limited to the combined output of the swing machine and the total set power of the droop machines. The minimum system load cannot be allowed to decrease below the output set for the droop machines. The machine with the highest output capacity should be operated as the swing machine, so that the system will accept the largest load changes within its capacity. Figure 12 presents the control concept of this method.

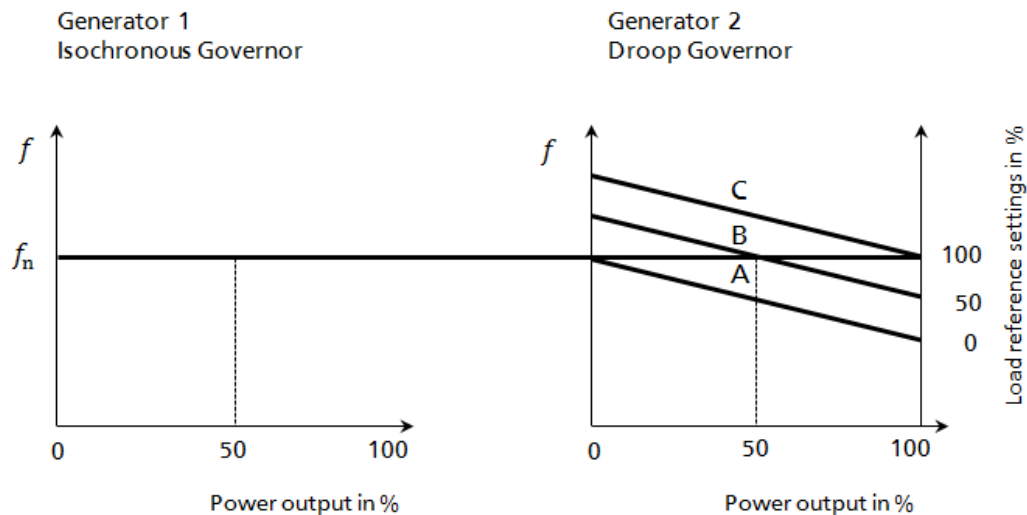


Figure 12: Operation of Droop/Isochronous load sharing on an isolated bus [26]

Three characteristics are shown representing three load reference settings. At the nominal frequency characteristic A results in zero output, characteristic B results in 50 % output and characteristic C in 100 % output. Thus, the power output of a generating unit at a given speed may be adjusted to any desired value by adjusting the load reference setting or in our case for a fixed power output the speed can be adjusted, so that the droop governors will run always at the frequency of the machine being in isochronous mode [26].

Isochronous frequency control

Isochronous load sharing operates all generator sets in a system in the isochronous mode. Load sharing is accomplished by adding a load sensor to each isochronous governor. The load sensors are interconnected by load sharing lines. Any imbalance in load between generating units will cause a change to the regulating circuit in each governor. While each generator continues to run at isochronous speed, these changes force each machine to supply a proportional share of power to meet the total load demand on the system [30]. Figure 13 presents the operation of this control concept.

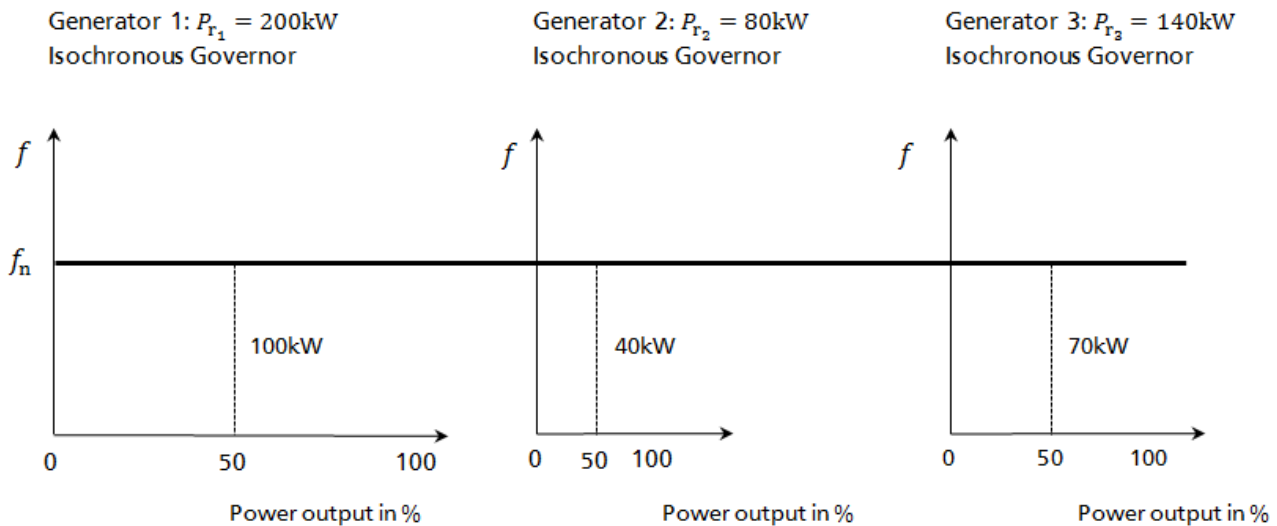


Figure 13: Isochronous load sharing [30]

With a proper set up each generator will supply each proportional share of the load as it can be seen in Figure 13. Thus, assuming a set of three generating units of different rated powers but all accomplished with an isochronous speed governor and assuming further that load sharing has been defined to be 50 %, then Generator 1 of $P_{r_1} = 200 \text{ kW}$ would feed the isolated bus with 100 kW, Generator 2 of $P_{r_2} = 80 \text{ kW}$ would feed the isolated bus with 40 kW and Generator 3 $P_{r_3} = 140 \text{ kW}$ of with 70 kW respectively.

Base load frequency control

Base Load is a method of setting a base or fixed load on a machine operating in parallel with an isolated bus. This is accomplished by using an isochronous load control and providing a reference at which load would be controlled. The governor will force the generator output to increase or decrease until the output of the load sensor is equal to the reference setting. At this point, the system is in balance.

This mode can only be used where other generator sets are producing enough power to meet the changes in load demand. This operating mode is ideal for either soft loading additional units into an IPS, or for derating or unloading a machine [30].

After presenting the most common and efficient control modes regarding DGs of IPSs, it has to be mentioned that the choice of the most appropriate mode is strongly related to the IPS and to its specific characteristics. As already referred to these characteristics in 2.2 and to the fact that a lot of combinations of them could be possible for an IPS, it supports the statement that attention has to be paid as far as the selection of the appropriate control concept is concerned, in order to ensure frequency stability.

3.4. Challenges regarding frequency stability of isolated power systems based on diesel power generation with high integration of wind power

In the former sections an overview of frequency control in interconnected and isolated power systems with conventional power generation has been provided. Consequently, in this section, an overview of challenges regarding frequency stability in case of high wind penetration is given as well. As high wind power penetration is meant a penetration of above 30 % in IPSs. In case of such a wind power penetration, fast wind changes and very high wind speeds may result in sudden loss of power generation as well, causing frequency excursions and dynamically unstable situations. This is due to the fact that frequency oscillations might easily activate frequency protection relays of the wind power plants. Setting of a too high under-frequency protection makes severe situations after a generation dropout even worse, because the frequency relays may disconnect the dispersed generators and even increase the lack of generation.

Additionally, in IPSs with a high wind power penetration, further operating constraints are imposed by the technical minima and the stability considerations of conventional thermal generating units, resulting in significant curtailment of the wind farm output powers [34].

According to the literature, the challenges related to high wind power integration can be summed up in three main categories of research work. The first one deals with studies trying to find out the best power mix between diesel and wind power plants, the second one trying to propose concepts supporting system frequency from wind power plants and the last one dealing with upgrading of diesel control loops to be able to confront a high wind power penetration.

Computational studies for defining the best wind-diesel power generation mix

Power system simulation software specifically dedicated to increase the use of RES in IPSs have been developed during last years [25]. The scope is commonly the development of computational environments to analyse the wind exploitation into small and medium size autonomous energy systems [35]. The proposed methods comprise algorithms and tools to analyse the impact of wind power integration from both technical and economical point of view [6]. A general simulation algorithm for the accurate assessment of isolated diesel-wind turbine systems interaction was developed in [36] able to perform transient stability analysis of isolated diesel-wind turbines power systems for accurate assessment of their interaction. Furthermore, other approaches aiming to optimise the operation of isolated and weakly interconnected systems by increasing the share of wind energy provide advanced on-line security functions, both in preventive and corrective mode. The main features of the control system comprise advanced software modules for load and wind power forecasting, unit commitment and economic dispatch of the conventional and renewable units and on-line security assessment capabilities. In this way, penetration of RES in IPSs can be increased in a secure and reliable way [37]. Additionally,

aspects as optimal energy flow control solution have been regarded by pursuing the minimum fuel consumption [38]. In this case the minimisation of production costs is performed through an on-line optimal scheduling of the power units, which takes into account the technical constraints of DGs, as well as short - term forecasts of load and of RES. The power system security is maximised through on-line security assessment modules, which enable the power system to withstand sudden changes in the production of RES [39].

Wind Generators frequency support

Normally, active power and frequency control in power systems are provided from synchronous generators. However, non-synchronous generators, such as WTGs, are nowadays requested in the most grid codes to participate in the active power-frequency control. This feature is especially interesting in IPSs. Regarding primary control taking place in wind turbine level, there are active power control concepts including power output control or curtailment and adjustable droop control for under/over frequency regulation. In addition, rapid injection of power would also be required after sudden frequency drop in order to forestall load shedding and generator tripping. There are two main methods for supporting system frequency on behalf of the wind turbines. On the one hand the so-called synthetic inertial response is the term for describing the frequency support coming from the wind power plants. The approach in inertial control is to modify the wind turbine controller so as to deliver a response similar to that from the inertia of synchronous generators [32]. According to inertia control principle, the WTG responds to ROCOF. The additional power provided by the inertial response of a wind turbine is restricted by the amount of kinetic energy stored in the actual inertia of the rotor, the acceptable variations of the rotor speed and the post disturbance effect of re-establishing rotor speed (and, therefore, kinetic energy) to the pre disturbance value. The inertial response however does not require a power reserve margin in the wind turbine. During the first instants following a major disturbance in the system, the virtual inertia provides fast output power response, effectively increasing total inertia of the power system. However, this effect is only transient in nature [12].

On the other hand, operating a wind turbine with curtailment means that there is a droop function defining the adaption of active power infeed with reference to frequency deviations. In droop control a dead band may also be included; no frequency response is required from wind turbines when frequency lies within the normal operating limits. Notably, in order for the droop function to be active in under-frequency events, sufficient power reserve should be maintained in wind turbines. Otherwise, the droop characteristic will only be active in over-frequency events. The droop parameters of wind turbines should be adjusted in coordination with the droop parameters of conventional generators, to obtain the desired active power sharing during transient conditions and steady-state frequency error in IPSs. The droop characteristic, on the other hand, provides a permanent response and contributes to the coordinated primary frequency control in the system.

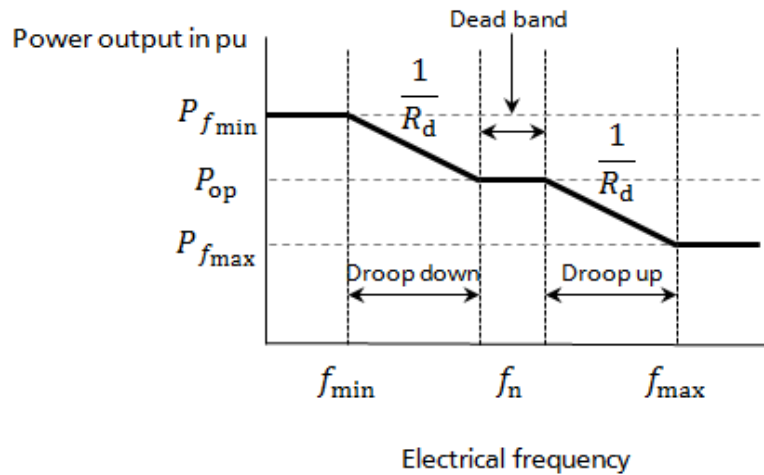


Figure 14: Droop control characteristic of wind turbines for primary frequency support [12]

In Figure 14 can be seen that within the dead band the wind turbines would not adapt their active power infeed, which would remain constant to P_{op} . In case that system frequency increases, then active power infeed could be proportionally adapted according to droop constant R_d and reach $P_{f_{max}}$ meaning the power corresponding to maximum frequency limit of droop control. This value of power output will be lower than the power corresponding to normal operation enabling frequency to restore permissible values within the dead band. Similarly, in case that system frequency decreases, then the wind turbines could feed proportionally more active power until reaching their maximum power output indicated as $P_{f_{min}}$ corresponding to minimum frequency of droop control.

Upgrade of diesel speed governor control and spinning reserves

There is need for fast automated control actions if the full potential of wind power plants is to be exploited [40]. It should be noted that it is possible to operate IPSs with a high level of wind penetration maintaining a high level of security. This is possible by providing adequate spinning reserve of conventional units. This is the result after simulating several fault cases (short circuits symmetrical and asymmetrical at different places). These studies have proven that an advanced control system will be helpful to determine spinning reserves and to manage system operation, especially during off-peak hours with very high wind power penetration, by suggesting: a) the most adequate DGs to be in operation or b) the disconnection of some WTGs. During off-peak hours, dynamic behaviour depends on the number and type of DGs in operation [41].

In order to protect IPSs against these disturbances and retain acceptable security levels, on-line dynamic security assessment functions are proven to be very valuable for their operation. According to literature, dynamic security assessment can be realised by two modules based on decision trees and neural networks, respectively. Decision trees are used to check security for operating schedules proposed by the

economic dispatch module, with respect to characteristic wind power fluctuations. Neural networks are used to give a real-time quantitative security evaluation of current operating state system, by emulating the expected frequency deviation to the predefine wind disturbance. In this way, wind power penetration can be increased without threatening system stability. In any case, response of IPSs to dynamic events depends critically on the amount of spinning reserve provided by conventional machines and the response of their speed governors [33].

Hence, assuring sufficient reserve capacity could be the technical solution for IPSs to withstand various disturbances. The determination of this reserve capacity was based on off-line stability analysis of credible contingencies under a variety of operating conditions. Carrying unnecessary reserve capacity however might significantly increase the cost of operation [42].

Load management control and storage systems

In case of wind diesel hybrid systems, a practice of control methods that uses energy storage devices and control methods for load management control is usually applied. Storage devices feed IPS with active power when it is needed and they are already charged. They constitute an additional support which otherwise could not be disposed in IPSs.

Load management and load shedding are used as methods of supporting system frequency. Loads are predefined into groups according to their priority. The low priority group consists of loads such as water or space heating. The high priority group loads are those to be served under any circumstances, such as lighting. When applying load shedding schemes, loads are switched in and out after they have been categorised as secondary. The low priority loads are switched in and out in a controllable manner by switching devices, thus effectively forming a governor from the load side. The decision of connecting or disconnecting a load is made according to pre-set values of frequency, specific for every controlled load or groups of loads [9].

3.4.1. Grid code requirements regarding frequency in isolated power systems

Characteristics of IPSs presented in 2.2, result in a different way of operation control. Due to these features, there are restrictions dealing with the main variables of a power system, like nominal frequency and voltage. The permissible frequency and voltage ranges for normal and under-fault operation are not as strict as in interconnected power systems, since these ranges cannot be met. The European standard EN 50160 on frequency and voltage defines that for an autonomous IPS, frequency must be within 49 - 51 Hz during 95 % of the week and within 42.5 and 57.5 Hz during 100 % of the week. The supply voltage under normal operating conditions (voltage interruptions excluded) must lie within ± 10 % of nominal voltage [43]. That is why in these power systems we can observe frequency excursions of more than 800 mHz without leading to system collapse, as it would be the case for the European interconnected

power system [44]. These rules can be modified from local network operators, but only so as to be *stricter* and not to permit higher ROCOFs or voltage. In this section only values related to frequency are presented, since focus lies on frequency stability.

All the analysed systems operate in a nominal frequency of $f_n = 50$ Hz. In Table 3 the lowest and highest permissible frequencies for several IPSs can be seen. For Iceland and Tasmania there are only the generator frequency requirements available.

Network Operator	Frequency in normal conditions in Hz	Frequency in abnormal conditions in Hz
Great Britain	49.5 - 50.5	47.0 - 52.0
Ireland	49.8 - 50.2	47.0 - 52.0
Madeira	49.5 - 50.5	
Malta	49.5 - 50.5 during 99.5% of a year	47.5 - 52.0 during 100 % of the time
Greece	49.0 - 51.0 during 95 % of a week	42.5 - 57.5 during 100 % of a week
Canary Islands	49.85- 50.15 for $t < 5$ min 49.75 - 50.25	
New Zealand	49.5 - 50.5	47.0 - 52.0
<i>Europe (ENTSO-E)</i>	<i>49.8 - 50.2</i>	<i>49.2 - 50.8</i>

Table 3: Frequencies in normal and abnormal conditions for isolated power systems and the European interconnected power system [14, 15, 16, 17, 19, 20, 21, 44]

With reference to the published grid code in 2013 of National Grid, the network operator in Great Britain, as well as from Eir Grid respectively for Ireland, a frequency between 49.5 to 50.5 Hz under normal conditions is permitted. For abnormal conditions these values can vary from 47.0 to 52.0 Hz. The largest ranges concerning frequency values for normal and abnormal conditions relate to requirements of *Hellenic electricity distribution network operator* (HEDNO). The range lies between 49.0 and 51.0 Hz in normal conditions and 42.5 to 57.5 Hz in abnormal conditions [20]. So, a difference between very small, small and large islands is visible. Some grids specify the time of the frequency range. This is the case of Canary Islands, Malta and Hellas [14, 19]. The grid code of Canary Islands allows in normal conditions that the system operates between 49.75 and 50.25 Hz for up to five minutes, for abnormal conditions no reference is made, and the same for island of Madeira [15]. The New Zealand grid code demands the same frequency range as the British [17].

The most important frequency requirement concerning the generating units conventional and renewable is that during frequency disturbances generating units must remain connected to the grid, as already mentioned above. The time they must remain connected to the grid is, among other, influenced by the time of the reaction of the unit to the deviation so that it can be assured that the generating unit will participate in the restoration of frequency. The most extreme condition for generating units are required for the island of Tasmania, which have to sustain frequency excursions between 47.0 Hz and 55.0 Hz for two minutes. In comparison, for normal conditions the generating unit only has to remain connected between 49.85 and 50.15 Hz. Here again a difference relating to requirements for small and large islands is to be noted. Great Britain and Ireland have the same requirements for abnormal conditions, i.e. 47.0 Hz for a maximum of 20 seconds and 52 Hz in Ireland for up to 60 minutes and 52 Hz in Great Britain for up to 90 minutes. The Irish generating units must then remain connected between frequencies of 49.5 and 50.5 Hz, whereas British generating units remain connected between 49.0 and 51.0 Hz.

As a result, taking as reference the values mentioned in Table 3 it can be stated that IPSs with frequency values for abnormal conditions within 47.0 and 52.0 Hz would remain stable. This restriction is necessary and could be met after comparing grid code requirements of several IPSs. Under this assumption the strictest requirement for IPS's frequency is fulfilled. As far as normal condition is concerned, values between 49.5 and 50.5 Hz have to be fulfilled. These assumptions are used for the introduced models in this thesis and serve the evaluation of frequency response for load steps. Hence, it can be ensured that conclusions could be applicable for all IPS with the same power generation mix.

3.5. Outlook and Discussion

In this chapter theoretical information about frequency stability in interconnected and IPSs has been presented. Furthermore, challenges of ensuring frequency stability have been mentioned and general operational principles as well as concrete control modes of speed governors in IPSs with integrated RES have been explained. At last, presentation of grid code requirements serve exploring and defining the permissible frequency values for further studies in the next chapters. Consequently, Chapter 4 deals with an introduction in control system theory and particular in diesel generator's speed governors, so as to enable the implementation and comparison of frequency control concepts realised from Chapter 5 in this thesis.

4. Introduction and modelling of speed governors for diesel generators in isolated power systems

In the former chapters we have presented operational principles of frequency stability for the interconnected power system as well for IPSs. In this section speed governing will be analysed in detail after providing the required theoretical background about control system theory. On focus are speed governors for synchronous DGs, since they are a common practice for power generation in IPSs.

4.1. Fundamental components and structure of a control system

A control system is an interconnection of components forming a system configuration that will provide a desired system response. The basis for analysis of a control system is the foundation provided by linear system theory, which assumes a cause-effect relationship for the components of a system. Therefore a component or the so called *process* to be controlled can be represented by a block as shown in Figure 15. The input-output relationship represents a cause-and-effect relationship of the process, which in turn represents a processing of the input signal to provide an output signal variable, often with a power amplification. An open-loop control system uses a controller and an actuator to obtain the desired response as it is a system without feedback. In contrast to an open-loop control system, a closed-loop control system utilises an additional measure of the actual output to compare the actual output with the desired output response. The measure of the output is called the *feedback signal*. A feedback control system tends to maintain a prescribed relationship of one system variable to another by comparing functions of these variables and using the differences as means of control. Figure 15 shows the typical structure of an open-loop and a closed-loop control system as well [45].

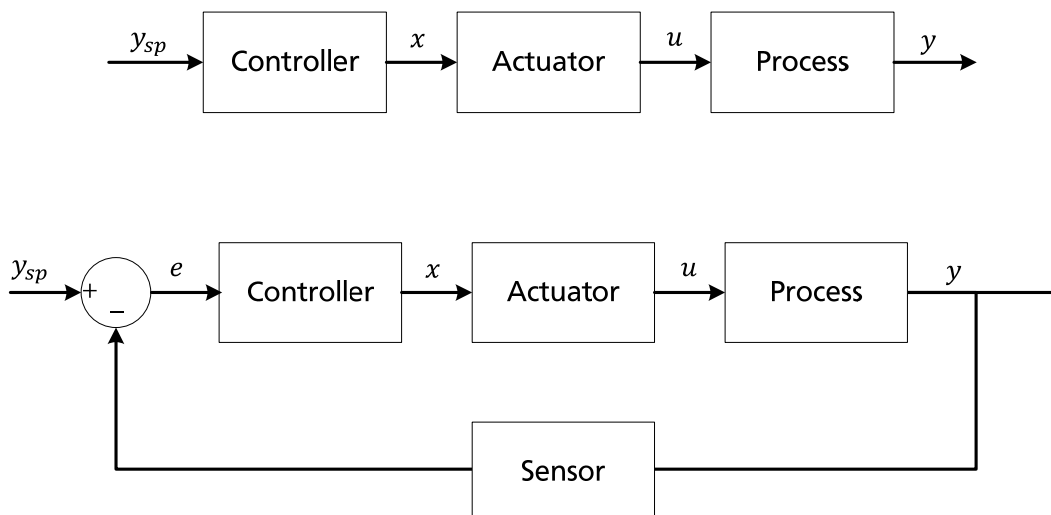


Figure 15: Open-loop (without feedback) and closed-loop control system with feedback [45]

It can be seen in Figure 15 that *Process* has one input, the manipulated or the so-called control variable u . The output is denoted by y . With y_{sp} the setpoint of the control system is denoted and x the output of the controller. In case of a closed-loop control system, there is an additional variable denoted by e and represents the control error, i.e. $e = y_{sp} - y$.

Introduction of PID controller: The most common solution for a control requirement

The most common technical solution to a control requirement is the three-term controller *PID*: proportional, integral and derivative, referring to the three elements of calculation. This form of control has been widely and successfully applied in the process industry over the last years. The three-term controller contains three essential components for an effective control system:

- A. *P* term: the proportional term offers a high proportional gain which gives a fast response to a developing error; The *P* term produces a multiple of current error. The greater the factor, the faster the control action and the more accurate the control. However, a *P* term alone cannot completely eliminate a control error, since an error is needed in order to generate the control action. The controller is a linear controller—so that it will behave in the same way whether the control demand is low or high. If the system under control is non-linear, as most of engine systems are severely non-linear, the parameters must be changed as the operating condition is changed. This technique of gain scheduling is widely applied in engine control.
- B. *I* term: the integral term ensures that there is no control error in the steady state since a proportional term alone can never finally correct a steady state error. The *I* term forms a sum of the control error over time. If there is a persistent control error, this term keeps accumulating the error producing a stronger corrective action. The *I* term can saturate if the control error persists for a long period.
- C. *D* term: the derivative term ensures that the control signal is modified if error changes so quickly that this term has a damping effect on control response. The *D* term differentiates the measurement and subtracts the result from the control output. This tends to damp the control response and acts as a stabilising influence on the control activity. The *D* term can amplify the effect of high frequency noise and must be accompanied by measures to filter (remove) noise from the measurement [46].

Integrator Windup

All actuators have limitations, for example a valve cannot be more than fully open or fully closed. For a control system with a wide range of operating conditions, it may happen that the control variable reaches the actuator limits. When this happens the feedback loop is broken and the system runs as an open loop because the actuator will remain at its limit independently of the process output. If a controller with integrating action is used, the error will continue to be integrated. This means, that the integral term may

become very large. The consequence is that any controller with integral action may give large transients when the actuator reaches his limits. One way to try to avoid integrator windup is to introduce limiters on the setpoint variation so that the controller output will never reach the actuator bounds. This often leads to conservative bounds and limitation on controller performance [46].

4.2. Diesel generator's speed governors

Diesel prime movers (also called the diesel speed governors) are attractive for applications requiring fast responding backups at the time of peak load demands or where local demand for additional power necessitates augmentation of power source [47].

Further analysing Figure 15 and explaining the relation of this general structure to a speed governor for a DG the following functionalities have to be mentioned.

1. The *sensor* obtains a measurement of a physical variable through a direct measurement or a combination of measurement and computation. A “soft sensor” delivers a value through an intermediate computation. Sensors can be specified to measure a range of physical quantities.
2. Electrical signals produced by sensors are relayed to the second major component of a control system, the *controller* (called control box in this thesis), so as to avoid the match with the supplementary controller and to refer directly to the term included in the speed governor structure that will be taken into consideration. The control box is often described as the brain of a control system where control actions are determined on the basis of calculations that will keep system performance at the required level. Additionally, it calculates a control action which will keep system performance at the required level. The majority of modern control systems are fitted with electronic control boxes built around microprocessors that are also programmable for added flexibility.
3. An *actuator* is set by the calculator to effect the required control action. The fuel injection equipment is the most fundamental actuator on the engine and is the mean of supplying energy to the cylinders [48]. The diesel engine represents the *process*.

4.3. Modelling of a diesel engine

The diesel engine model gives a description of the fuel consumption rate as a function of speed and mechanical power at the output of the engine. The diesel engine is usually modelled by a simple first order model relating the fuel consumption (fuel rack position) to the engine mechanical power represented by first order lags with time constant denoted usually as T_D . In this work the diesel engine has been modelled exactly in this way which mainly considers the inertia of the engine. This modelling option for diesel engines is a common simplification which can be found also in [34, 40, 49–52].

4.4. Modelling of diesel speed governors

In Chapter 3 information about diesel governors and their structure was presented. In this chapter two most commonly used speed governors are implemented after presenting their control loops in detail. The scope is tuning their parameters in order to optimise their dynamic response according to selected goals during their operation in isolated power systems.

4.4.1. Introduction of isochronous speed governor

The isochronous speed governor will be presented at the very beginning. With reference to Figure 2 we focus on “Speed Governor” and “Turbine” components.

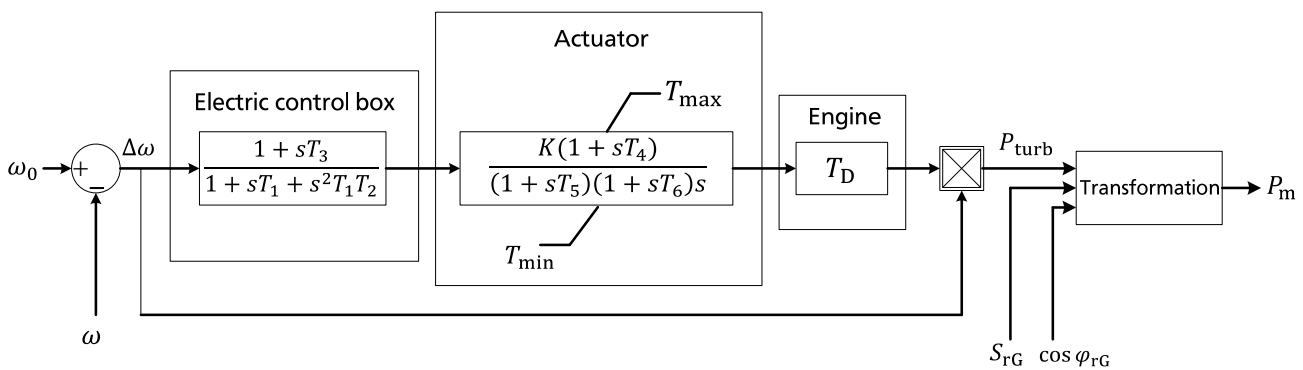


Figure 16: Block diagram of isochronous speed governor

The input signals are as expected the rotor speed corresponding to nominal frequency ω_0 as well the actual rotor speed ω . Rotor speed in per unit is used instead of frequency, since all variables in the closed control loop are expressed in per unit. The rotor speed deviation $\Delta\omega$ is inserted as input signal to the electric control box, which according to each transfer function represents a PT-element of second order. The analytical form of transfer function can be seen in Figure 16. The next component is the “Actuator”, where in this implementation of the speed governor the limitation is applied corresponding to torque limit values T_{min} and T_{max} respectively. The engine is modelled as a time delay implicated as T_D as explained in 4.3. that is the common practice.

The output signal after multiplication of the output signal from the diesel engine with the rotor speed ω is called P_{turb} . The signals P_{turb} and P_m are already in per unit and they represent the respective signals of turbine power and of mechanical power used as input for the generator. That’s the reason why the additional box named “Transformation” exists, since the rated power of the turbine is in most cases a little higher than this of the generator. In this box the following calculation is performed $P_m = \frac{P_{turb} * P_N}{S_{rG} * \cos \varphi_{rG}}$ where P_N is the prime mover rated power given in MW and can take values from zero up to P_G . The product $S_{rG} * \cos \varphi_{rG}$ represents the rated active power of the generator given in MW as well. In this way these basic values can be separated. The rated power of the machine S_{rG} as well as its power factor

$\cos \varphi_{rG}$ are required as input signals for this calculation box. The output signal of the speed governor will be the mechanical power P_m provided to the generator in order to be transformed to electrical power.

Modelling of isochronous speed governor

In the context of this section, the modelling process of isochronous speed governor in MATLAB Simulink is presented. The structure that has been implemented is the one presented in Figure 16.

In Figure 17 can be seen that the governor has four inputs (ω_0 , ω , S_{rG} and $\cos \varphi_{rG}$) and one output, P_m . The inputs ω_0 and ω as well as the output P_m are measured in per unit, whereas inputs S_{rG} and $\cos \varphi_{rG}$ are not given in per unit. The main reason of using a mask is to enable a better overview and to reduce the complexity of the models where the speed governor has to be integrated. Under the mask the block elements of the speed governor are to be seen in the following figure.

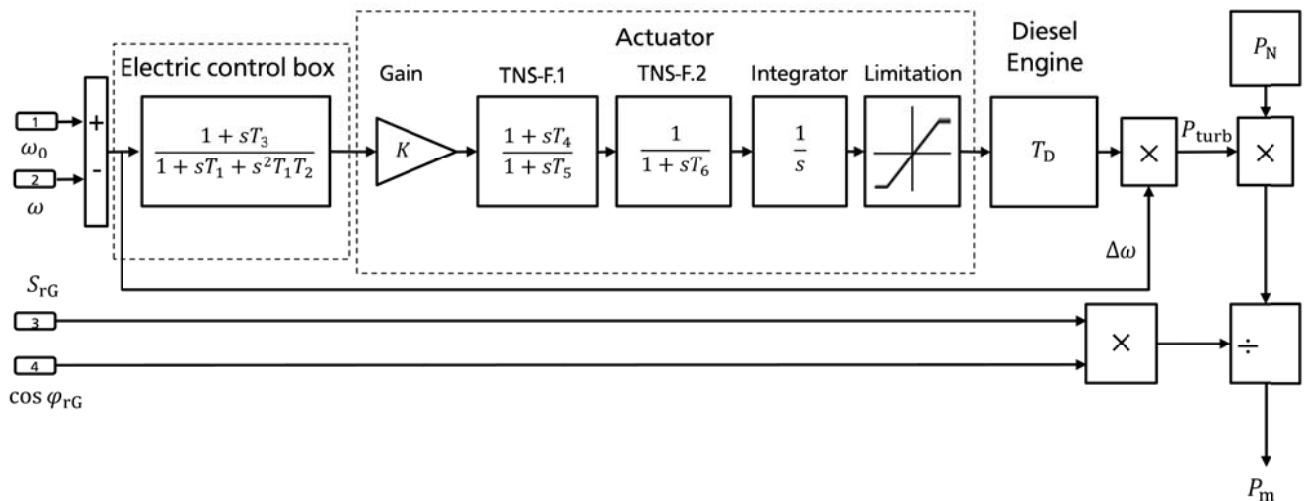


Figure 17: Block diagram of isochronous speed governor modelled in MATLAB Simulink

The main elements are the electric control box, the actuator and diesel engine. The input signals referred to the rotor speeds have been presented and analysed. The deviation in rotor speed, denoted as $\Delta\omega$ is implemented at the very beginning by subtracting the actual speed ω from the nominal speed ω_0 and the resulting signal is inserted and processed from the electric control box and consequently from the actuator.

Presenting in detail the transfer functions of the actuator, there is at first a signal processed from a proportional element with gain K before it is processed further from two transfer functions. These two transfer functions are denoted as TNS-F.1 and TNS-F.2 and have the analytical form presented in Figure 17. TNS-F.1 represents a PD-element (nominator) in combination with a time delay through the PT_1 -element (denominator). A PD-element consists of a P-element with a proportional gain and a

differentiating element. The transfer function TNS-F.1 has therefore amplifying differentiating properties, combined with a time delay through the PT_1 -element. The transfer function TNS-F.2 represents a normal PT_1 -element, concerning the actuator. As a last element of the actuator the signal is processed by an integrator and limitation is applied, which expresses at the same time the upper limit T_{\max} and the lower limit T_{\min} . The main task of the integrator is to regulate and minimise the control deviation, which allows the actuator to work precisely and without a remaining error. Since the actuator is a real mechanical element, it can only operate within certain limits. The task of the actuator within the governor is to open and close the valve for the fuel injection to the diesel engine. The limits of the actuator therefore correspond to the limits of the valve opening and closing.

The signal after the electric control box and the actuator represents the torque and gives this value to the diesel engine through the valve gate opening. The diesel engine in reality converts the fuel in mechanical torque and its output represents the torque. As a next step, the torque of the diesel engine is multiplied with the actual, measured speed of the connected synchronous generator, which results in the signal P_{turb} . This signal is afterwards multiplied with the constant P_N inside the multiplication block element. At the end the product between P_N in MW and the signal P_{turb} is divided through the product of power factor $\cos \varphi_{rG}$ and the rated apparent power S_{rG} in MVA, which results in the power P_m representing the power through the connected synchronous generator which has to be converted into electrical power.

4.4.2. Introduction of droop speed governor

The droop controller will be presented at the very beginning. With reference to Figure 2 we focus on “Speed Governor” and “Turbine” components. In Figure 18 it can be seen that a similar structure to isochronous speed governor is valid also for the droop speed governor. The input signals are as before the rotor speed corresponding to nominal frequency ω_0 as well as the actual rotor speed ω expressed in per unit. The rotor speed deviation $\Delta\omega$ is inserted as input signal to the electric control box after it has been added with the reference value of the active power P_{setp} expressed in per unit that has to be fed and the input P_G stands for the active power of the connected synchronous generator in per unit as well. The structure of the electric box and of the actuator is completely the same as for isochronous speed governor. The additional control loop of droop can be seen and can be activated using two possible ways: either with the throttle feedback (1) or with electric power feedback (2) as denoted in Figure 18. Responsible for this function is the “Droop Control” switch. Actually, the actual rotor speed ω causes this reaction. The block with the transfer function $\frac{1}{1+sT_E}$ serves to measure the power, since it is not measured directly but with a time delay caused from this PT_1 element. The output signal is a torque. Afterwards, the block named “Transformation” serves as for isochronous speed governor to generate the final signal for mechanical power P_m applied as input for the generator.

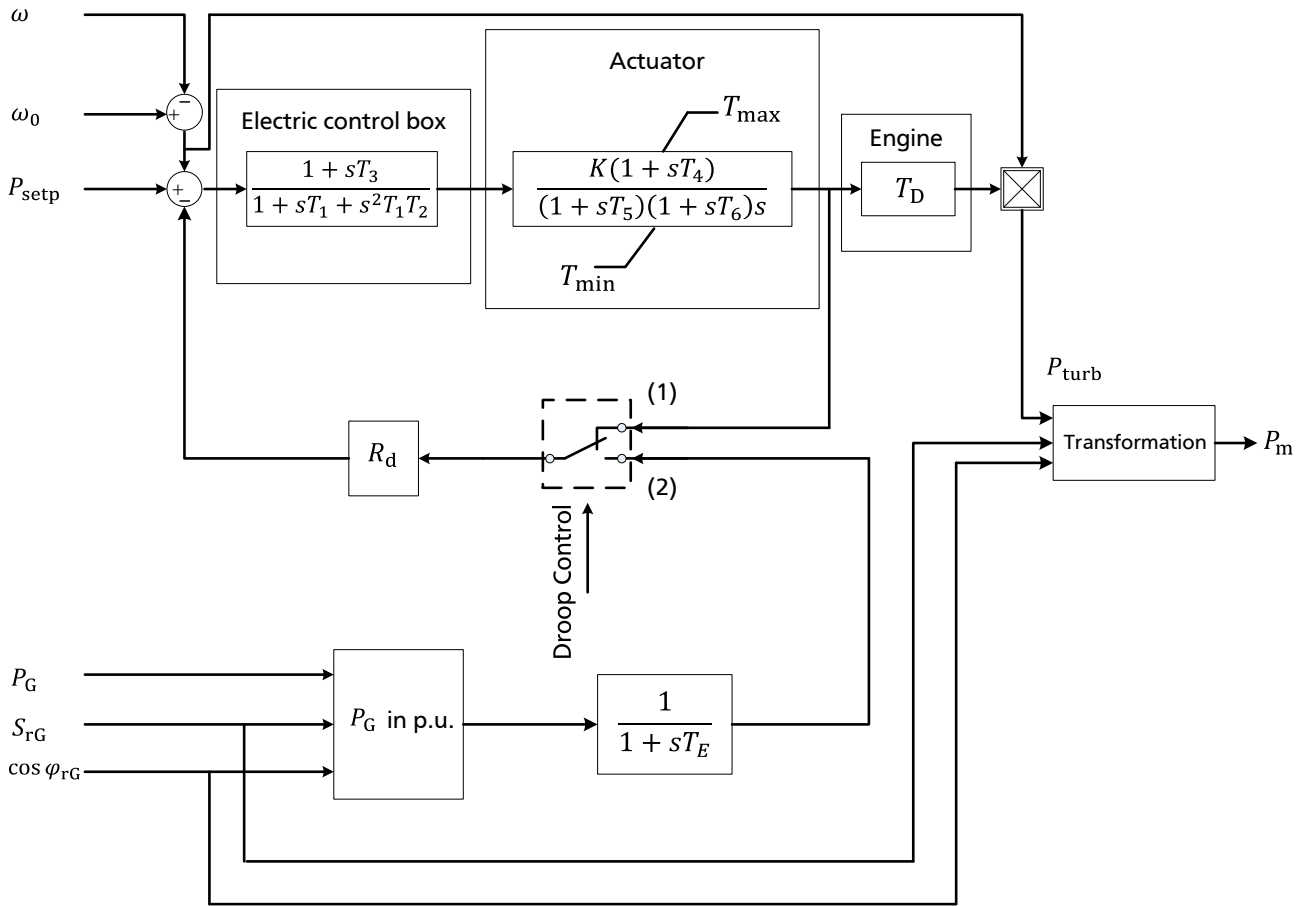


Figure 18: Block diagram of droop speed governor

It can be seen that there is a difference between Figure 2 and Figure 18 concerning the droop constant R_d , since in Figure 2 in the control loop the ratio $1/R_d$ is used, but in Figure 18 only the term R_d . This is due to the units. As already mentioned in Figure 2, R_d is expressed in Hz / p.u. and in this implementation R_d is given in per unit as all input signals.

Modelling of droop speed governor

After presenting the modelling process of isochronous speed governor in this upcoming section the modelling process of droop governor is presented as well. As seen in Figure 19 droop governor possesses five inputs. The input signal P_G has not been included, since the possibility of activating droop through throttle has been implemented. As output, mechanical power P_m is expected. The option for this implementation is based on the fact that only one from both options can be activated and therefore in this thesis only option (1) of Figure 18 is realised.

In Figure 19 feedback loop can be seen. Feedback is between output of the actuator and input of the summation element before the electric control box. Comparable to isochronous speed governor, the rotor speed deviation $\Delta\omega$ is produced between the reference speed and the measured speed. For that, actual

rotor speed ω (signal input 2) is subtracted from rotor speed corresponding to nominal frequency ω_0 (signal input 3). Through P_{setp} (signal input 3) the rated power is given, which is afterwards summarised with the rotor speed deviation $\Delta\omega$. From this sum, the signal of the feedback path is subtracted and fed into the electric control box. The signal path is from the electric control box, over the actuator, consisting of the gain K transfer elements with transfer functions “TNS-F.1” and “TNS-F.2” as well as an integrator, to the diesel engine with time delay T_d which are equal to the above described loop of the isochronous speed governor. Transfer functions are identical as well.

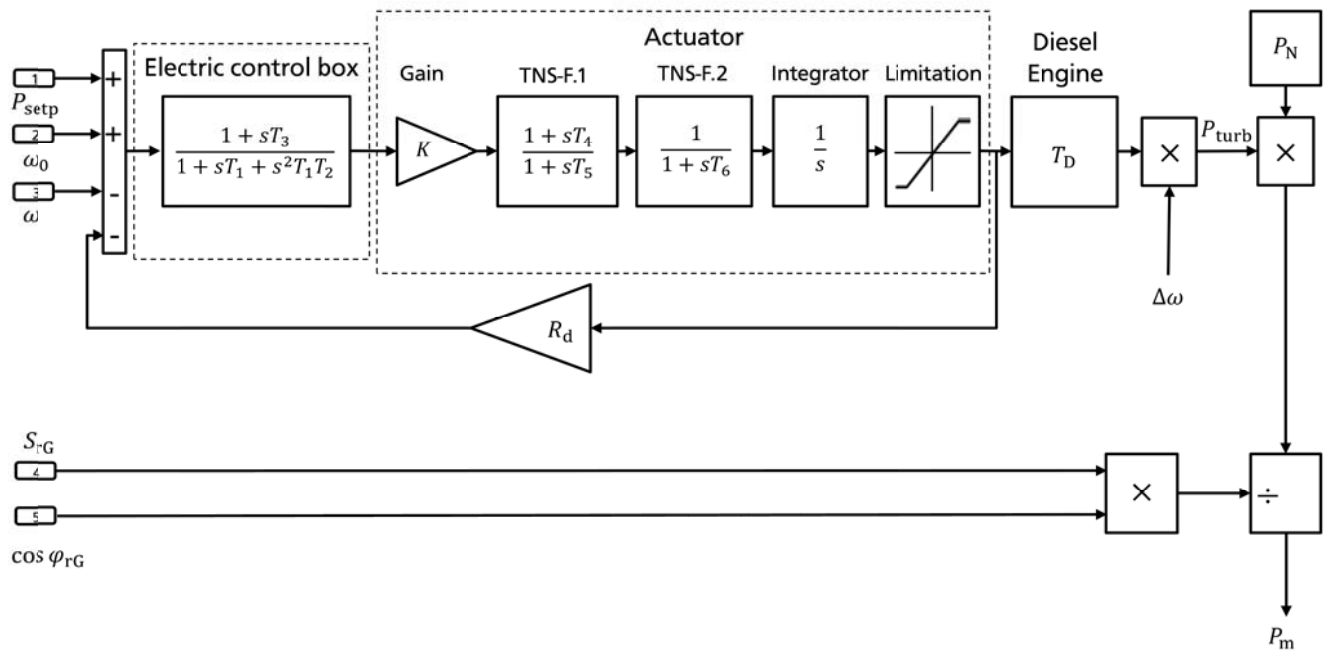


Figure 19: Block diagram of droop speed governor modelled in MATLAB Simulink

Feedback junction is located before the diesel engine’s block. This is the case here, since as mentioned before the direct feedback has been implemented and the option with the signal $T_{throttle}$ is used. The result will be a linear decrease in frequency when increasing load using a linear droop.

The block elements after the diesel engine are identical to the elements implemented for the isochronous speed governor. The mathematical description and connections are identical as well.

4.5. Validation of implemented speed governors

The developed speed governors will be validated in this subchapter before being integrated in a simple power system, to ensure their proper functionality. In order to realise the validation the analytical expression of the transfer functions of the electric control box and the actuator is presented.

Values of time constants and gains

As far as the values of the time constants of the transfer functions are concerned, they can be found in Table 4. The most important values are these one of T_{\min} and T_{\max} , since they limit the integrator and prevent the control system from windup. Default values concerning time constants and gains are used only for the validation in this section and can be found in simulation examples in the bibliography [27, 46].

Time constants in s		Gains in p.u.	
T_1	0.2	T_{\min} (Actuator minimum output torque)	0
T_2	0.1	T_{\max} (Actuator maximum output torque)	1.1
T_3	0.5	K (Actuator gain)	15
T_4	1		
T_5	0.1		
T_6	0.2		
T_D	0.01		

Table 4: Default time constants and gains for isochronous speed governor

A further approach concerning the appropriate values for time constants and gains will be presented and in detail in Chapter 5, where the goal is to define which of these variables plays a major role for the dynamic behavior of the control system and if the default values can be used without consideration or if they have to be modified dependent on the whole system.

4.5.1. Speed governor's validation

The validation of both speed governors takes place after their connection to a synchronous generator and a load. At this way the "Generator-Load Model" block presented in all control loops of chapter 3 is replaced. The generator's rated power S_{rG} is thought to be 2 MVA and $\cos \varphi_{rG}$ is equal to 0.8. A load of 1 MW active power and 0.45 Mvar reactive power is connected. The validation is realised for isochronous and droop governor. The dynamic event considered is a load step of 0.3 MW. This load step is applied at $t = 2$ seconds and remains connected.

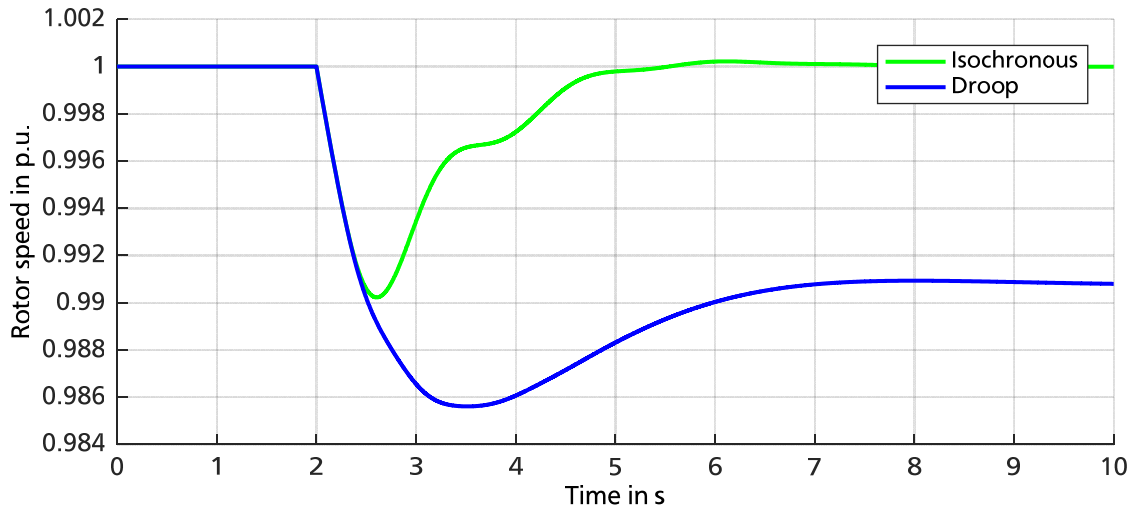


Figure 20: Rotor speed ω of isochronous as well as for droop speed governor for a load step of 0.3 MW

In Figure 20 can be seen that rotor speed ω remains stable for the first two seconds of the simulation and after the load step is applied both curves have the same gradient, which corresponds to synchronous generator's inertia that is the same for both cases. Within the next two and half seconds from $t = 2.5$ seconds until $t = 5$ seconds, speed governors react until rotor speed reaches a constant value again corresponding to the new loading condition. As it was expected the isochronous speed governor reaches the nominal value of 1 per unit again. The rotor speed deviation for droop speed governor can be validated to be the correct one according to 3.3, so it is in per unit $\frac{\Delta\omega}{\Delta P} \times 100 = \frac{0.991-1}{0.82-0.64} \times 100 = 5\%$ droop, as the used default value. The values of rotor speed and mechanical power are in per unit and have been taken from Figure 20 and Figure 21.

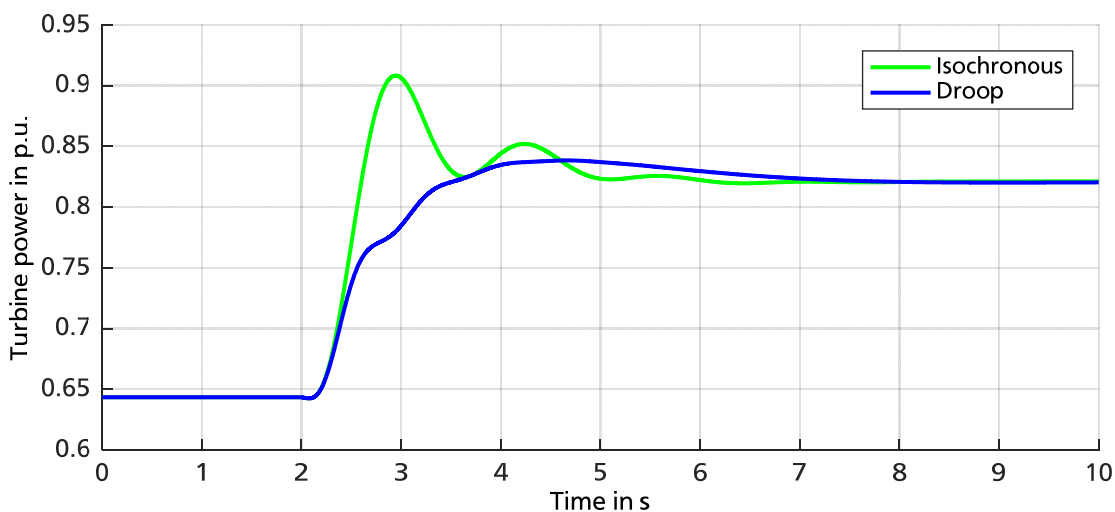


Figure 21: Turbine power P_{turb} output of isochronous as well as for droop speed governor for a load step of 0.3 MW

Similarly in Figure 21 the turbine power output in per unit can be seen. Both governors have the same initial value and the same final value, as it has been expected. Power demand at the beginning of the simulation and after the load step is the same, so that the turbine power of the speed governors and therefore the mechanical power to be the same. In the time between $t = 2$ seconds until $t = 7$ seconds speed governors are trying to adapt their turbine power output. Isochronous reacts not as smooth as droop because of the integrator and the proportional component of droop enables this response.

4.6. Control systems tuning

Considering again the components of a control system presented in 4.1 we now focus on its core element, the control box. Control box has several parameters that can be adjusted. The control loop would react properly if these parameters are selected accordingly and would perform poorly in any other case. The procedure of defining proper values for these parameters is called *tuning*. When solving a control problem it is necessary to understand what the primary goal of this control is. The two most common types of problems are whether to follow the set-point or to reject disturbances. As far as the restrictions are concerned, it has to be mentioned that the diesel speed governors are non-linear and a typical specification of this control system deals with set-point following [46].

Specifications on set-point following may include requirements on rise time, settling time, decay ratio, overshoot and steady-state offset for step changes in the set-point. In Figure 22 these quantities can be seen and are defined consequently [46].

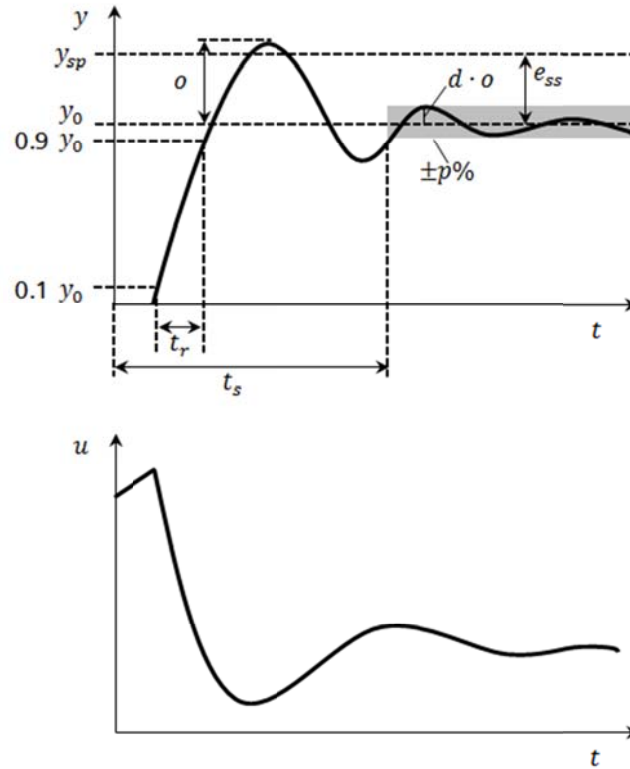


Figure 22: Specifications on set-point following based on time response to a unit step in the set-point [46]

The variables mentioned in Figure 22 are described below:

- The rise time t_r is either defined as the inverse of the largest slope of the step response or the time it takes the step to pass from 10 % to 90 % of its steady state value.
- The settling time t_s is the time it takes before the step response remains within p % of its steady state value.
- The decay ratio d is the ratio between two consecutive maxima of the error for a step change in setpoint or load.
- The overshoot o is the difference between the first peak and the steady state value of the step response.
- The steady-state error e_{ss} is the value of control error e in steady state. With integral action in the controller, the steady state error is always zero.

4.6.1. Tuning methods

There is a wide variety of tuning methods and techniques and a large number of tuning criteria. Most of them are considered for design purposes so as to provide the appropriate values for the parameters of a new implemented controller. Detailed analysis of tuning methods as well as innovative tuning techniques can be found in the literature in [45, 46]. These techniques are, from a classical point of view, the Ziegler-Nichols and related methods as well as the analytical methods, up to the modern methods with fuzzy logic

and particle swarm optimisations and generic algorithms [53–58]. Common used criteria for tuning are time-weighted absolute error (ITAE) [59]. However, in case of already known control system structures automatic tuning is a common practice. This method is described in brief in 4.6.3., where tuning process for droop and isochronous is described.

4.6.2. Tuning methods for diesel generator's speed governors in isolated power systems with integrated renewable energy sources

Tuning plays a major role in LFC since the operating point of a power system changes continuously and thus controller's response in a system may not be optimal. As a matter of fact, to keep dynamic response near the optimal value, it is desirable to track the operating point of the system and accordingly update its parameter to achieve a better control scheme [60].

A literature overview regarding LFC techniques for diesel speed governors operating in IPSs with RES is presented, since there are several concepts that have been proposed. Bhatt et al. suggested a PI load frequency controller to be installed on the DG to generate command signals to raise or lower the speed-gear ratio in response to the error in frequency [61]. Simulation results showed that this recommendation would succeed for optimum transient response to that of the DG. Kamwa studied the dynamic modelling and control of wind diesel hybrid systems by having a programmable smoothing-load controlled by a standard PID controller installed on the DG [62]. In [38] the problem was approached in two levels: a high level dealing with the total energy of wind turbines, DGs and storage and dump load and a low level containing three independent controllers which determine, respectively, each wind turbine state and power dispatch. Uhlen implemented and compared two robust controllers on a Norwegian wind-diesel prototype system. Optimum values of gain settings of the PI controller were given by using the integral squared error (ISE) technique [35]. A study of dynamics of a small autonomous wind-diesel system using simplified models and classic control theory techniques is presented in [51]. For better dynamic performances of wind-diesel system under wind and load disturbance conditions, two control schemes are used. In the first case, a PI controller and in the second case a PID controller are used. Gain parameters of PI and PID controllers have been optimised by using genetic algorithm and particle swarm optimisation considering eigenvalue based objective function and quadratic objective function [63]. Improvement of frequency stability in mini-grids with a high wind power penetration have been realised using an online generic algorithm for tuning [64]. Furthermore, an additional paper with the same problematic of LFC for isolated microgrids considers several speed governors [65].

4.6.3. Tuning of isochronous and droop speed governors

At the very beginning of this subsection a brief description of automating tuning is given.

Automatic tuning

By automatic tuning is meant a method where the controller is tuned automatically or by demand from a user. An automatic tuning procedure consists of three steps:

1. Generation of a process disturbance
2. Evaluation of the process disturbance
3. Calculation of controller parameters

The process must be disturbed in some way in order to determine the process dynamics. This can be done in many ways, e.g. by adding steps, pulses or sinusoids to the process input. The evaluation of the disturbance response may include a simple characterisation of the response.

There are several approaches for automatic tuning such as adaptive techniques, which refer to adaptive control or gain scheduling. Other options are model-based methods such as transient response methods including open-loop and closed-loop tuning, frequency response methods or rule-based methods [46].

The selected and applied tuning process is composed of several steps that have to be realised in order to set-up a tuning session. Figure 23 provides an overview of these steps. In case of non-linear models, as it is the case for the diesel speed governors and synchronous generators, a linearization has to take place before tuning. Since linearization is referred to a specific operation point, tuning will take place after speed governors have been connected to a power system with synchronous generators and loads. Hence, the process is divided in two main categories, the first one of linearization and the second one of tuning.

Linearization refers to two subtasks:

1. Selection of a linearization point and
2. Application of a linearization algorithm

Similarly, tuning is realised in four subtasks:

- Selection of elements to be tuned
- Definition of tuning goals
- Running (execution) of tuning algorithm
- Interpretation of tuning results

Consequently these steps are analysed and applied to isochronous and droop speed governor.

Selection of linearization point

The selection of linearization point depends on controller initialising conditions. The time delay caused from the diesel engine leads to unstable behaviour for the first 0.01 seconds. Due to this fact, the initial

conditions are not appropriate for the linearization. Therefore, a time point after the appropriate initialisation is preferred. In that case, the model for the time point selected is linearized using the values of the variables for this time point. In our case, this time point is always after $t = 1$ seconds.

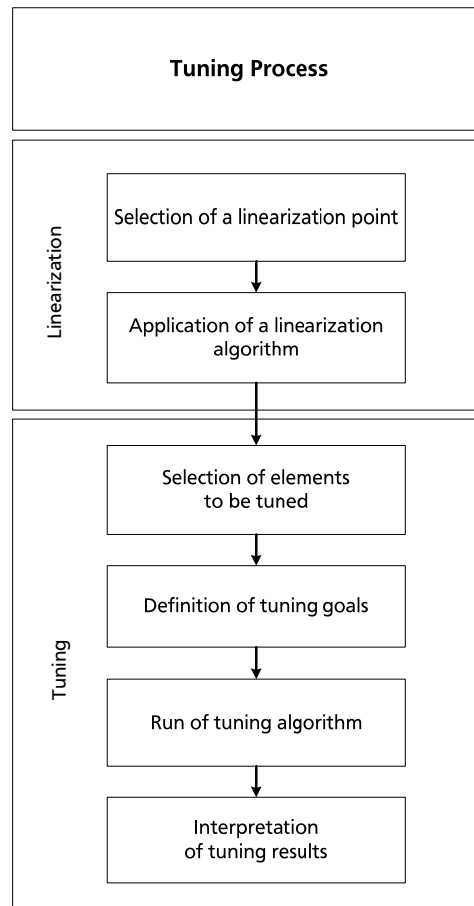


Figure 23: Applied tuning process

Application of linearization algorithm

The method of analysis employed in this work is based on frequency domain techniques, using linearized models of the system components. Therefore, in a strict mathematical sense, the results obtained are quantitatively accurate only in the vicinity of the specific initial operating point, around which the model equations have been linearized. However, the conclusions drawn regarding the modes of the system and their dependence on the various factors (controller parameters, generator types etc.) are qualitatively correct and valid for any normal operating condition. The same applies regarding the influence of the particular values used in the parameters of the system.

For the model linearization a block-by-block approach is used, instead of using full-model perturbation. This block-by-block approach individually linearizes each block in the model and combines the results to produce the linearization of the specified system.

The block-by-block linearization approach has several advantages to full-model numerical perturbation:

- Most blocks have pre-programmed linearization that provides an exact linearization of each block at the operating point.
- Blocks can be configured to use custom linearization without affecting model simulation.
- Non-minimal states are automatically removed.

In case of blocks that do not have pre-programmed linearization, they are automatically linearized by using numerical perturbation. Block linearization is computed by numerically perturbing the states and inputs of the block about the operating point of the block.

The block perturbation algorithm introduces a perturbation to the nonlinear block and measures the response to this perturbation. The default difference between the perturbed value and the operating point value is $10^{-5}(1 + |x|)$, where x is the operating point value. This perturbation and the resulting response are used to compute the linear state-space of this block.

In general, a continuous-time nonlinear block in state-space form is given by:

$$\dot{x}(t) = f(x(t), u(t), t) \quad 4.1$$

$$y(t) = g(x(t), u(t), t) \quad 4.2$$

In these equations, $x(t)$ represents the states of the block, $u(t)$ represents the inputs of the block and $y(t)$ represents the outputs of the block. A linearized model of this system is valid in a small region around the operating point $t = t_0, x(t_0) = x_0, u(t_0) = u_0$ and $y(t_0) = g(x_0, u_0, t_0) = y_0$.

To describe the linearized block, we define a new set of variables of the states, inputs and outputs centered about the operating point

$$\delta x(t) = x(t) - x_0 \quad 4.3$$

$$\delta u(t) = u(t) - u_0 \quad 4.4$$

$$\delta y(t) = y(t) - y_0 \quad 4.5$$

The linearized state-space equations in terms of these new variables are

$$\delta \dot{x}(t) = A\delta x(t) + B\delta u(t) \quad 4.6$$

$$\delta y(t) = C\delta x(t) + D\delta u(t) \quad 4.7$$

A linear time-invariant approximation to the nonlinear system is valid in a region around the operating point.

The state-space matrices A , B , C , and D of this linearized model represent the Jacobians of the block. To compute the state-space matrices during linearization, the following operations are realised.

- Perturbation of the states and inputs, one at a time, and measurement of system's response to this perturbation by computing $\delta \dot{x}(t)$ and $\delta y(t)$.
- Computation of the state-space matrices using the perturbation and the response.

$$A(i) = \frac{\dot{x}|_{x_{p,i}} - \dot{x}_o}{(x_{p,i} - x_o)} \quad 4.8$$

$$B(i) = \frac{\dot{x}|_{u_{p,i}} - \dot{x}_o}{(u_{p,i} - u_o)} \quad 4.9$$

$$C(i) = \frac{y|_{x_{p,i}} - y_o}{(x_{p,i} - x_o)} \quad 4.10$$

$$D(i) = \frac{y|_{u_{p,i}} - y_o}{(u_{p,i} - u_o)} \quad 4.11$$

where $x_{p,i}$ is the state vector whose i th component is perturbed from the operating point value

x_o is the state vector at the operating point

$u_{p,i}$ is the input vector whose i th component is perturbed from the operating point value

u_o is the input vector at the operating point

$\dot{x}|_{x_{p,i}}$ is the value of \dot{x} at $x_{p,i}$, u_o .

$\dot{x}|_{u_{p,i}}$ is the value of \dot{x} at $u_{p,i}$, x_o

\dot{x}_o is the value of \dot{x} at the operating point

$y|_{x_{p,i}}$ is the value of y at $x_{p,i}$, u_o

$y|_{u_{p,i}}$ is the value of y at $u_{p,i}$, x_o

y_o is the value of y at the operating point

In this way, nonlinear models can be linearized in a selected linearization point and consequently can be tuned with the following steps.

Selection of elements that have to be tuned

Moreover the elements that are tuned have to be selected. In Figure 17 and Figure 19 the implemented structure of both speed governors is presented. The elements that can be physically tuned after the construction of a speed governor are the electric control box and the droop constant in case of a droop

function. Therefore, the variables that will be tuned are time constants T_1, T_2, T_3 of electric control box for isochronous and droop speed governors: Additionally droop constant R_d of droop speed governor is tuned.

Definition of tuning goals

There is a variety of tuning goals that can be selected in order to tune the selected elements referred above. Some of them are in frequency domain and other in time domain. Tuning goal used in this thesis is the Step Rejection Goal which specifies how a step disturbance injected at a specified location in the control system affects the signal at a specified output location and tries to keep the gain from disturbance to output below the defined permissible gain.

The disturbance signal is a step signal applied in the reference rotor speed ω_0 and as output we consider rotor speed ω of the speed governors. The simultaneous consideration and tuning of isochronous and droop in an IPS is required since for almost all the cases these speed governors operate cooperatively in an IPS and they should not react competitively to each other for restoring frequency to the nominal value. The custom target time-domain response according to which the selected elements have to be tuned are the following and is presented graphically in Figure 24.

- Time constants have to remain positive values
- Droop constant R_d of droop has to be positive and smaller than 10, since then it would not be any physically applicable value and
- Permissible of overshoot o of 0.1 p.u.
- A permissible settling time t_s of one second
- The steady-state error e_{ss} has to be zero.

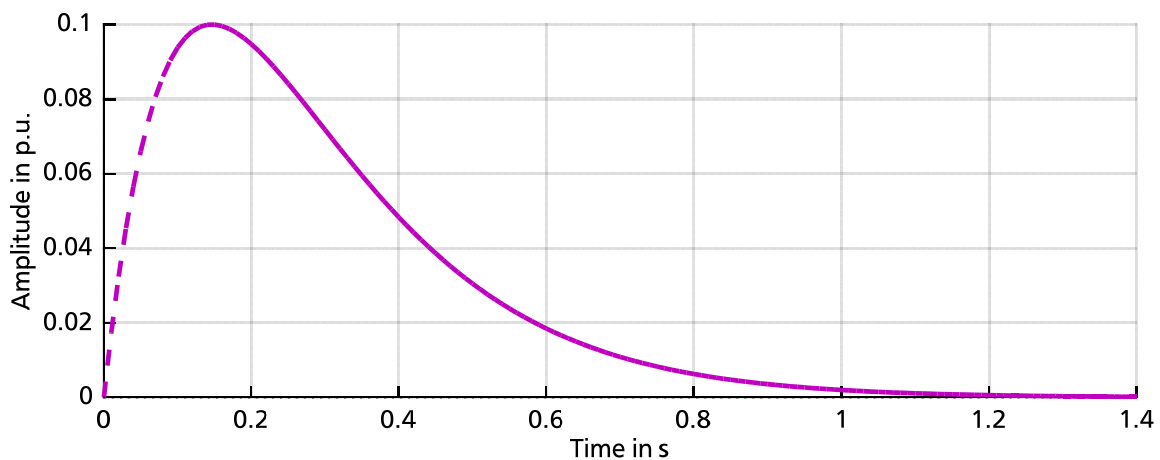


Figure 24: Custom target time-domain response to a disturbance used for tuning

A permissible overshoot of 0.1 per unit corresponds to a permissible rotor speed deviation of 0.1 p.u. which physically corresponds to 5 Hz. Therefore, the frequency limits for abnormal conditions are 45 - 55 Hz. These frequency margins are common for IPSs, as presented in Table 3, and the speed governors have to react effectively for such frequency events.

In Figure 24 the worst case response is presented. It can be seen that the worst case that is set as a margin for the amplitude of overshoot between the disturbance signal which is the step function and the output signal which is the actual rotor speed cannot overexcite the value of 0.1 p.u., after 0.6 seconds from the time point when the disturbance is applied this amplitude have to lie under 0.02 p.u. After one second the steady-state error is zero. Transforming these limits from per unit in frequency values as before, means that in case of a disturbance the speed governors have to be tuned in such a way that the frequency remains always between 45 to 55 Hz and after 0.6 seconds from the time point that the disturbance has been applied frequency has to remain between 49 and 51 Hz, which are the frequency limits during normal operation for many IPS's operators. As a result, when the speed governors are tuned with regard to these criteria, then frequency stability can be assured and a system collapse can be prevented for IPSs.

Once the tuning goal has been defined, tuning algorithm is executed, so as to reach the custom target system response.

Execution of tuning algorithm

Applied tuning belongs to the category of automatic tuning and is especially one of the Model-Based tuning methods and it is called closed-loop tuning, as already mentioned in 4.6.1. According to this method, the steps or pulses are then added either to the set point or to the control signal. In these cases it is necessary to detect that the perturbations are sufficiently large compared to the noise level [46].

In our case, the algorithm running for implementing the specified tuning goal of step rejection connects the goal into a normalized scalar value $f(x)$. Here, x is the vector of tunable parameters of the control system. The algorithm then adjusts the parameter values to minimise $f(x)$. In our case the aim is to keep the amplitude of gain below the gain of the reference model presented in Figure 24. The scalar value of the requirement $f(x)$ is given by

$$f(x) = \frac{T(s,x)}{T_{ref}(s)} \quad 4.12$$

where $T(s, x)$ is the closed-loop transfer function from the input to the output and $T_{ref}(s)$ is the reference model used to custom the target time domain response for tuning.

Interpretation of tuning results

Once tuning has been realised, results concerning the selected values for tuning are available. A physical interpretation or further simulations could be necessary for clarifying the modified values of time constants or the droop value.

4.7. Outlook and discussion

In this chapter fundamental information regarding control systems has been provided. The basic components and their function have been analysed as well as an introduction of PID controllers is given. The two commonly used speed governors for diesel engines (isochronous and droop) have been also presented. Control loops are explained and the implemented models are described. Furthermore, default for time and gain parameters are provided, as well as a validation of the implemented speed governors as part of a simple model has been realised. Moreover, information about control system tuning is provided and the tuning method used in this thesis as well as the tuning process is explained.

In the next chapter combinations of the two speed governors are introduced and tuned for a model with two synchronous generators. It is worth mentioning that speed governors in this thesis are tuned after their integration in an IPS aiming to present their response as part of a power system and their interaction. Tuning sessions should provide a tendency concerning the values of time constants and gains that ensure frequency stability.

5. Introduction of “DIGLO IPS” for tuning and comparing frequency control concepts

In this chapter, after having explored and developed the isochronous and droop speed and after explaining the tuning process and tuning goal, a complete model will be presented. This model is thought to represent a typical IPS’s topology.

5.1. Model “2 DIGLO IPS”

From now on, the model composed from Diesel Generators and Loads, denoted as DIGLO, its attributes and components will be described in detail. In Figure 25 an overview of “2 DIGLO IPS” model can be seen. It composed from an APS of two SGs, denoted as SG1 and SG2, the already mentioned speed governors (isochronous and droop) and two *automatic voltage regulators* (AVRs) of type ST1A. Additionally, a transformer is connected at the terminal of each generator. The transformers are denoted as TR1 and TR2 respectively. Two loads are connected, representing the power demand. The first one, denoted as L1, is the largest one corresponding approximately to the 70 % of the whole power demand connected at the end of a 10 km transmission line and a second one, denoted as L2, is connected directly at the point of power generation near the APS and represents 70 % of the whole power demand.

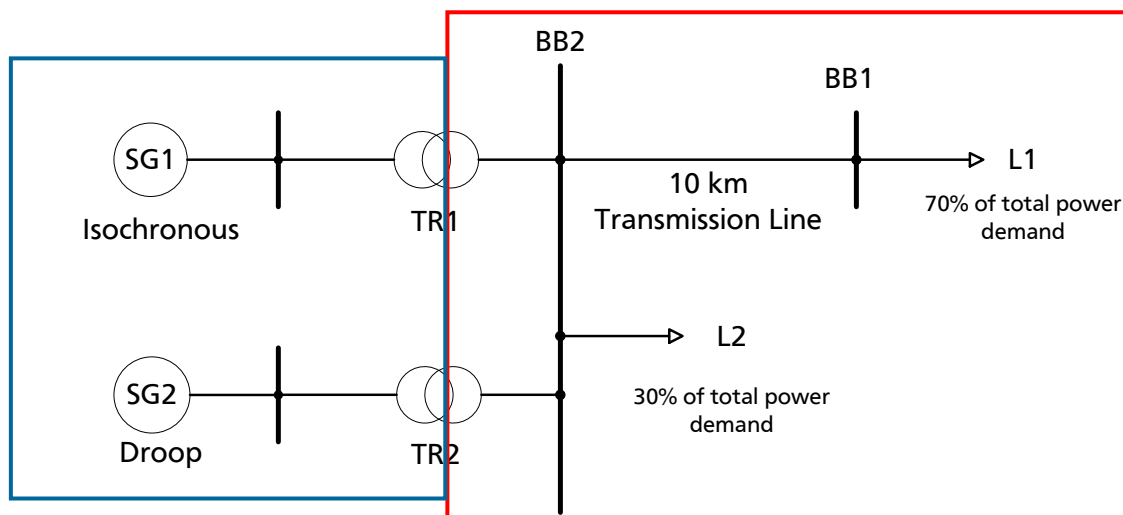


Figure 25: Overview of “2 DIGLO IPS” model

5.1.1. Voltage Levels

The voltage in “DIGLO IPS” is divided into two levels. The nominal voltage of SGs, their governors and the excitation systems is 400 V. Nominal voltage of the transmission line and of load L1 is 20 kV. The general concept is to demonstrate a typical IPS topology consisting of a small APS (400 V zone in the blue box in Figure 26) feeding a load connected directly to this substation (L2) and the rest of loads (L1) placed far away from it. Power transmission takes place with the transmission line for a relatively short distance of 10 km, which is realistic in IPSs (20 kV zone in the red box in Figure 26).

5.1.2. Transformers

The model “2 DIGLO IPS” includes two three-phase transformers with two windings. These step-up transformers, one for each generator with a rated power of 2.5 MVA enable voltage transformation from the low voltage of 400 V to the medium voltage of 20 kV.

5.1.3. Transmission Line

The transmission line connecting the small APS with the large load has a length of 10 km and a positive sequence resistance $R_1=0.1153 \Omega/\text{km}$, zero sequence resistance $R_0=0.413 \Omega/\text{km}$, positive sequence inductance $L_1=0.00105 \text{ H}/\text{km}$, zero sequence inductance $L_0=0.00302 \text{ H}/\text{km}$, positive sequence capacitance $C_1=11.33 \cdot 10^{-9} \text{ F}/\text{km}$ and zero sequence capacitance $C_0=5.01 \cdot 10^{-9} \text{ F}/\text{km}$.

5.1.4. Synchronous Generators

In “2 DIGLO IPS” model presented in Figure 28, two synchronous generators, denoted also as SG have been used. SG1 has a rated power of $S_{rG SG1} = 2 \text{ MVA}$ and SG2 has a rated power of $S_{rG SG2} = 1.32 \text{ MVA}$. The selection of these SGs is based on their rated power to enable a realistic modelling of an IPS as well as the comparison between the “2 DIGLO IPS” model with the extended versions introduced in the next chapters. As is usually the case, IPSs consist of sets of DGs of different rated power. The inertia time constant related to rated apparent power S_{rG} is three seconds for both of them. The parameters can be seen in the following tables for each machine.

Synchronous Generator SG1	
Rated apparent power $S_{rG SG1}$ (MVA)	2
Nominal Voltage (kV)	0.4
Inertia constant related to $S_{rG SG1}$ (s)	3

Stator resistance $R_{s\ SG1}$ (p.u.)	0.0095	
Leakage reactance x_l (p.u.)	0.05	
Synchronous reactance (p.u.)	$x_d = 2.11$	$x_q = 1.56$
Transient time constants (s)	$T_{d'} = 0.33$	$T_{q'} = 0.5$
Transient reactance (p.u.)	$x_{d'} = 0.17$	$x_{q'} = 0.3$
Subtransient time constants (s)	$T_{d''} = 0.03$	$T_{q''} = 0.03$
Subtransient reactances (p.u.)	$x_{d''} = 0.13$	$x_{q''} = 0.23$

Table 5: Parameters of SG1 of "2 DIGLO IPS" model

Synchronous Generator SG2

Rated apparent power $S_{rG\ SG2}$ (MVA)	1.32	
Nominal Voltage (kV)	0.4	
Inertia constant related to $S_{rG\ SG2}$ (s)	3	
Stator resistance $R_{s\ SG2}$ (p.u.)	0.0132	
Leakage reactance x_l (p.u.)	0.04	
Synchronous reactance (p.u.)	$x_d = 2.78$	$x_q = 2.05$
Transient time constants (s)	$T_{d'} = 0.29$	$T_{q'} = 0.5$
Transient reactance (p.u.)	$x_{d'} = 0.24$	$x_{q'} = 0.3$
Subtransient time constants (s)	$T_{d''} = 0.03$	$T_{q''} = 0.03$
Subtransient reactances (p.u.)	$x_{d''} = 0.17$	$x_{q''} = 0.21$

Table 6: Parameters of SG2 of "2 DIGLO IPS" model

The values listed in Table 5 and in Table 6 are the ones used to develop the models of these synchronous generators and correspond to a sixth order model.

5.1.5. Automatic voltage regulators

Voltage regulation of a synchronous generator is responsible for regulating terminal voltage according to the predefined value. This regulation is as important as speed regulation, since it ensures the power supply without disturbances. Goal of voltage regulation is to keep the difference between terminal voltage actual value and terminal voltage set point within the acceptable defined limits. Usually the regulation includes a component realising the dependency of set point from reactive current that enables reactive power distribution within parallel connected synchronous generators.

With regard to an accurate adjustment the integral component of the voltage regulator is the one who enables a very fast response of the control loop. At this way it is ensured that short-term load changes and the resulting reactive power and voltage oscillations up to 0.4 Hz can be regulated [66].

When the behaviour of SGs is to be simulated accurately in power system stability studies, it is essential that the excitation systems are modelled in sufficient detail. AVRs are a part of the excitation system. Figure 26 presents a general functional block diagram of an excitation system for a SG as provided in [67].

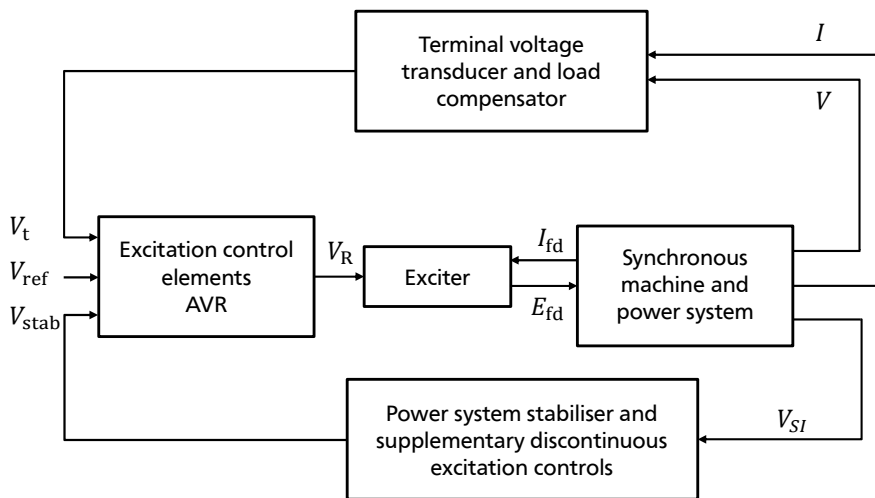


Figure 26: General functional block diagram for synchronous machine excitation control system

Several types of compensation are available on most excitation systems. Active and reactive current compensation of synchronous generators are the most common. Either reactive droop compensation and/or line-drop compensation may be used, simulating an impedance drop and effectively regulating at some other node than the terminals of the machine.

Droop compensation takes its name from the drooping (declining) voltage profile with increasing reactive power output on the unit. Line-drop compensation, also referred to as transformer-drop compensation, refers to the act of regulating voltage at a point partway within a generator’s step-up transformer or, less frequently, somewhere along the transmission system. This form of compensation produces a rising

voltage profile at the generator terminals for increases in reactive output power. When load compensation is not employed, then this block diagram reduces to a simple sensing circuit. The terminal voltage V of a synchronous generator is sensed and is usually reduced to a dc quantity after is compared with a reference that represents the desired terminal voltage setting, as shown on each of the excitation system models. The equivalent voltage regulator reference signal V_{ref} is calculated to satisfy initial operating conditions. It will, therefore, take on a value corresponding to assumed generator's load condition. The resulting error is amplified as described in the appropriate excitation system model to provide field voltage and subsequent terminal voltage to satisfy steady-state loop equations. Without load compensation, the excitation system, within its regulation characteristics, attempts to maintain a terminal voltage determined by the reference signal [67].

The IEEE type ST1A excitation system represents AVRs that provide the field voltage E_{fd} input to the synchronous generator. The maximum exciter voltage available from such systems is directly related to the generator terminal voltage V . In this type of system, the inherent exciter time constants are very small, and exciter stabilisation may not be required. As it can be seen in Figure 26 in this model the stabiliser has not been implemented and is grounded. The input value for voltage reference V_{ref} is set to be 1 p.u.. The required input signals V_t and I_{fd} come from the synchronous generator. As the AVRs and the excitation systems are in the field of this thesis as well as for frequency stability studies not considered principally, the selected AVR has been used for the implemented model with the default values and without any further modifications.

5.1.6. Loads

The implemented model "2 DIGLO IPS" includes two loads L1 and L2 as seen in Figure 26. Both are regarded as constant impedances and are connected in the 20 kV zone. Load L1 represents 70 % of the total power demand and load L2 represents approximately 30 % of total power demand, meaning that for example in case of 1 MW active power required from loads, 0.7 MW correspond to L1 and 0.3 MW to L2. The specific parameters of the loads are given in the following section referred to as power infeed scenarios. Loads have an inductive power factor of 0.9.

5.2. Load - flow results of "2 DIGLO IPS"

There are three power infeed scenarios implemented and regard different loading conditions. *Scenario A* means a 30 % loading of the generators, *Scenario B* corresponds to 50 % and *Scenario C* to 70 % loading respectively. This loading refers to generators condition regarding active and reactive power supply. Load - flow results are listed in the following sections for each scenario separately. The purpose is to have three scenarios for different loading conditions that correspond to operating conditions in IPSs dependent of the time of year.

Load - flow results for each scenario can be seen in the following figures. For load flow the synchronous generator with the larger rated apparent power, SG1, is set to be the swing machine and the second synchronous generator, SG2, is defined as PQ bus type.

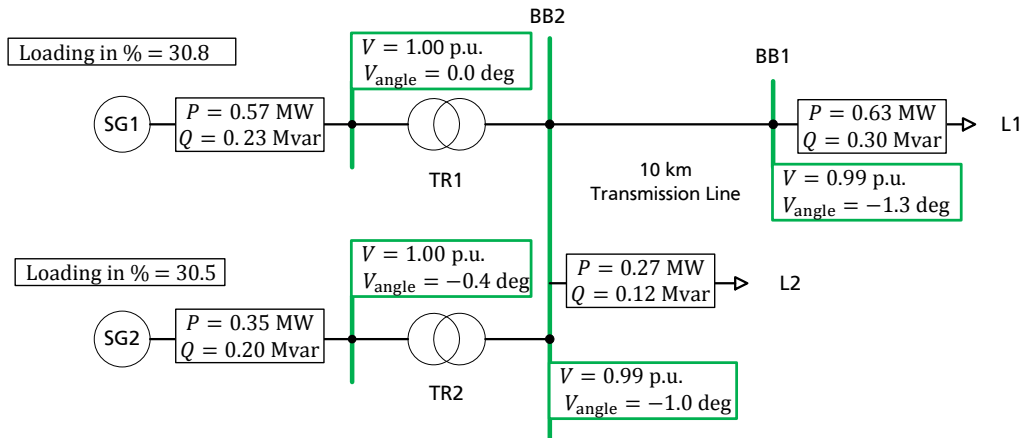


Figure 27: Load - flow results for Scenario A of "2 DIGLO IPS"

Figure 27 presents the results with reference to Figure 25 based on the overview of the IPS. Busbars are underlined green in case that resulted values of voltage magnitude V in per unit remain within the acceptable limits. These are under normal operation for example in Iceland 0.91 p.u.-1.05 p.u., in Madeira and Greece 0.9 p.u.-1.1 p.u., in Malta and New Zealand 0.95 p.u.-1.05 p.u. [14, 16, 17, 19, 20]. Hence, from now the strictest values of 0.95 p.u.-1.05 p.u. are used as limits. Voltage angle V_{angle} is provided as well and the values of active and reactive power for the synchronous generators and the loads.

In the same way in Figure 28 the load - flow results are presented for Scenario B. Loads have been modified so that the synchronous generators have a loading of approximately 50 %.

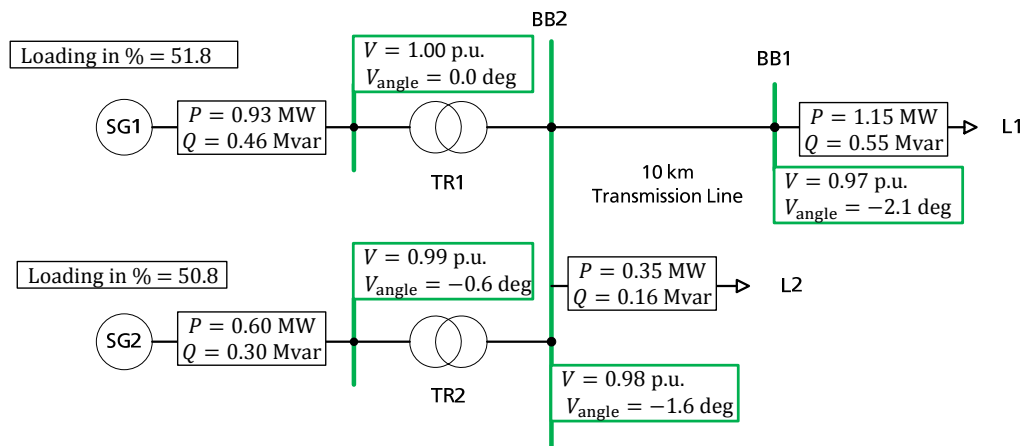


Figure 28: Load - flow results for Scenario B of "2 DIGLO IPS"

Similarly in Figure 29 the load - flow results for Scenario C can be seen. As before, the modified values concerning both loads so that loading of synchronous generators is approximately 70 %.

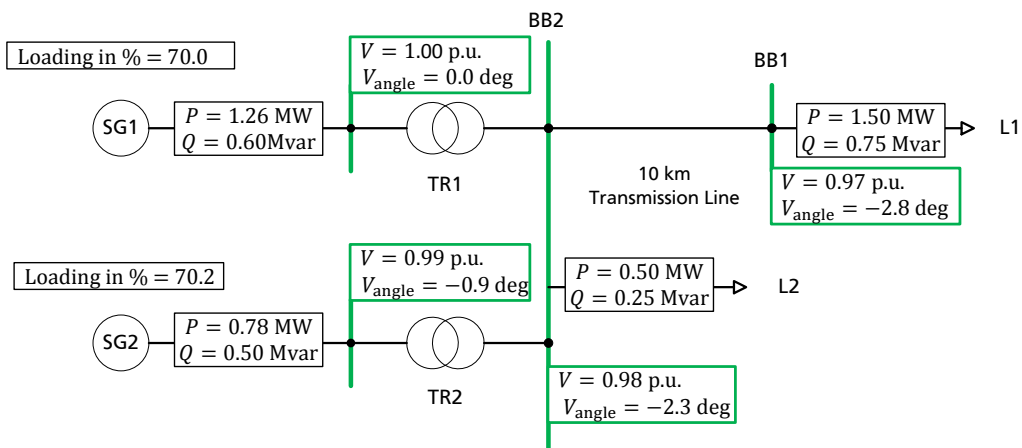


Figure 29: Load - flow results for Scenario C of "2 DIGLO IPS"

Once power infeed scenarios have been configured and load - flow calculations have been performed, tuning can be performed.

5.3. Tuning speed governors of “2 DIGLO IPS”

Tuning of governors serves to assure that the time and gain values are the appropriate ones for a specific power model and the operation point selected. In this section, tuning of both speed governors is realised. Tuning enables to improve system’s response to a disturbance affecting its frequency and is performed as explained in 4.6.

Time constants of the electric control box have the default values presented in Table 4. In the following table the values after tuning for the time constants and the droop are listed for each scenario and to enable the comparison the default values before tuning are listed in the very first column.

Before tuning		Tuning results: Scenario A, B and C			
		Speed governor	Scenario A	Scenario B	Scenario C
0.2	T_1	Isochronous	0.25	0.04	0.19
		Droop	0.46	0.15	0.16
0.1	T_2	Isochronous	0.08	0.57	0.11
		Droop	0.014	0.14	0.52
0.5	T_3	Isochronous	0.39	0.6	0.12
		Droop	0.36	0.52	0.49
0.05	Droop R_d SG2		0.02	0.04	0.06

Table 7: Tuned values for time and droop constant R_d of isochronous and droop speed governors - Scenario A, B and C

Initially, tuned values for the droop constant R_d are given. For Scenario A, the droop constant has been reduced from 0.05 to 0.02. As mentioned in section 3.3.1., a generator with a low droop will react more intensive to a load frequency change in comparison to a generator with a high droop value. Since in Scenario A the loading of the synchronous generators is approximately 30 % and SG1 is not restricted by any constant concerning the additional power which can be fed, tuning proposes for a better dynamic response and according to the tuning goal to reduce the value of droop for SG2 so as to enable a larger power infeed in case of the same frequency deviation. Based on this explanation, the values of droop constant R_d regarding Scenario B and Scenario C can be respectively explained. In Scenario B where loading is approximately 50 %, the conventional value of 0.04 is proposed and for Scenario C where loading of generators already equals to 70 % a higher value of 0.06 is selected, which is normal, because

also in case of a low droop value the generators could not exceed their physical limit generating more power than the rated power of the turbine.

Regarding the time constants, there is not a clear tendency to be seen. This has been expected and can be explained, since these time constants influence the behaviour of the output signal of the electric control box, which is placed before the actuator and its limitation. That means, that the time constants take values that enable running of tuning algorithm but they do not have a physical meaning for further study concerning the power system.

In order to prove that the time constants do not influence the behaviour of the control loop, since their results are restricted due to limitation, the transfer function of the electric control box and the actuator is simulated for the default values and for the values after tuning for all scenarios. A step pulse is applied as input signal.

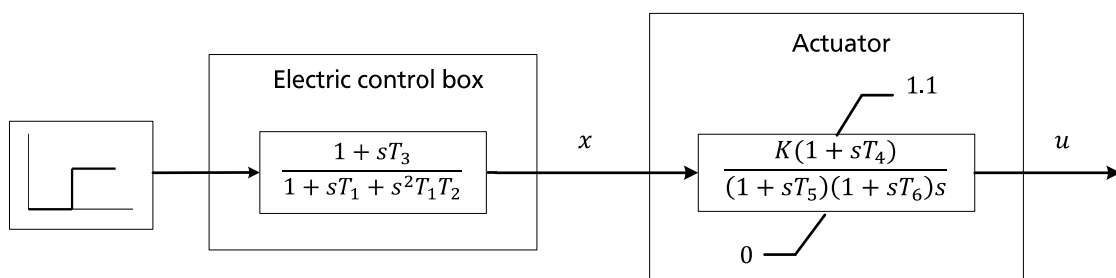


Figure 30: Block diagram of electric control box and actuator for demonstrating the effect of time constants before and after tuning

The simulation results can be seen in the following figures. It cannot be recognised a tendency between the default values of time constants before tuning and the ones after tuning, as referred above. It is to be seen in Figure 31 that the overshoot of the output signal of electric control box, denoted as x in Figure 15, is after tuning for Scenario B and Scenario C bigger than before tuning. This can be explained as mentioned above because of the fact that time constants are selected to be tuned and they enable running of tuning algorithm but in reality they do not influence the control loop output because of the limitation.

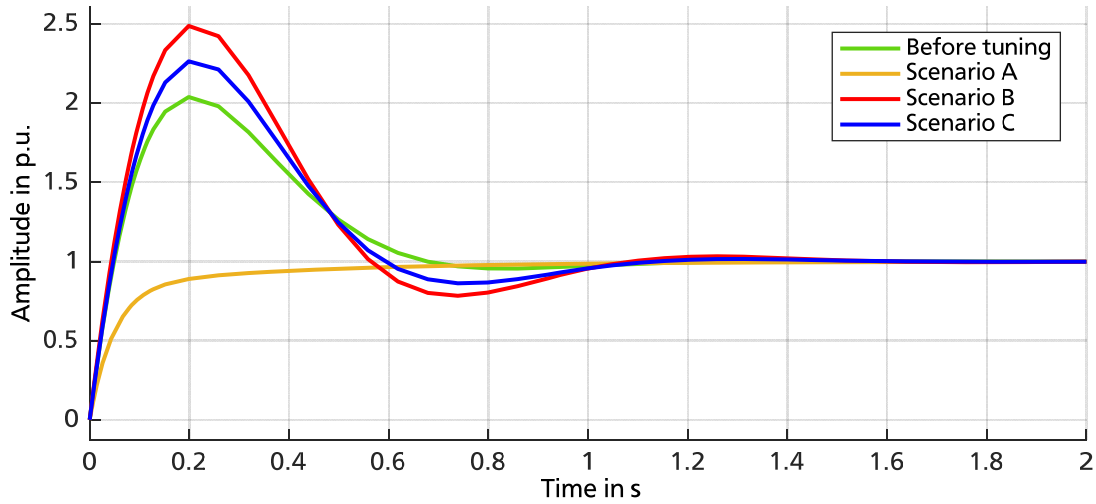


Figure 31: Output signal x of electric control box before and after tuning for Scenario A, B and C

Figure 32 presents the output signal of the actuator that acts as input for the diesel engine. The role of limitation is clearly to be seen. All signals x coming from the electric control box are limited to 1.1 which is the value of T_{max} as given in Table 4.

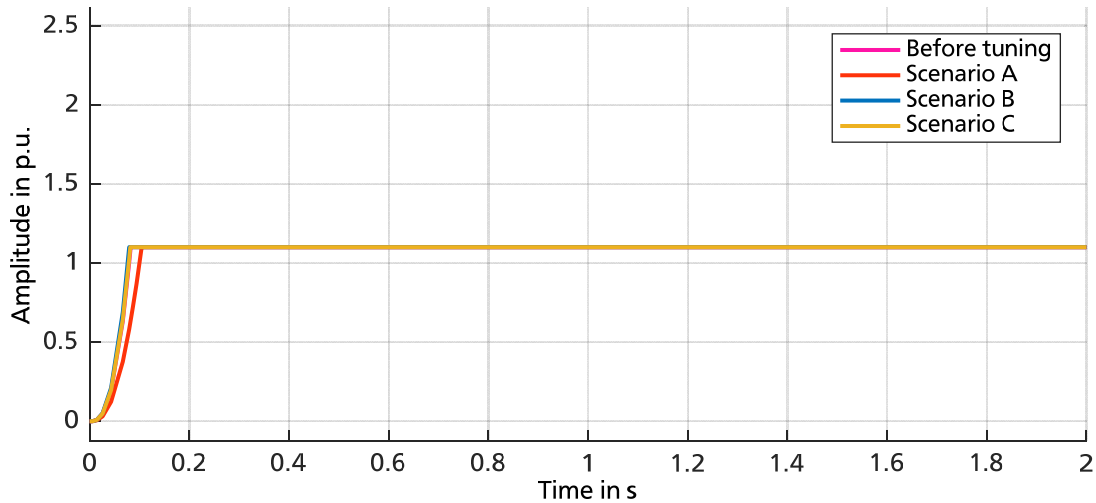


Figure 32: Output signal u of actuator before and after tuning for Scenario A, B and C

To conclude this section, tuning of isochronous and droop speed governors has been realised simultaneously and the results can be applied for dynamic simulations so as to demonstrate the influence of the droop value for frequency stability in this simple model of two synchronous generators.

5.4. Dynamic simulations

The previous sections of Chapter 5 deal with the introduction of “2 DIGLO IPS”, its components, the power infeed scenarios and the tuning results. Dynamic simulations presented in this section refer to a load change. Because of the linearization that has to take place before tuning, it makes sense to simulate dynamic events that would not damage the assumed selected operation point for linearization. Therefore the results before and after tuning that will be compared to each other concern only the case of a load change.

Load step

A load change is realised by connecting an additional load at BB1 of the model, as presented in Figure 28. For Scenario A, the active power of the additional load equals to 0.3 MW, for Scenario B equals to 0.4 MW and for Scenario C equals to 0.5 MW. Moreover the additional load is applied at $t = 2$ seconds. Electrical frequency measured at BB2 before and after tuning is presented for the three scenarios.

In Figure 33 can be seen that the electrical frequency has the first two seconds the nominal value of 50 Hz and at $t = 10$ seconds frequency reaches again its nominal value. As it can be seen in Figure 25, SG1 has an isochronous speed governor and SG2 has a droop governor. Frequency gradient of the first second after applying the additional load is the same for both curves, because it depends only from power system’s inertia. A slight better performance relating to frequency nadir after tuning can be recognised for Scenario A. What is more, in case of low loading (Scenario A) the isochronous governor regulates the electrical system frequency, so that a possible frequency deviation caused from the droop speed governor cannot be seen in Figure 33.

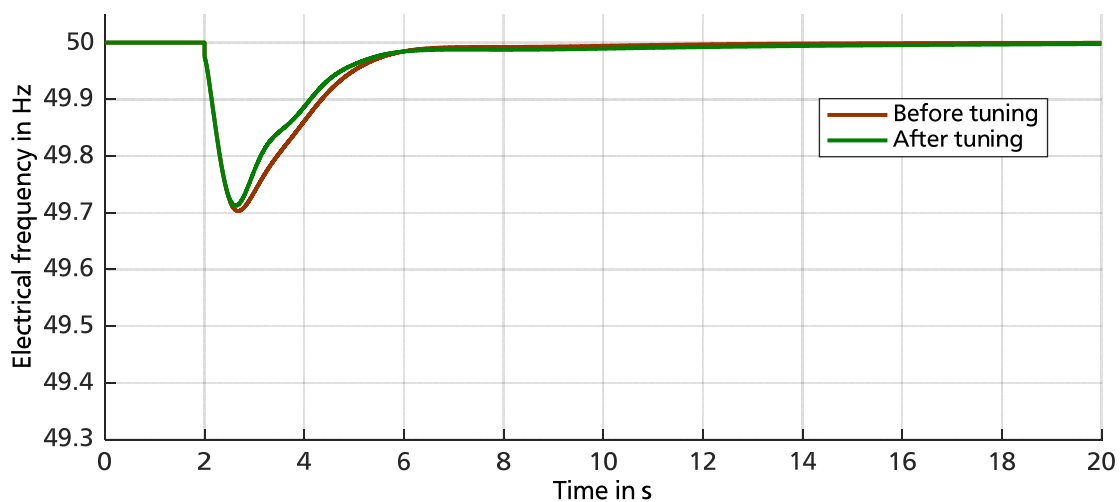


Figure 33: Electrical frequency before and after tuning in case of 0.3 MW load step for Scenario A

Similarly Figure 34 presents the response of electrical frequency for an additional load of 0.46 MW. In Scenario B both curves almost coincide. This was to be expected because of the fact that the droop constant R_d before and after tuning differs only of 1 %. Furthermore isochronous speed governor in case of two machines is the one regulating system's frequency and no frequency deviation can be seen.

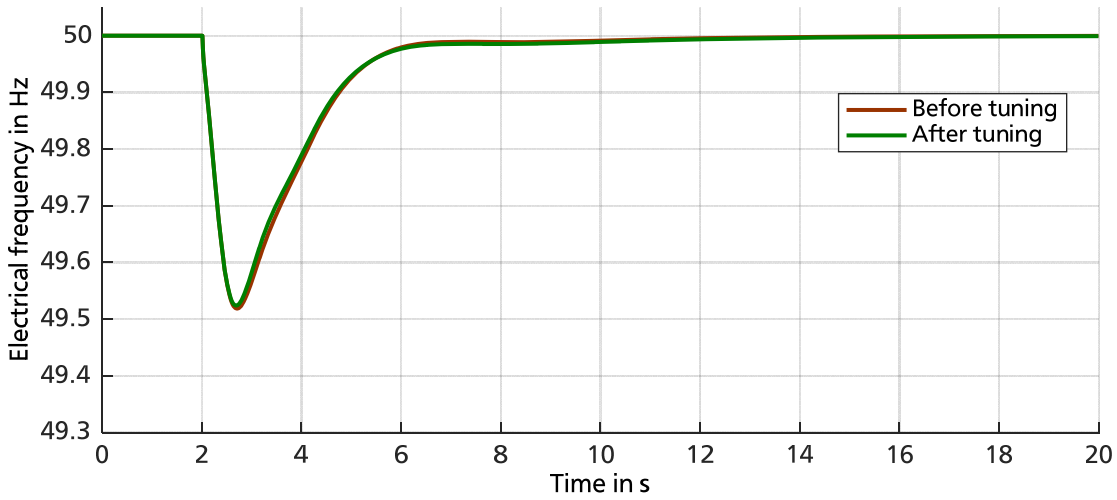


Figure 34: Electrical frequency before and after tuning in case of 0.4 MW load step for Scenario B

For Scenario C, the only difference that can be recognised with comparison to Scenario B is only the value of frequency nadir, which is 0.04 Hz. According to Figure 34 and Figure 35 it can be stated that for two synchronous generators for the cases between 50 % and 70 % loading, frequency response for a load change before and after tuning is approximately identical.

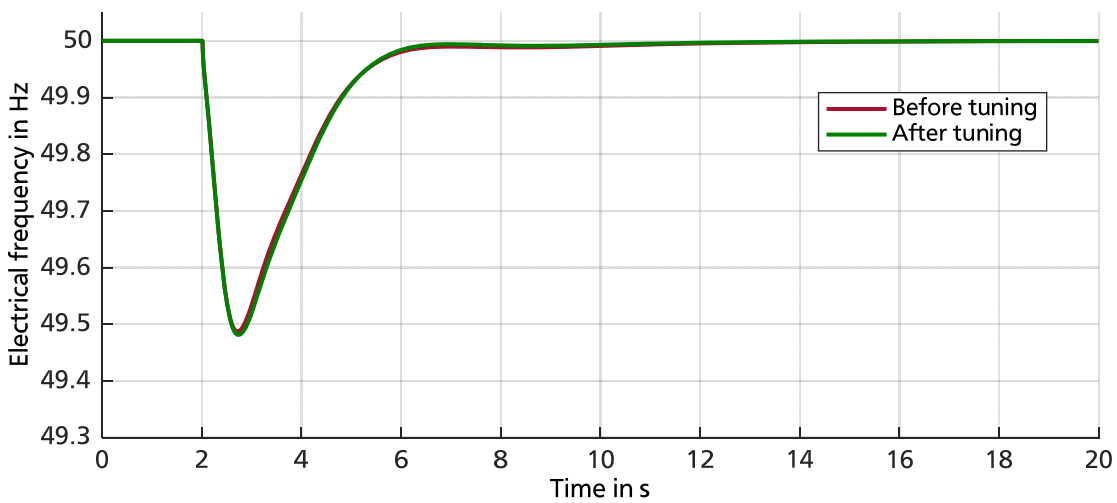


Figure 35: Electrical frequency before and after tuning in case of 0.5 MW load step for Scenario C

It should be mentioned as well that for all scenarios frequency nadir remains within the acceptable limits in case of abnormal conditions for most IPSs which are between 47 and 52 Hz, as presented in Table 3. After performing dynamic simulations and demonstrating the effects of tuning for the “2 DIGLO IPS”, it is worth exploring further the interaction of speed governors and tuning results as well as frequency response for IPSs with more synchronous generators.

5.5. Conclusion - Discussion

The chapter deals with the introduction of the “2 DIGLO IPS”, load-flow results for three loading scenarios, simultaneous tuning of isochronous and droop governor and dynamic simulations. Tuning algorithm run for all three scenarios and tuning results concerning time constants and droop values have been analysed. There are two main conclusions that must be underlined at the end of this chapter:

1. Tuning of time constants in electric control box of isochronous and droop speed governor enables tuning algorithm to run, but due to actuator’s limitation these parameters cannot influence frequency response in reality.
2. Tuning droop constants R_d of speed governors has the expected results. The lower the loading of a generator, the lower its droop constant, so as to feed the power system with as much additional power as possible.
3. Interaction of both speed governors has been taken into consideration because tuning takes place simultaneously for isochronous and droop speed governor, as it is the case in reality for most IPSs, that these speed governors operate simultaneously with a common control concept.

6. Extension of “DIGLO IPS” with more synchronous generators and tuning

In this chapter two extended versions of “2 DIGLO IPS” model are presented. The purpose of these extensions is to demonstrate the effect of speed governor combinations reacting simultaneously in a model with more synchronous generators.

6.1. Model “3 - and “4 DIGLO IPS”

A first extension of “2 DIGLO IPS” model is realised by adding a synchronous generator denoted as SG3 of $S_{rG\ SG3} = 1.32$ MVA parallel to the two existing ones. The modified power system topology can be seen in Figure 36. The 20 kV side remains without changes consisting of two loads L1 and L2 and a 10 km transmission line as presented in Figure 28. The third SG will have either an isochronous or a droop speed governor. According to the simulated combination the desired speed governor is connected.

Furthermore, “3 DIGLO IPS” model is further extended by adding one more synchronous generator. The same procedure is followed. As a result, the power system is be parted from two additional SGs of rated power $S_{rG} = 2.0$ MVA denoted as SG1 and SG4 and two SGs of rated power of $S_{rG} = 1.32$ MVA. The overview is to be seen in Figure 36 as well. In this model the third synchronous generator SG3 uses always a droop speed governor. Lastly, the fourth synchronous generator denoted as SG 4 is the one having either an isochronous or a droop speed governor with reference to defined combinations.

Power infeed scenarios remain the same as defined for the “2 DIGLO IPS” model corresponding to a 30 % (Scenario A), 50 % (Scenario B) and 70 % (Scenario C) loading. Load - flow results are independent of the combination of speed governors and are presented in section 6.2.

Table 8 provides an overview of scenarios and speed governors combinations taken into consideration.

	3 DIGLO IPS		4 DIGLO IPS	
SG1 $S_{rG} = 2.0$ MVA	Isochronous	Isochronous	Isochronous	Isochronous
SG2 $S_{rG} = 1.32$ MVA	Droop	Droop	Droop	Droop
SG3 $S_{rG} = 1.32$ MVA	Droop	Isochronous	Droop	Droop
SG4 $S_{rG} = 2.0$ MVA			Droop	Isochronous

Table 8: Overview of realised speed governors’ combinations

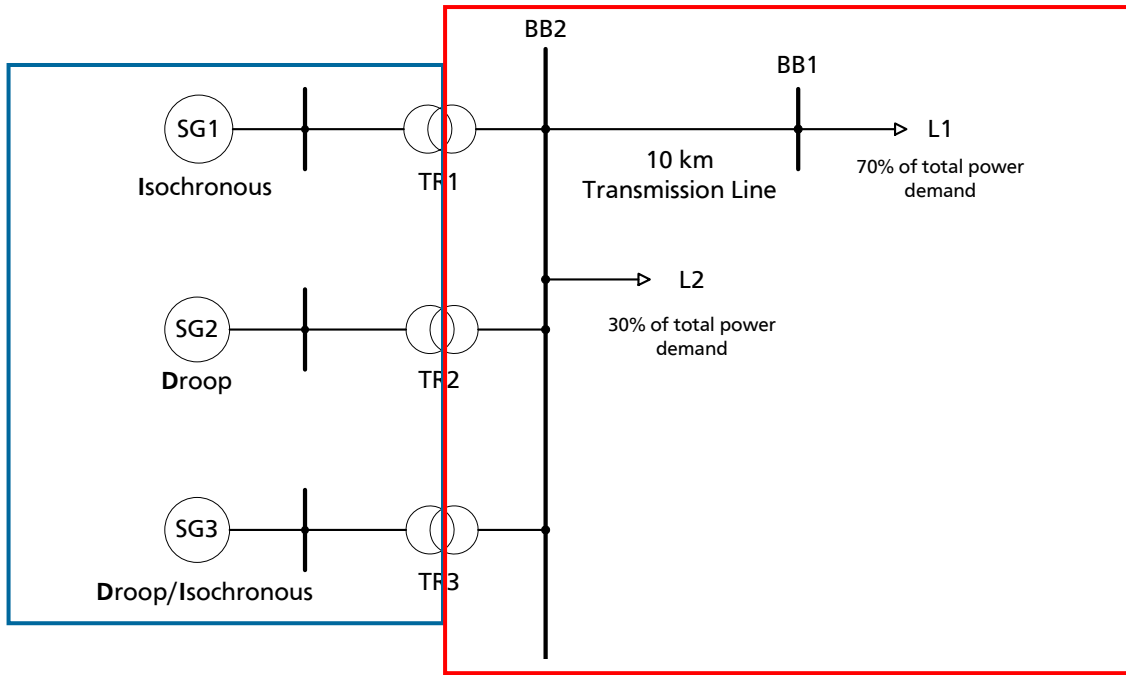


Figure 36: Overview of "3 DIGLO IPS"

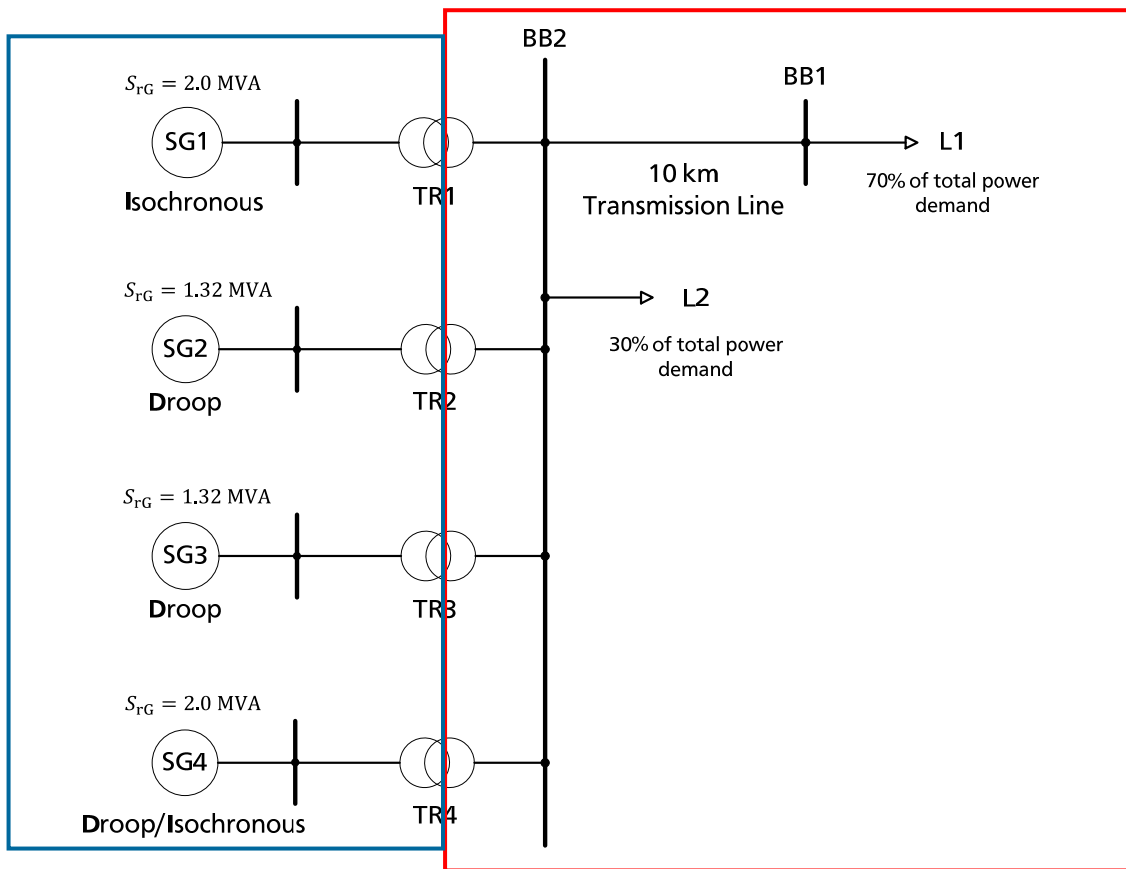


Figure 37: Overview of "4 DIGLO IPS"

As it can be seen in Figure 36 and Figure 37 the system topology is based on this of “2 DIGLO IPS” model. The nominal voltage of SGs, their governors and the excitation systems is 400 V. Nominal voltage of the transmission line and of load L1 is 20 kV. Speed governors are denoted with a bold initial letter, since this is the abbreviation used to describe from now on the combinations. The abbreviation results from listing the speed governor corresponding to each synchronous generator beginning from SG1 to SG3.

In reality the concepts of IDDD and IDDI has been developed to represent the Droop/Isochronous load sharing on an isolated bus – IDDD – and Isochronous load sharing on an isolated bus – IDDI –. Operation principles of both frequency concepts have been presented in 3.3.3. At this way a comparison of these frequency control concepts is enabled.

6.2. Load-flow results of “3 – and “4 DIGLO IPS”

In this section load-flow results for the three scenarios are presented for the extended IPSs. These results are important, because they relate to the initial operating point regarding dynamic simulations that take place at the end of this chapter for “3 – and “4 DIGLO IPS”.

A. “3 DIGLO IPS”

There are three power infeed scenarios implemented and regard different loading conditions. *Scenario A* means a 30 % loading of the generators, *Scenario B* corresponds to 50 % and *Scenario C* to 70 % loading respectively. Load - flow results are demonstrated at the same way based on IPS overview as presented in Figure 37 for each scenario separately. As before SG1 is set to be the swing machine and synchronous generators SG2 and SG3 are defined as PQ bus types.

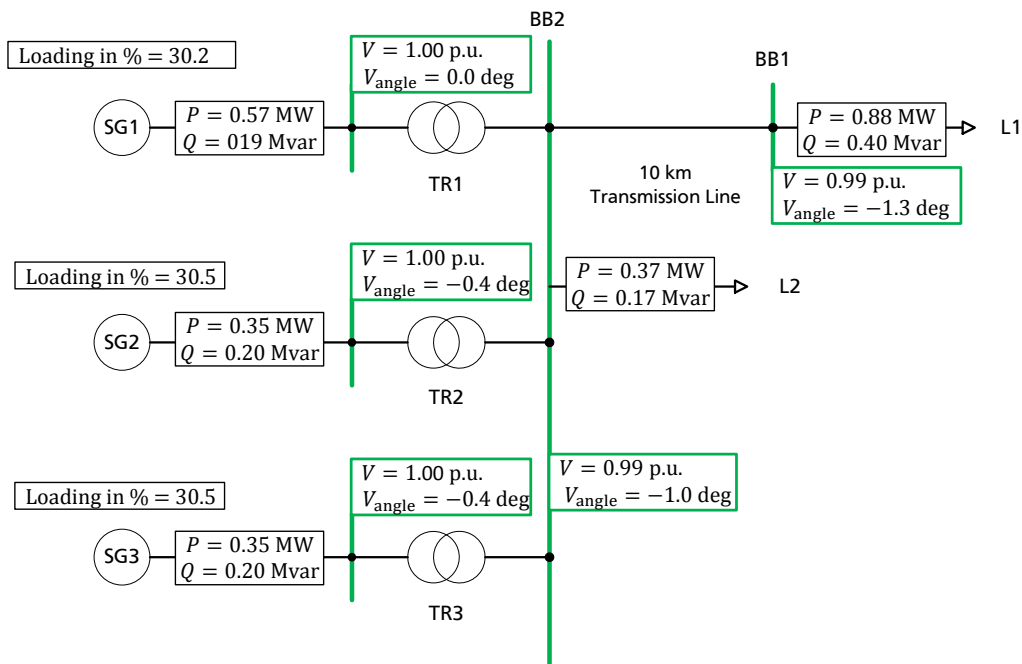


Figure 38: Load - flow results for Scenario A of "3 DIGLO IPS"

In Figure 38 can be seen that busbars are underlined green since voltage remains within the acceptable limits. Load - flow results for Scenario B and Scenario C can be found in Appendix and are presented in Figure 1A and Figure 2A.

B. "4 DIGLO IPS"

Load - flow results are demonstrated at the same way based on IPS overview as presented in Figure 37 for each scenario separately. As before SG1 is set to be the swing machine and synchronous generators SG2 and SG3 and SG4 are defined as PQ bus types.

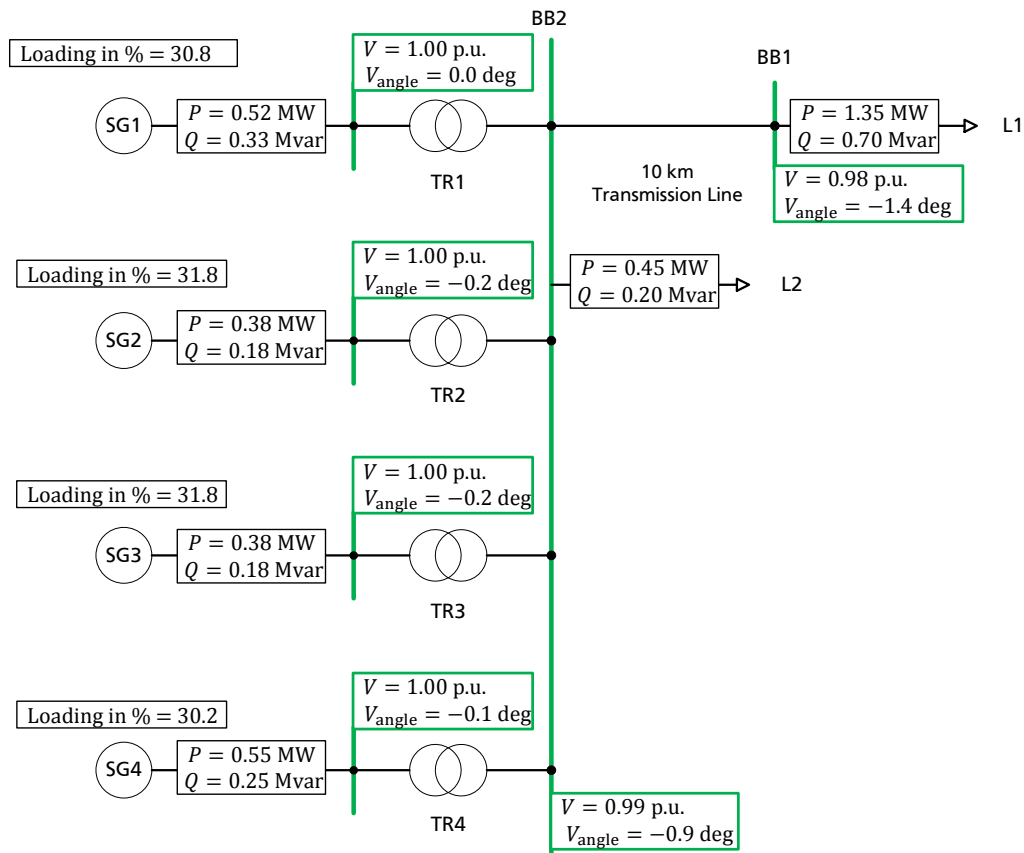


Figure 39: Load - flow results for Scenario A of "4 DIGLO IPS"

In Figure 39 can be seen that busbars are underlined green since voltage remains within the acceptable limits. This is the case as well for Scenario B and Scenario C, where the load - flow results can be found in Appendix and are illustrated in Figure 3A and Figure 4A.

Load - flow results have been presented for all loading scenarios of "4 DIGLO IPS". These results constitute the initial values for dynamic simulations that are performed in section 6.4.

6.3. Tuning speed governors of "3 - and "4 DIGLO IPS"

As presented in Section 5.3, tuning time constants enables running algorithm but does not influence speed governors' response for dynamic simulations because of actuator's limitation. Therefore, the tuned values of droop constants R_d and the system response after tuning will be presented for each loading scenario.

3 DIGLO IPS

		Before tuning	Scenario A	Scenario B	Scenario C
IDD	SG2	0.05	0.02	0.03	0.05
	SG3	0.05	0.02	0.03	0.05
IDI	SG2	0.05	0.02	0.02	0.03

Table 9: Tuned droop constants R_d of "3 DIGLO IPS" for Scenario A, B and C

With reference to Table 9 it can be seen that droop constants R_d have the same tendency as for "2 DIGLO IPS" model. The higher the loading the larger the droop constants are. This is valid for both combinations and for all scenarios. As far as the difference between IDD and IDI is concerned it can be seen that the droop constant is being primary influenced by isochronous speed governors which are the majority in case of IDI and react more intensive than droop speed governor in frequency changes. Therefore droop constants remain as low as possible in IDI to interact appropriately with droop governor's response.

4 DIGLO IPS

		Before tuning	Scenario A	Scenario B	Scenario C
IDDD	SG2	0.05	0.02	0.03	0.03
	SG3	0.05	0.02	0.03	0.03
	SG4	0.05	0.02	0.02	0.03
IDDI	SG2	0.05	0.02	0.02	0.03
	SG3	0.05	0.02	0.02	0.03

Table 10: Tuned droop constants R_d of "4 DIGLO IPS" for Scenario A, B and C

The arguments explaining tuning results of Table 9 are further applicable for the explanation of Table 10. Droop constants R_d are higher the higher the loading of the generators, meaning that Scenario B and Scenario C have larger droop constants than Scenario A. Furthermore in Scenario B for SG4 droop constant remains low, since rated power of this machine is larger than of the two others. Similarly, droop constants between combinations have the tendency to remain close to the lowest value the more

isochronous speed governors are connected, meaning that e.g. SG2 and SG3 have for IDDI a lower value in comparison to IDDD.

6.4. Dynamic simulations

For dynamic simulations and tuning two combinations are explored for “3 – and “4 DIGLO IPS”. The first one denoted as IDD assumes a droop speed governor of SG3 for “3 DIGLO IPS” model and consequently the second combination, denoted as IDI refers to an isochronous speed governor for SG3. Similarly for “4 DIGLO IPS” the combination denoted as IDDD regards a droop for SG4 and the last combination denoted as IDDI regards an isochronous speed governor for SG4.

Load step

As for “2 DIGLO IPS” a load step is simulated. The additional load is adapted to each scenario and is applied at $t = 2$ seconds. In the following figures a comparison of both frequency control concepts before and after tuning is demonstrated. Before tuning means that all variables of speed governors have the values presented in Table 4. The same variables and according to the simulated scenario take the values presented in Table 10 after tuning.

Model “3 DIGLO IPS”

In Figure 40 response of electrical frequency for Scenario A can be seen. Frequency gradient is the same for all curves, as it has been expected and frequency nadir differs slightly between them. Additionally a frequency nadir of 49.5 Hz is within the acceptable limits, which are within 47.0 and 52.0 Hz for abnormal conditions and have been introduced in section 3.4.1.

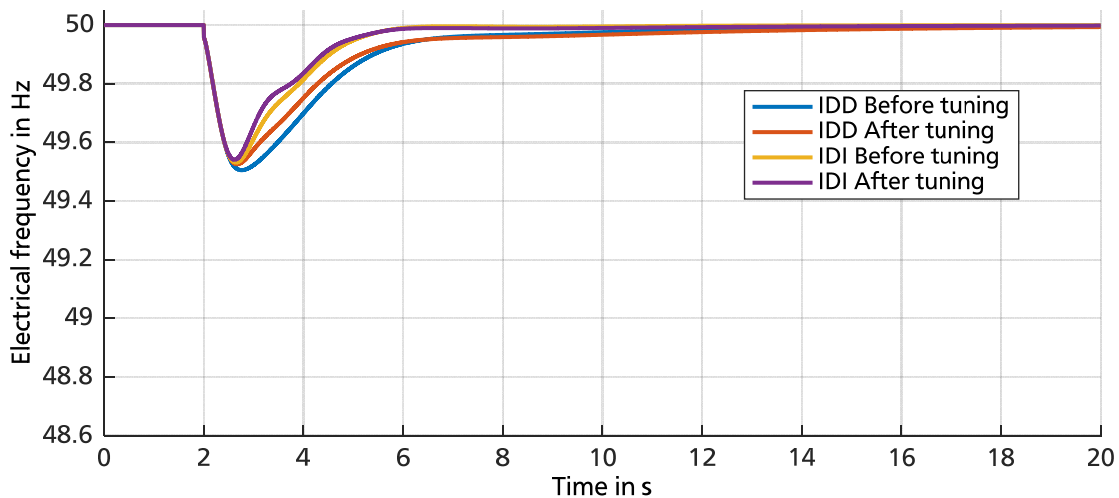


Figure 40: Electrical frequency for a load step of 0.63 MW for Scenario A - “3 DIGLO IPS”

It can be seen that there is no steady - state frequency deviation independent of frequency control concept and of tuning for Scenario A. That means that isochronous speed governor reacts as primary and secondary control and restores frequency to the nominal value. This is the case for IDI frequency control concept, since the settling time is of about three seconds shorter than for the IDD frequency control concept. Furthermore tuning does not influence response of electrical frequency in a significant way.

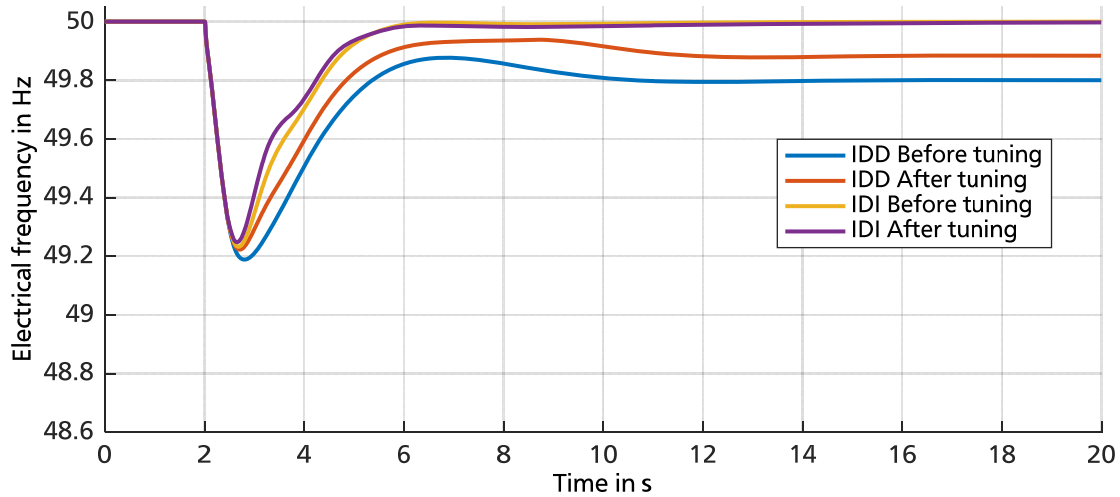


Figure 41: Electrical frequency for a load step of 1 MW for Scenario B - "3 DIGLO IPS"

In Figure 41 electrical frequency response for Scenario B can be seen as well. Frequency nadir remains as before within the acceptable limits. Comparing for this case frequency control concepts can be seen that IDD has a steady-state frequency deviation corresponding to the droop constants and for IDI frequency takes the nominal value. This steady-state frequency deviation remains within the acceptable limits of 49.5 and 50.5 Hz, as they have been introduced in 3.4.1. It can also be stated that tuning does not influence significantly IDI frequency control concept, but improves steady - state frequency deviation for IDD. Frequency deviation for IDD before tuning can be validated to be the correct one according to 3.3, and considering one synchronous generator the values in per unit, it is $\frac{\Delta f}{\Delta P} \times 100 = \frac{0.004\text{p.u.}}{0.08\text{p.u.}} \times 100 = 5\%$ droop. After tuning can be calculated at the same way with per unit values, it is $\frac{\Delta f}{\Delta P} \times 100 = \frac{0.002\text{p.u.}}{0.076\text{p.u.}} \times 100 = 3\%$ droop. Per - unit values of power deviation have been calculated according to the base value of power.

Generally, IDD presents a relatively worse response in comparison to IDI. This was expected because of the existence of more than one isochronous speed governors for the combination IDI. The fact that isochronous speed governor tries to restore frequency to the nominal value enables a better performance than droop speed governor. As a result, IDI with two isochronous speed governors and one droop reaches a slightly better steady state frequency than the one of IDD.

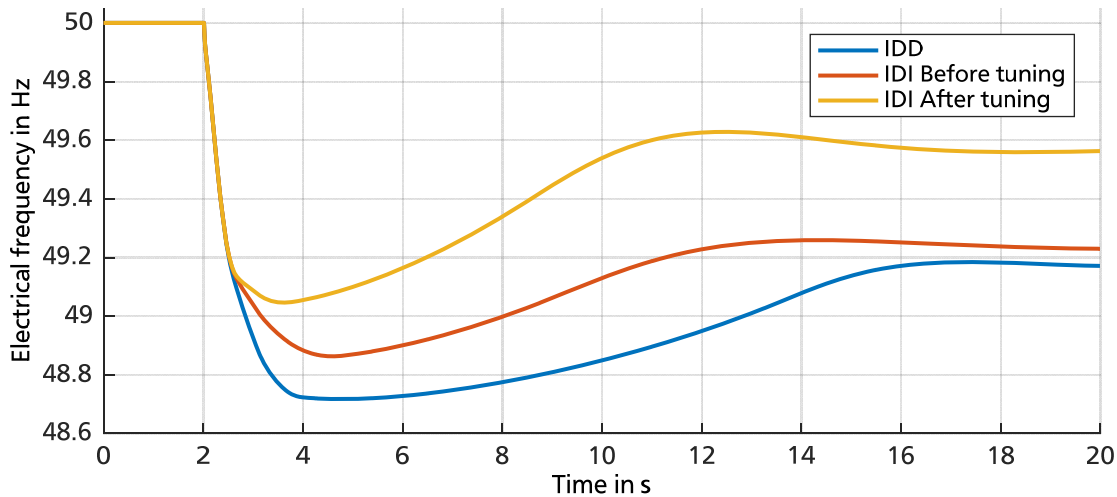


Figure 42: Electrical frequency for a load step of 1.28 MW for Scenario C - "3 DIGLO IPS"

In Figure 42 response of electrical frequency for Scenario C can be seen. Frequency nadir is 48.7 Hz but remains within the acceptable limits. For a high loading of synchronous generators as it is the case in this scenario the differences between control concepts are recognised clearly. For IDD there is only one curve, because droop constant R_d equals to 5 % before and after tuning. Although frequency nadir fulfils frequency limits, this is not the case for two frequency concepts concerning steady-state frequency deviation. IDD and IDI Before tuning have a frequency deviation of 49.18 Hz and 49.22 Hz respectively. In this scenario it can be clearly recognised that without tuning such a load step would threat frequency stability.

Model "4 DIGLO IPS"

Simulating a load step for the "3 DIGLO IPS" has demonstrated that combining appropriately speed governors and tuning in high loading conditions can improve significantly electrical frequency response. Therefore a load step is simulated for the "4 DIGLO IPS" to explore the effects for one more generator.

In Figure 43 response of electrical frequency for Scenario A can be seen. Frequency gradient is the same for all curves, as it has been expected and frequency nadir of 49.5 Hz is within the acceptable limits. The differences between the frequency control concepts concern settling time and frequency nadir. Settling time for IDDI equals to one second and for IDDD approximately to ten seconds. Frequency nadir can be improved of about 0.1 Hz for IDDD frequency control concept, but there are no limits violated that would recommend tuning. Additionally, it can be seen that an appropriate selection of the frequency control concept prevents a possible adaptation of speed governors' values, since electrical frequency response between IDDI before tuning almost coincides with frequency response of IDDD after tuning. This should

be expected, since tuned values have shown that droop constant R_d is adapted to approach zero, meaning that droop speed governors assimilate the dynamic behaviour of isochronous speed governor.

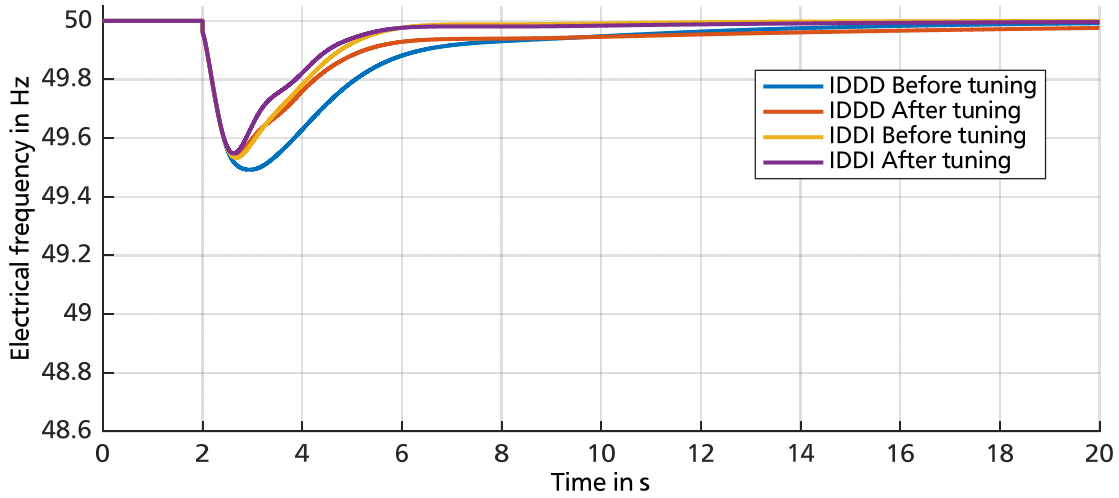


Figure 43: Electrical frequency for a load step of 0.9 MW for Scenario A - "4 DIGLO IPS"

Figure 44 presents electrical frequency response for Scenario B. Frequency nadir as well as steady - state frequency deviation remain within the acceptable limits for all frequency control concepts. Tuning has a positive effect for IDDD but not an obvious effect for IDDI. There are two reasons explaining these behavior: firstly in IDDD there are more droop governors and therefore tuning influences system's response more than for IDDI and secondly according to the tuned values the droop constant of SG4 for Scenario B is lower than of SG2 and SG3.

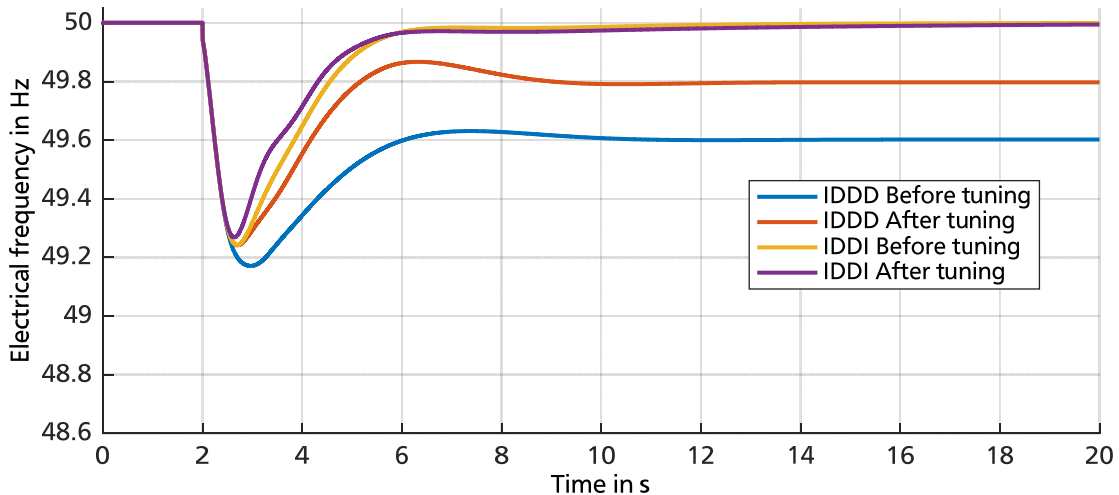


Figure 44: Electrical frequency for a load step of 1.5 MW for Scenario B - "4 DIGLO IPS"

Figure 45 shows electrical frequency response for Scenario C simulating the same load step as for Scenario B. In case of additional active power load generators could not supply the required power because of high loading condition.

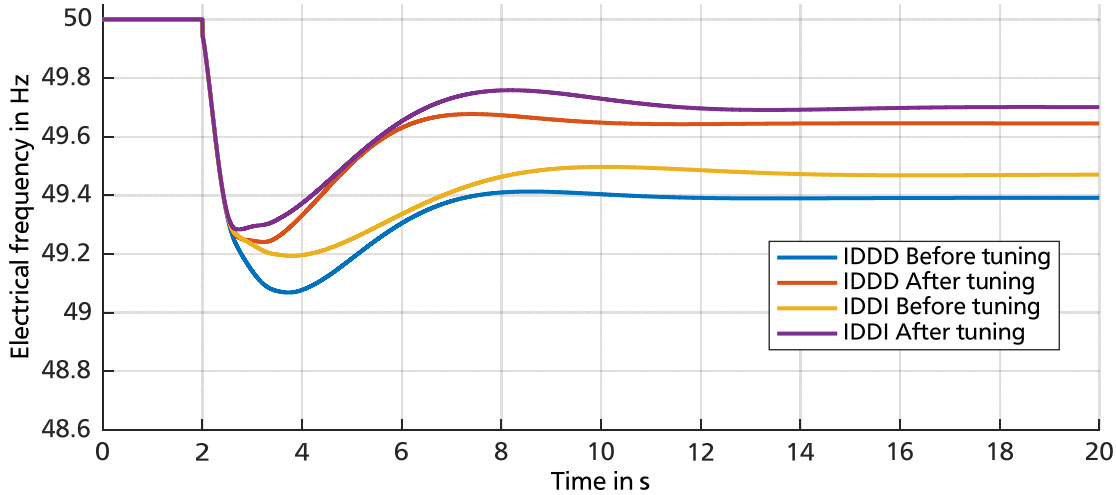


Figure 45: Electrical frequency for a load step of 1.5 MW for Scenario C - “4 DIGLO IPS”

In Figure 45 can be seen that frequency nadir is almost the same as in Figure 44, since additional active power required is the same. Its value equals to 49.1 Hz for IDDD before tuning and 49.2 Hz for IDDI and IDDD after tuning. It is interesting that for a high loading condition and a large load step none of these frequency control concepts succeeds to restore nominal value of frequency. It can also be recognised that the steady - state frequency deviation remains within the acceptable limits for IDDI after tuning.

Three - phase short circuit

In IPSs short circuits could cause a power system collapse and are considered in most of frequency stability studies. For the models of “3 DIGLO IPS” and “4 DIGLO IPS” a three - phase short circuit is simulated to explore electrical frequency response and to compare the effect of both frequency control concepts. Before and after tuning is not taken into consideration, since tuning has been realised based on load step disturbances.

Model “3 DIGLO IPS”

A three - phase short circuit of duration of 200 ms is applied to generators terminal at $t = 2$ seconds. Instead of electrical frequency, rotor speed of generators is demonstrated. Figure 46 shows rotor speed in per unit for all loading scenarios and frequency control concepts. What is more, it can be stated that the loading of generators plays a major role regarding dynamic response in case of a three - phase short circuit. Maximum value of rotor speed differs between Scenario A and Scenario B about 0.01 p.u. and

between Scenario B and Scenario C about 0.005 p.u.. This is because of the amount of active power which is fed into the grid and during the short circuit is transformed to kinetic energy accelerating the rotor of synchronous generators. Therefore, the more loaded a synchronous generator is, the more active power has been fed and the larger the amount of resulting kinetic energy which accelerates the machine's rotor. The result is a higher rotor speed for Scenario C in comparison to Scenario A, as it was to be expected.

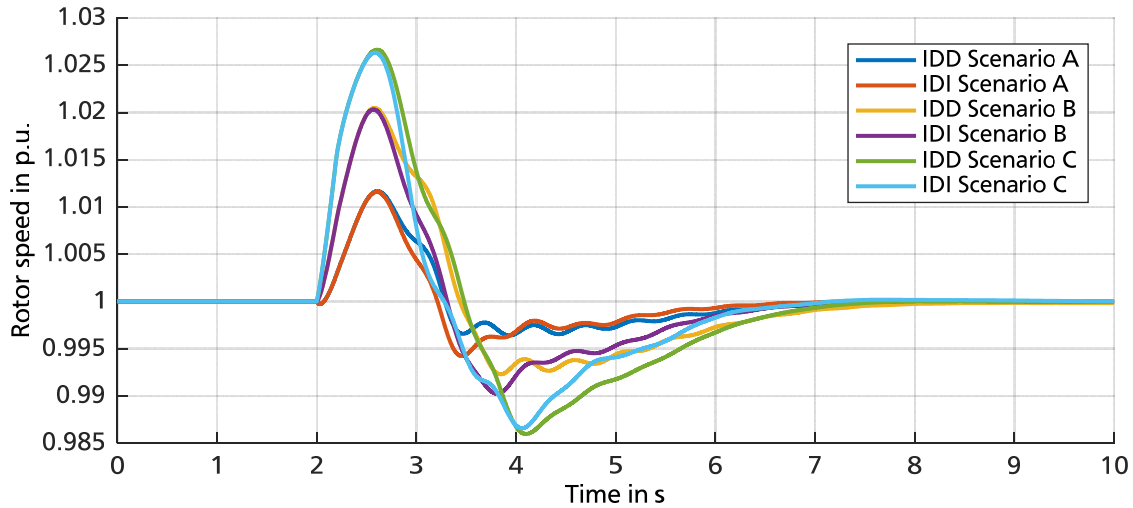


Figure 46: Rotor speed of SG1 in case of a three - phase short circuit for IDD and IDI of Scenario A, B and C - “3 DIGLO IPS”

Regarding the frequency control concepts IDD and IDI there is a slightly better response of IDI for all loading scenarios. This is important because in case of deciding to apply the IDI concept based on the better behaviour of electrical frequency for a load step, it is necessary to evaluate dynamic response of rotor speed for other disturbances, such as three - phase short circuits.

Model “4 DIGLO IPS”

For reasons of similarity, a three - phase short circuit of duration of 200 ms is simulated for “4 DIGLO IPS” as well. All scenarios and combinations are presented in Figure 47. Maximum value of rotor speed differs for each scenario about 0.01 p.u.. Comparing rotor speed behaviour of “4 DIGLO IPS” with the one of “3 DIGLO IPS” it can be seen that overshoot is the same. The number of synchronous generators does not influence rotor speed behaviour of SG1. The frequency control concepts affect rotor speed response at the same way as in “3 DIGLO IPS” model.

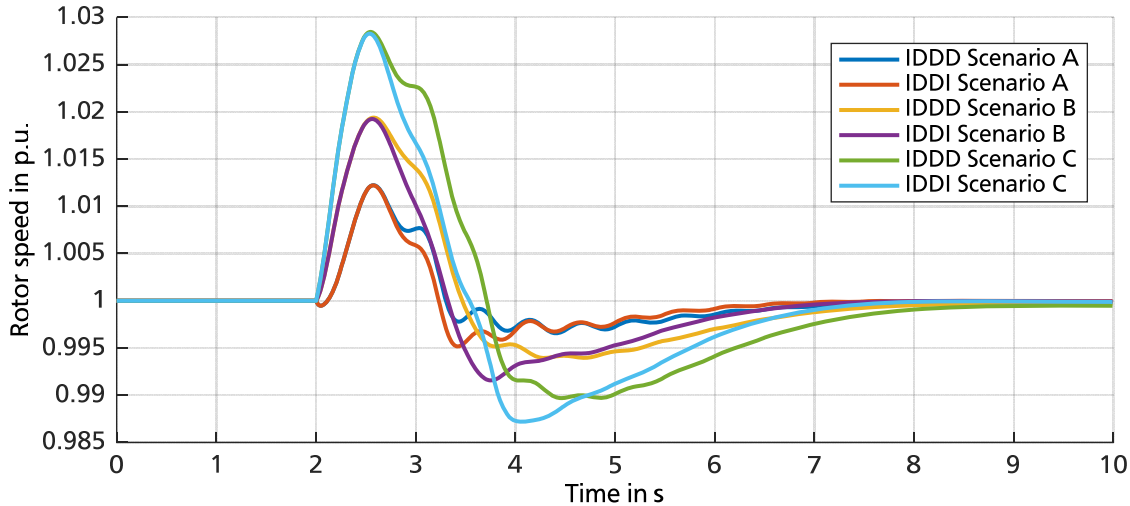


Figure 47: Rotor speed of SG1 in case of a three - phase short circuit for IDDD and IDDI of Scenario A, B and C - “4 DIGLO IPS”

Terminal voltage of SG1 is presented in Figure 48 for all scenarios and frequency control concepts. As it has been expected there is no difference between IDDD and IDDI regarding the terminal voltage. It can be seen that during short - circuit duration voltage reaches a minimum value of 0.2 p.u. and after short-circuit clearance increases again to reach the nominal value from $t = 4$ seconds.

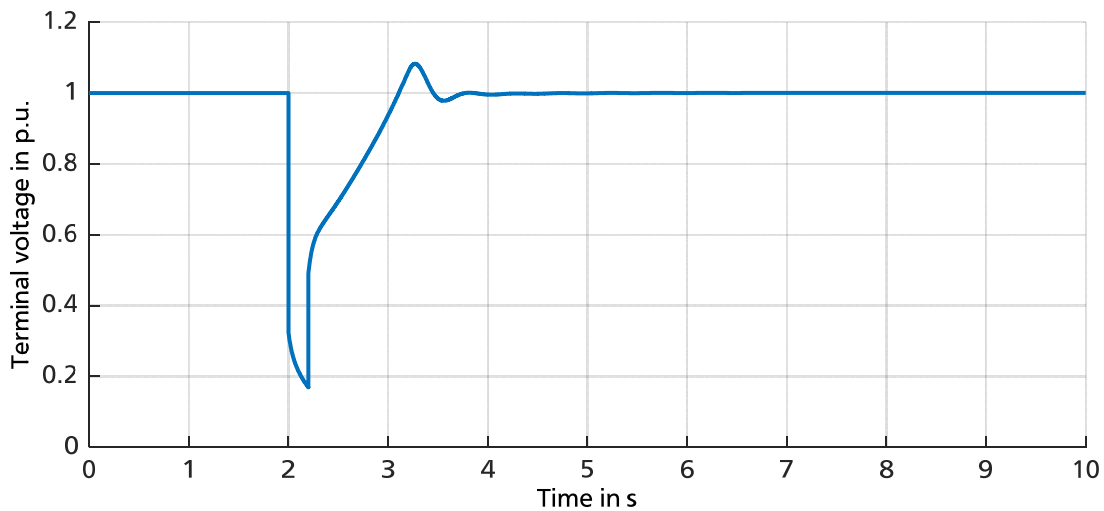


Figure 48: Terminal voltage of SG1 in case of a three - phase short circuit for both frequency control concepts of Scenario A, B and C - “3 and 4 DIGLO IPS”

Dynamic simulations prove that the comparison and proposal of frequency control concepts plays a more important role for load steps than for three - phase short circuits. However, rotor speed behaviour is not worsen but slightly improved.

6.5. Conclusion - Discussion

In this chapter two extended “DIGLO IPS” have been implemented. Consequently, setting - up load - flow scenarios has been realised successfully and afterwards dynamic simulations have been performed. Tuning droop values and comparing the selected frequency concepts, denoted as IDD and IDI - representing the number of isochronous and droop speed governors- for model of three SGs and respectively IDDD and IDDI for “4 DIGLO IPS” has been performed as well. The most important conclusions are summarised in this section.

1. The more isochronous speed governors are connected to an IPS the more stable dynamic system behaviour is. This is the case in all “DIGLO IPS” regarding basic and extended versions.
2. Tuning has a positive effect particularly for Scenario B and Scenario C in “3 DIGLO IPS” and in “4 DIGLO IPS”.
3. Steady - state frequency deviation is not within the acceptable limits before tuning for both frequency control concepts in Scenario C of “3 DIGLO IPS” and in “4 DIGLO IPS”. This is the case when tuning is necessary.
4. Tuning droop constants simultaneously enables considering the interaction of more than one speed governors. The resulted values are influenced from two parameters:
 - a. The loading condition of generators;
 - b. The number of isochronous speed governors in operation.
5. Since tuning goal is step rejection it can be clearly seen that tuned values of droop constants result in a better dynamic response in case of a load step and they slightly improve speed governor’s dynamic response in case of short circuits.
6. Tuning tries to adapt droop constant in this way to approach low values near zero. A droop constant with a zero value transforms a droop speed governor to an isochronous. Therefore IDDD which includes more droop and only one isochronous after tuning has almost identical response as IDDI before tuning including more isochronous speed governors.

Generally, it can be stated that the higher the loading of a synchronous generator, the lower the droop constants and the more isochronous speed governors in operation in a model, the lower the droop constants. Comparing frequency control concept of Droop/Isochronous load sharing on an isolated bus to Isochronous load sharing on an isolated bus has shown for this first approach that the second concept in general and for most cases provides a better dynamic response concerning rotor speed before and after tuning.

7. Extension of “4 DIGLO IPS” model including a fully rated wind energy converter

In this chapter the “4 DIGLO IPS” model is extended with a fully rated wind energy converter that simulates power generation coming from renewable energy sources without contributing to power system’s inertia.

7.1. Modelling of Fully Rated Wind Energy Converter

In order to simulate a high wind power penetration coming from wind power plants without inertia support but exclusively from power electronic converters, a fully rated wind energy converter model is presented in detail concerning load flow as well as stability analysis functions [68].

Wind generators that are connected to the grid using a full-size converter can also be modelled as static generators, because behaviour of the plant is determined by the converter. Static generator is meant any kind of non-rotating generator. The model consists of various components, all connected in a unified model. These for instance include the block for active and reactive power control, for active power reduction and also the current controller. The frequency measurement, the *phase locked loop* (PLL) and further measurement devices are also included. An overview of control loops can be seen in Figure 49.

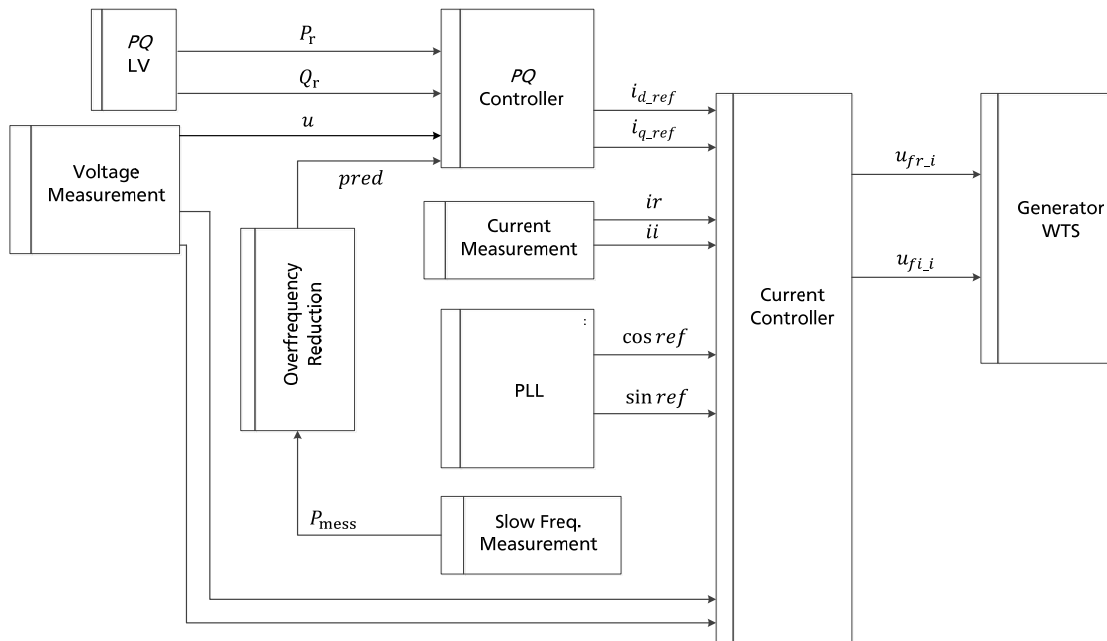


Figure 49: FRWEC model including the current controller

The main concept of the model’s control is that the *Generator WTS* receives the voltage set points calculated by the FRWEC model that will define its operating point. However, each block in the control frame has its own function. Specifically, the *PQ Controller* takes as inputs the measured values of active power P and reactive power Q , the measured value of voltage u and, if existent, the value of the reduced active power denoted as $pred$. Then it compares the measured P and Q values with the reference values

and gives as output the reference values for the d and q axis currents, which are the inputs for the current controller. The *PQ* Controller is the outer control loop of the unified controller.

The inner control loop of the *PQ* Controller is the current controller. It takes as inputs the d and q axis current reference values and compares them with the measured current values. Other inputs are the reference values of sine and cosine which are the outputs of the PLL block and are necessary for the d-q transformation. The values i_d and i_q are obtained from the d-q transformation block by applying the following equations

$$i_d = i_r \cdot \cos \varphi + i_i \cdot \sin \varphi \quad 7.1$$

$$i_q = -i_r \cdot \sin \varphi + i_i \cdot \cos \varphi \quad 7.2$$

Consequently, the PLL block provides the values $\sin ref$ and $\cos ref$ which are used by the current controller for the d-q transformation and the d-q back transformation. The *Slow Frequency Measurement* block provides the measured frequency to the active power reduction block, called *Overfrequency Reduction*.

The *Overfrequency Reduction* block receives as input the measured frequency from the *Slow Frequency Measurement* block and outputs the value for the reduced active power which is fed to the *PQ* Controller. The active power is set to be reduced when frequency reaches the value of 50.2 Hz and ends when frequency reaches the value of 50.05 Hz. The gradient of active power reduction is set to 40 % / Hz based on rated power in accordance with the values indicated by the grid code requirements [69]. The output of *Overfrequency Reduction* block is transmitted to the block which accomplishes the function of gradient limiting for power change. As a result, the outputs of the *Current Controller* are the stator voltages which are fed to the generator.

7.1.1. Load flow

The local controller responsible for load - flow calculations can be set to one of the following different modes, which are described further in detail.

Constant V

This option corresponds to a PV bus type and its block diagram is shown in Figure 50 where (2) $\rightarrow P, U$ is activated. Voltage control is done locally, i.e. the reactive power output of the generator is controlled to achieve the specified local voltage at its terminal. The dispatched active power output is kept constant. The reactive power will be increased or decreased till either the voltage set point or the reactive power limit is reached.

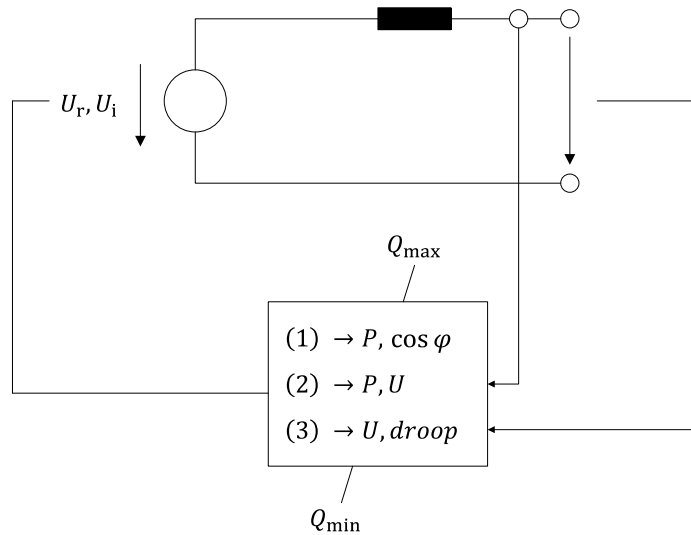


Figure 50: Options for local controller of FRWEC [68]

Constant Q

This option corresponds to a PQ bus type and its block diagram is shown in Figure 50 where (1) $\rightarrow P, \cos \phi$ is activated. With this type of control, active and reactive power outputs at which the static generator will be operated can be specified. The way to specify these values will depend on the *Input Mode* selected. The voltage and droop value boxes are disabled for the *Power Factor* control option.

Voltage Q-Droop

The block diagrams for this option are shown in Figure 51. The droop control corresponds to a proportional control. This means that the amount of reactive power is calculated in proportion to the deviation from the voltage set point entered in the element. The droop control can be used if several voltage controlling machines are placed close to each other [68].

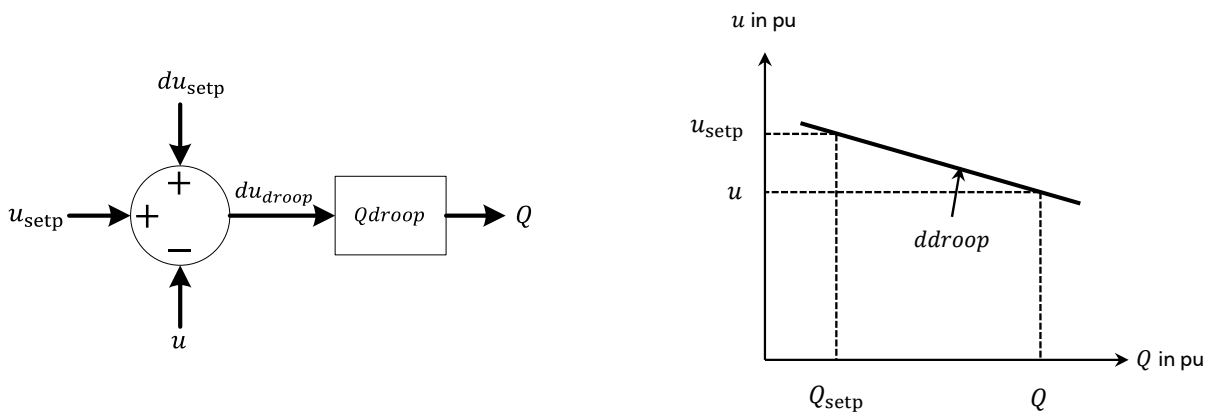


Figure 51: Voltage Q-Droop control of FRWEC model [68]

When set to *Voltage Q-Droop* control, a droop value can be entered. The voltage at the local busbar is then controlled according to the equations below. The equation is shown graphically in Figure 51. It can be inferred that a droop value of 1 % and a voltage deviation of 0.01 p.u. result in an additional reactive power of 100 % of the nominal apparent power of the generator. Similarly a droop value of 2 % and the same voltage deviation of 0.01 p.u. results in an additional reactive power of 50 % of generator's nominal apparent power.

$$u = u_{\text{setpoint}} - \Delta u_{\text{droop}} \quad 7.3$$

$$\Delta u_{\text{droop}} = \frac{Q - Q_{\text{setpoint}}}{Q_{\text{droop}}} \quad 7.4$$

$$Q_{\text{droop}} = \frac{S_{\text{rated}} \cdot 100}{ddroop} \quad 7.5$$

where

u is the actual voltage value at the terminal busbar

u_{setpoint} is the specified voltage setpoint of the static generator

Δu_{droop} is the voltage deviation

Q is the actual reactive power output of the static generator

Q_{setpoint} is the specified dispatch reactive power of the static generator

Q_{droop} is the additional reactive power for 1 % voltage deviation

S_{rated} is the rated apparent power

$ddroop$ is the droop value specified in percentage

Voltage I_q -Droop

The block diagram for this option is shown in Figure 52 *Voltage I_q -Droop* control corresponds to a reactive current controller, in which the reactive current is calculated in proportion to the deviation from the voltage set point entered in the element. The voltage reactive current droop in per unit. is based on the nominal active current of the machine and calculated as follows, using 7.6, 7.7 and 7.8. The dispatched reactive current is calculated by using the nominal voltage of the current connected busbar.

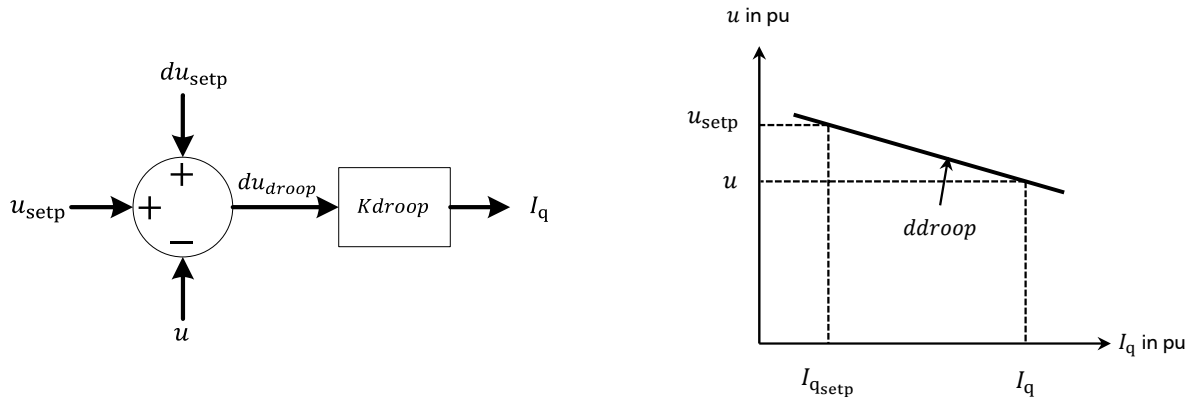


Figure 52: Voltage I_q -Droop control of FRWEC model [68]

The voltage at the local busbar is then controlled according to the equations below.

$$u = u_{\text{setpoint}} + du_{\text{setpoint}} - \Delta u_{\text{droop}} \quad 7.6$$

$$\Delta u_{\text{droop}} = \frac{I_q - I_{q_{\text{setpoint}}}}{K_{\text{droop}} \cdot I_{p_{\text{nom}}}} \quad 7.7$$

$$K_{\text{droop}} = \frac{100}{ddroop} \quad 7.8$$

where

u is the actual voltage value at the terminal busbar

u_{setpoint} is the specified voltage setpoint of the static generator

Δu_{droop} is the voltage deviation

du_{setpoint} is the voltage deviation coming from the static generator

I_q is the reactive current output of the machine

$I_{q_{\text{setpoint}}}$ is the reactive current setpoint of the machine

K_{droop} is the gain

$I_{p_{\text{nom}}}$ is the nominal active current

$ddroop$ is the droop value specified in percentage

The principal functions about the load flow calculation for the used FRWEC model have been presented. Next sections present stability analysis functions of this model.

7.1.2. Stability Analysis

The static generator supports two different models. The first one called *current source model* and the second one *voltage source model*. Depending on the connected input signals the current or the voltage source model is used. If both signals are connected the voltage source model is used. If no input signal is connected, the static generator behaves like a constant current source and the current values from the load flow are used [68].

Current Source Model

In case of a current source model there are input signals that have to be connected and they are the following ones:

$i_{d.ref}$: d-axis current reference in p.u.

$i_{q.ref}$: q-axis current reference in p.u.

$\cos ref$: cosine (dq-reference angle)

$\sin ref$: sine (dq-reference angle)

As far as $\cos ref$, $\sin ref$ signals are concerned, they can be connected from a PLL model. Figure 53 presents the current source model of FRWEC model.

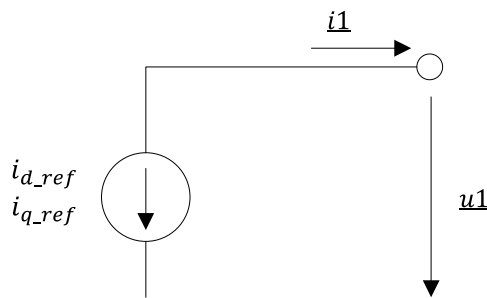


Figure 53: Current source model of FRWEC [68]

Following equations are used:

$$\underline{i1} = (i_{d.ref} \cdot \cos u - i_{q.ref} \cdot \sin u) + j \cdot (i_{d.ref} \cdot \sin u - i_{q.ref} \cdot \cos u) \quad 7.9$$

If the input signals $\cos ref$ and $\sin ref$ are connected, then

$$\cos u = \cos ref \text{ and } \sin u = \sin ref \quad 7.10$$

If the input signals are not connected, then $\cos u$ and $\sin u$ are internally calculated by using the terminal positive sequence voltage u_1 . If the voltage underruns the *Min. Operating Voltage* then $\underline{i}_1 = 0$ and the machine is switched again when the voltage is higher than 5 % of the minimum operating voltage.

Voltage Source Model

Similarly to the current source model, the voltage source model requires input signals as well. These are:

u_{1r_in} : Voltage Input, real part of positive sequence in p.u.

u_{1i_in} : Voltage Input, imaginary part of positive sequence in p.u.

In addition to the input signals, there are input parameters required in order to fulfil the values needed for the calculation. These parameters are:

u_k : series reactor, short circuit impedance

P_{cu} : series reactor, copper losses

The voltage source model is presented in Figure 54 and is used if the two input signals “ u_{1r_in} ” and “ u_{1i_in} ” are connected, otherwise the current source model is used.

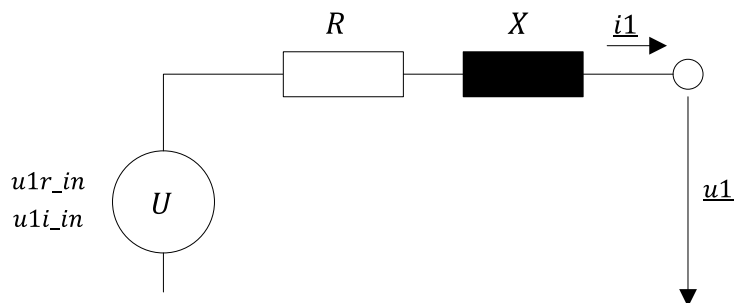


Figure 54: Voltage source model of FRWEC [68]

Following equations are used:

$$u_{1r_in} + j \cdot u_{1i_in} = \underline{u}_1 + \underline{z} \cdot \underline{i}_1 \quad 7.11$$

with $\underline{z} = R + j \cdot X$ which are calculated from the input parameters u_k and P_{cu} . If the voltage underruns the minimum operating voltage, then $\underline{i}_1 = 0$ and the machine is switched again when the voltage is higher than 5 % of the minimum operating voltage.

7.2. Model “4 DIGLOW IPS”

The power system presented in Figure 37 will be extended using the model of FRWEC analysed in 7.1. As far as the topology is concerned, the FRWEC of rated power $S_{rG} = 4.0$ MVA with power factor of 0.9 will be connected at the same busbar of L1 so as to be far away from APS, as it is mostly the case in IPSs. A step/down transformer 20kV/400V is required as well. In Figure 55 an overview of “4 DIGLOW IPS” can be found.

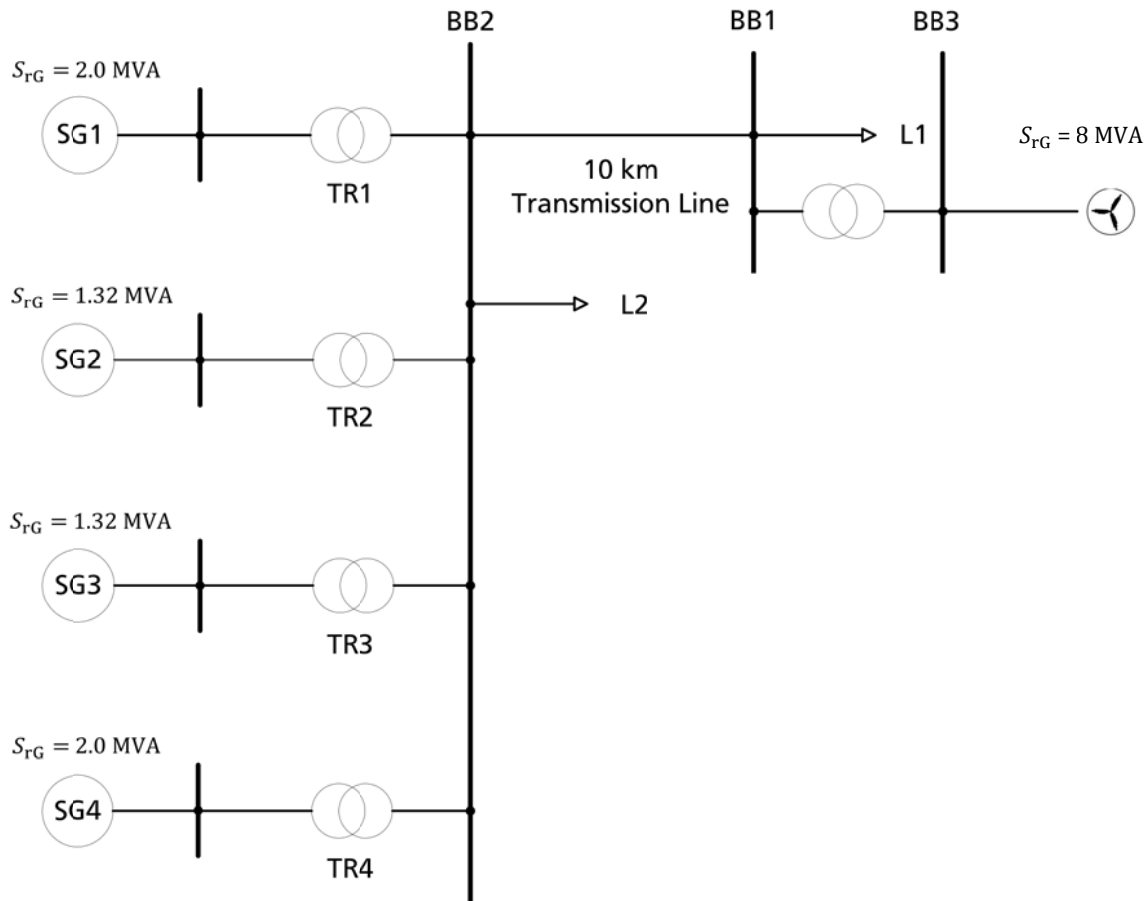


Figure 55: Overview of “4 DIGLOW IPS”

According to this power system model, power infeed scenarios are developed and dynamic simulations demonstrate the effect of power generation units without inertia response respectively.

7.2.1. Load-flow results of “4 DIGLOW IPS”

The concept of three loading scenarios is followed further. The loads are adapted so as to consume the additional power coming from the wind power converter. For further exploration of wind power penetration, Scenario A and Scenario C with different wind power penetration limits are presented, because they are the most crucial ones and represent the worst case for a stability analysis with a high

wind power penetration. Load - flow results for for Scenario A_WP30 can be seen in Figure 56. *Scenario A_WP30* means a wind power penetration of 30 % (with reference to the loads) and *Scenario A_WP70* means a wind power penetration of 70 %. The same is valid for *Scenario C_WP30* and *Scenario C_WP70*. The notation of Scenario A and Scenario C remains as the generator loading and equals approximately to 30 % and 70 % respectively. Load - flow results for all remaining scenarios can be found in Appendix and are illustrated at the same way in Figure 5A, Figure 6A and Figure 7A.

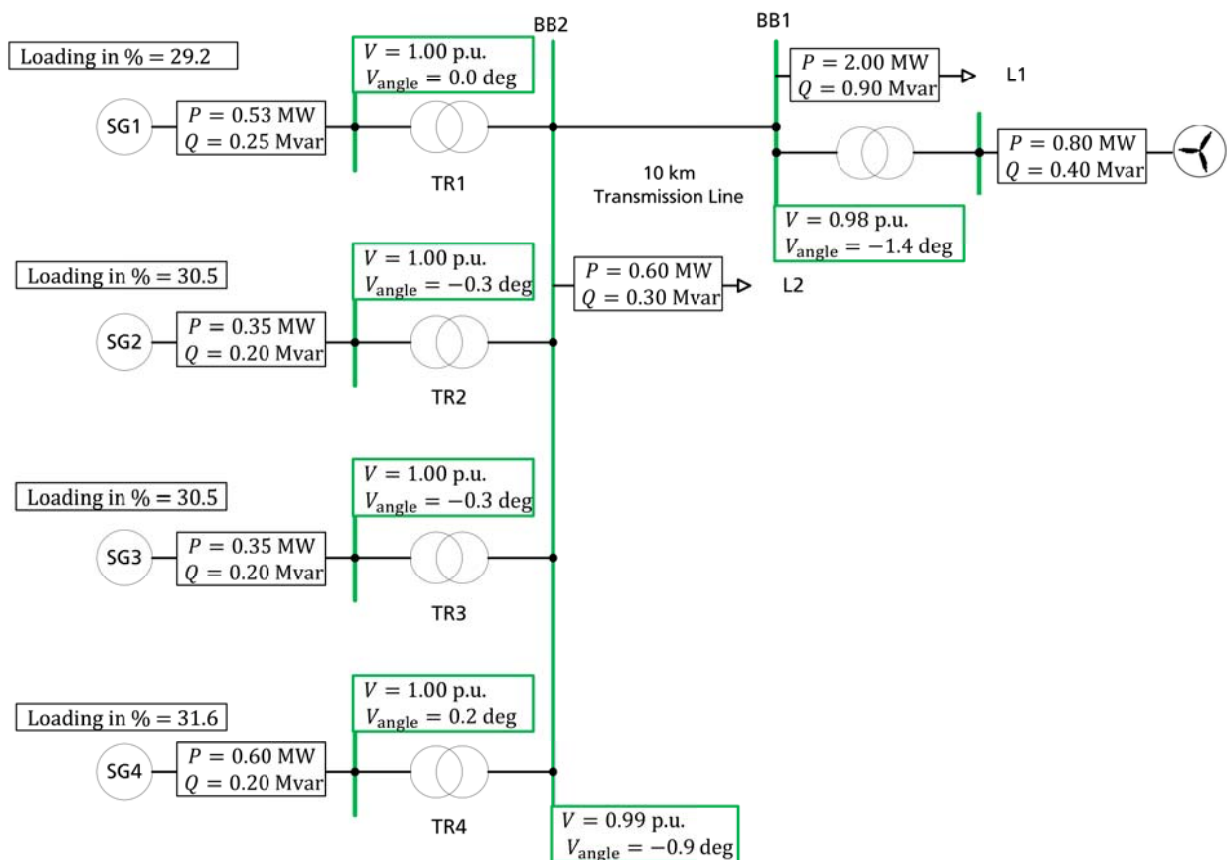


Figure 56: Load - flow results for Scenario A_WP30 of "4 DIGLOW IPS"

7.2.2. Dynamic simulations

Dynamic simulations now demonstrate the influence of power generation sources without inertia support. The most extreme cases are simulated with the values before and after tuning, corresponding to initial "4 DIGLO IPS" so as to prove if tuned values for power systems without RESs would have a positive influence on power systems including them as well. A generator tripping for Scenario A_WP30 and

Scenario C_WP30 and tripping of a *wind power plant* (WPP) for Scenario A_WP70 and Scenario C_WP70 are simulated, since these cases represent a worst case scenario. Consequently a three - phase short circuit is simulated. In this way, it can be validated whether the power system would remain stable after such an event and if the tuned values improve dynamic response. Acceptable frequency limits remain as mentioned in 3.4.1.

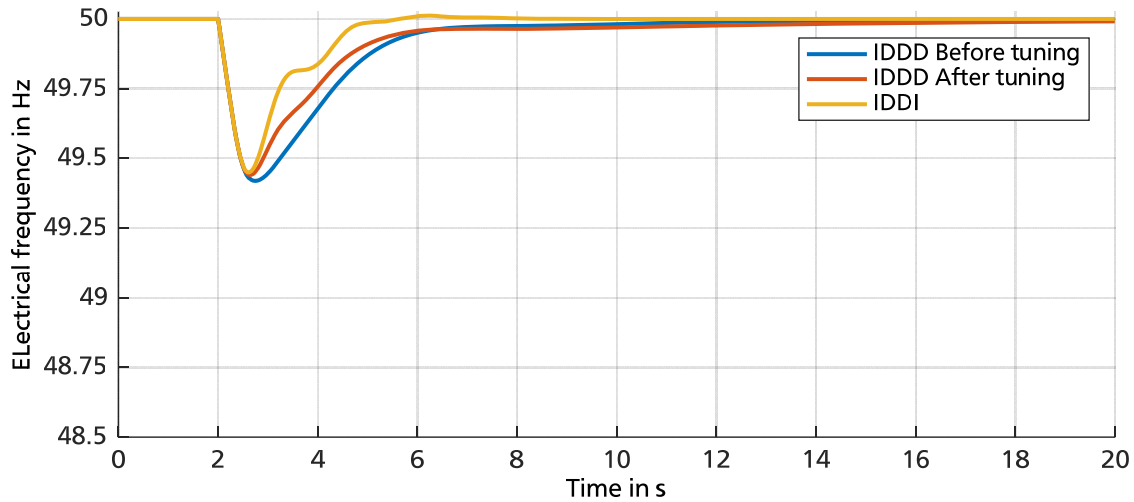


Figure 57: Electrical frequency before and after tuning in case of SG2 and SG3 tripping for Scenario A_WP30 – “4 DIGLOW IPS”

Figure 57 presents electrical frequency response in case of SG2 and SG3 tripping at $t = 2$ seconds and corresponds to a power loss of 0.7 MW. It can be seen that the system remains stable and tuning improves the dynamic behaviour slightly. IDDD cannot be tuned, since SG2 and SG3 with a droop speed governor are out of operation after tripping and tuning does not influence dynamic behaviour. It can also be seen that there is no frequency deviation after fault. This is the effect of isochronous speed governor, which simultaneously implements primary and secondary frequency control in IPSs.

Consequently, WPP tripping at $t=2$ seconds corresponding to 2.5 MW and to 36% of the whole fed power of the power system is presented in Figure 58.

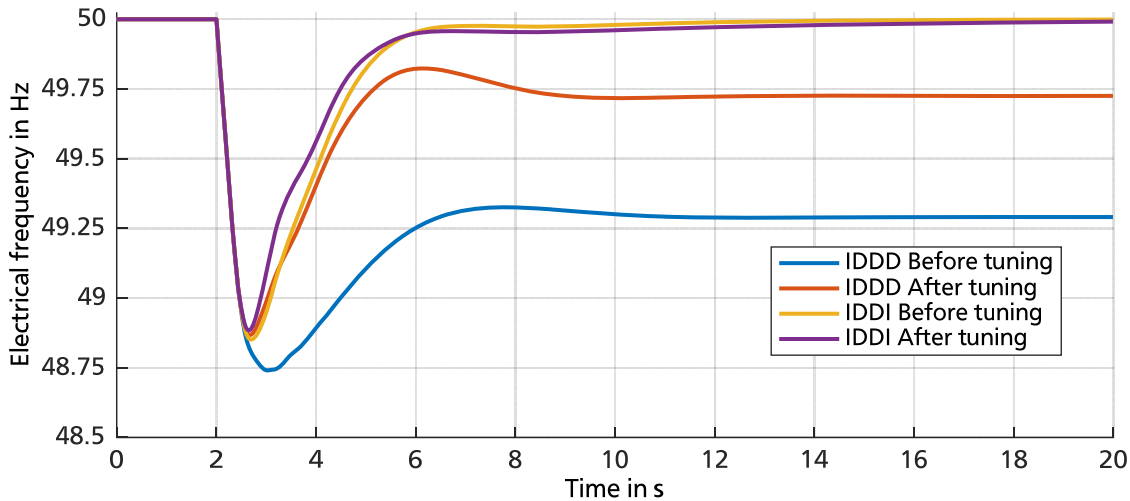


Figure 58: Electrical frequency before and after tuning in case of WPP tripping for Scenario A_WP70 – “4 DIGLOW IPS”

It can be seen that the system remains stable after this simulation event as well, because electrical frequency nadir is bigger than 47 Hz. Tuning has a very positive effect with reference to IDDD since frequency deviations for normal condition after $t = 10$ seconds is before tuning 49.26 Hz and does not fulfil the limit of 49.5 Hz. However, after tuning IDDD reaches permissible value for steady state frequency deviation, as it is the case for IDDI before and after tuning. What is more, IDDI ensures stability during and after the load step in comparison to IDDD, independently of tuning effect.

After the exploration of Scenario A for both cases of wind power feed, Scenario C is presented at the same way. In Figure 59 tripping of SG2 and SG3 corresponding to a 1.7 MW power loss can be seen.

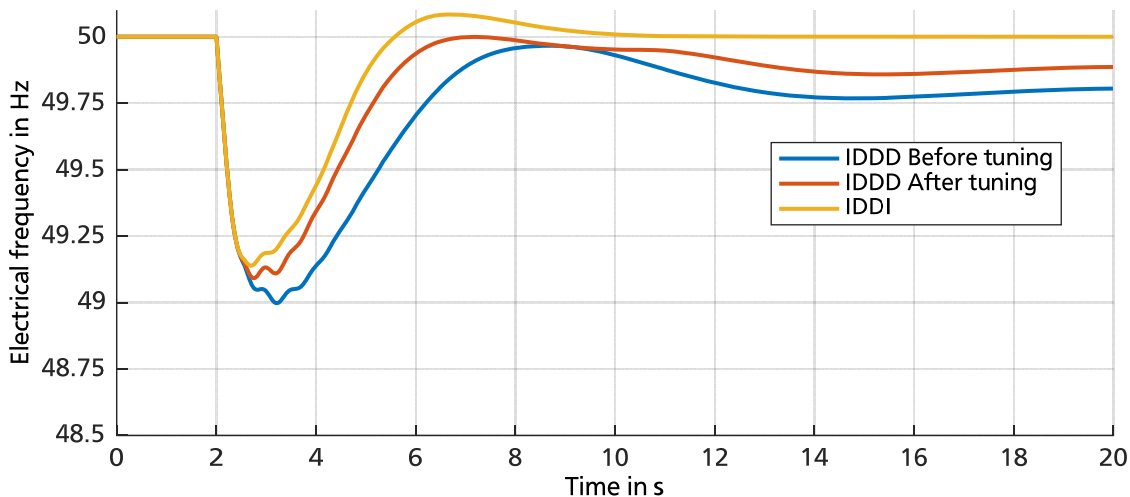


Figure 59: Electrical frequency before and after tuning in case of SG2 and SG3 tripping for Scenario C_WP30 – “4 DIGLOW IPS”

Comparing now Figure 59 to Figure 57 it can be seen that due to a higher loading of the synchronous generators in operation, final frequency deviation is not any more equal to zero for the same tripping,

although it remains within the permissible values for normal operation. The limit of 47 Hz regarding abnormal conditions is further fulfilled and the system would remain stable.

Furthermore, a wind power loss of 2.8 MW is presented in Figure 60. The model “4 DIGLOW IPS” remains stable, since frequency remains above the under limit of 47 Hz. The positive effect of tuning is further to be seen. Comparing Figure 58 to Figure 60 it is interesting to remark that for the case of an approximately same power loss, frequency nadir for Scenario C is not so low for Scenario A, caused by the fact that power loss is in relation to the total power demand not as big as the WPP tripping presented in Figure 58. Electrical frequency does not reach the nominal value for any combination or tuning condition. However, IDDD does not fulfil the criterion of reaching a value above 49.5 Hz after the event. Final frequency deviation lies between the permissible values for all other combinations and tuning conditions.

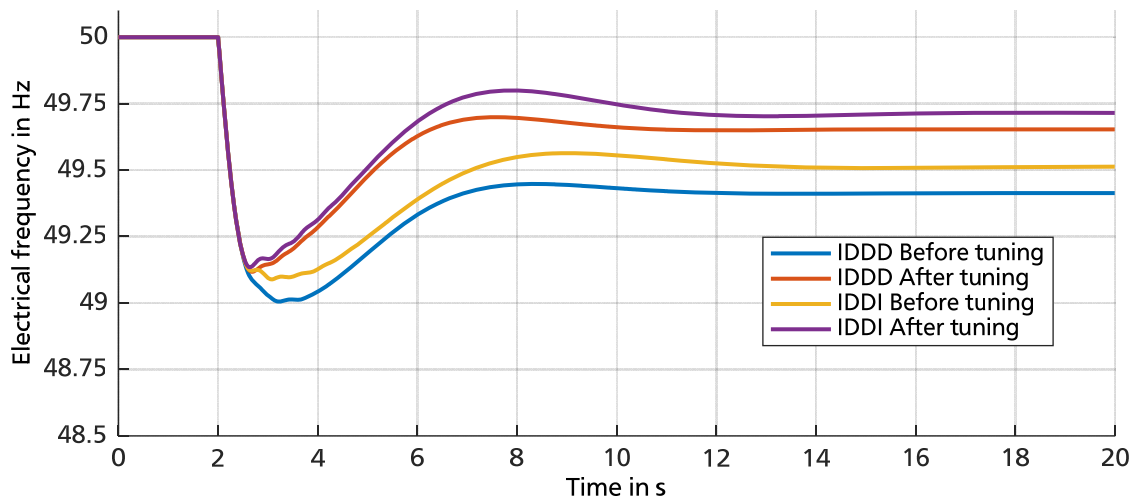


Figure 60: Electrical frequency before and after tuning in case of WPP tripping for Scenario C_WP70 – “4 DIGLOW IPS”

At last for both scenarios with different wind power infeed a three - phase short circuit is simulated.

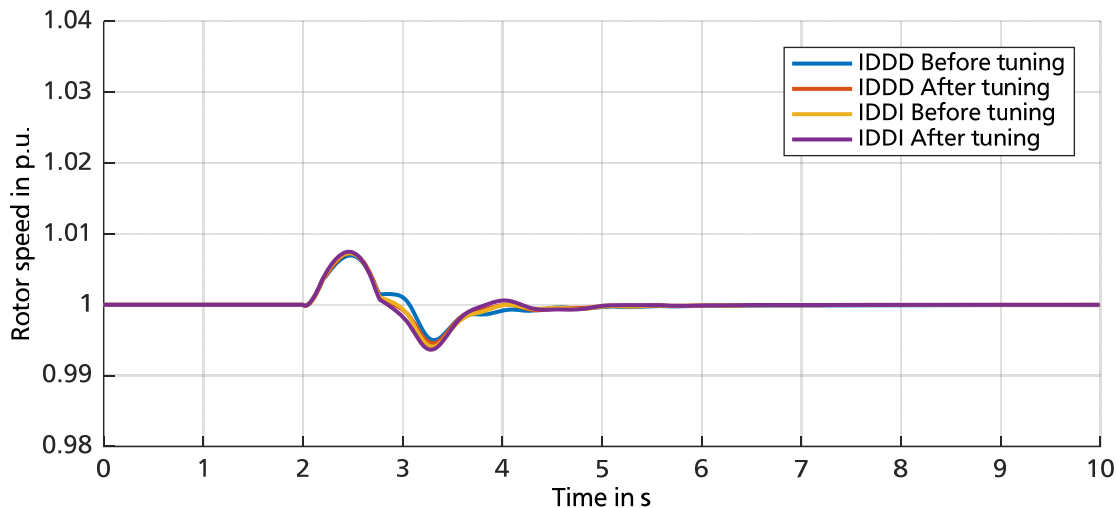


Figure 61: Rotor speed of SG1 before and after tuning in case of a three - phase short circuit for Scenario A_WP70 – “4 DIGLOW IPS”

Figure 61 presents rotor speed response in case of a short circuit for Scenario A_WP70. It can be seen that in case of high wind power penetration, a short circuit does not threaten power system stability. Additionally, selection of speed governing concept as well as tuning does not affect dynamic response as already mentioned, since tuning goal is selected to reject steps.

Consequently, for Scenario C and the same wind power infeed, a three - phase short circuit is presented in Figure 62. It can now be seen that a 70 % loading of generators influences maximum value of synchronous generator SG1 rotor speed, as it was expected. The reason is that the additional active power accelerates the rotor of the machine more than in case of a 30 % loading.

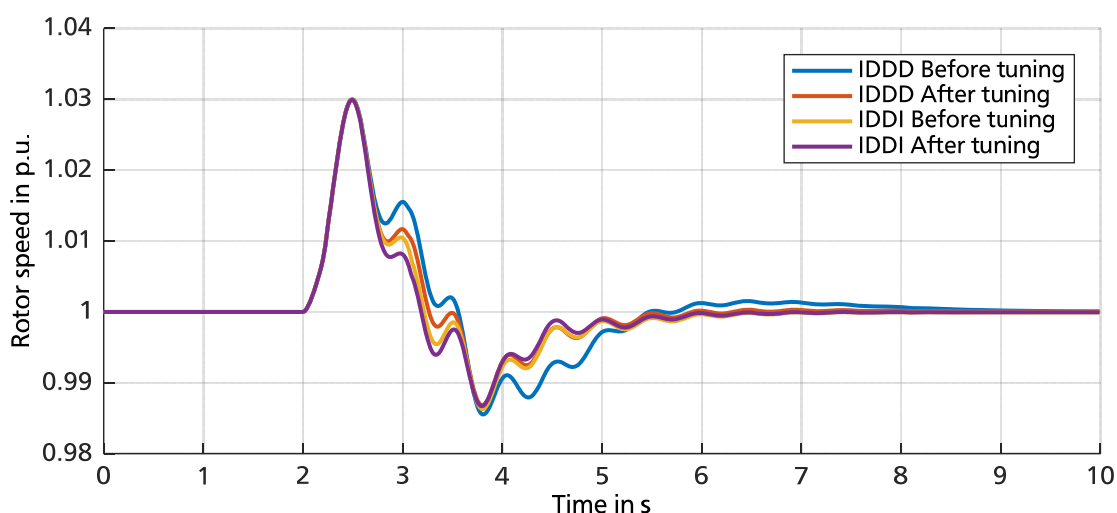


Figure 62: Rotor speed of SG1 before and after tuning in case of a three - phase short circuit for Scenario C_WP70 – “4 DIGLOW IPS”

To sum up, at the end of this chapter a brief conclusion session is provided to underline the results regarding the extension of “4 DIGLOW IPS”, the application of tuning in this model and its dynamic response.

7.3. Conclusion and discussion

In this chapter the extension of “4 DIGLOW IPS” is implemented by integrating a fully rated wind energy converter. The intension is to compare dynamic response of the power system without renewable energy sources to a model having ones, as well as to demonstrate the effect of tuning also for models with renewable power generation.

It has been demonstrated that:

1. Tuning values improve dynamic response “4 DIGLOW IPS” model, meaning that although tuning has been realised for the model without FRWEC, the tendency of decreasing the value of droop works for systems with power generation coming from non-conventional generators.
2. Tuning has a very positive effect especially for IDDD concerning final frequency deviations, which are before tuning outside the permissible values.
3. The effect of combinations is also valid for this model. IDDI proves a more stable behaviour in comparison to IDDD, especially demonstrating the effect of integrated secondary control in IPSs having a larger amount of speed governors without droop function.

A general conclusion from Chapters 5, 6 and 7 is that *the more isochronous speed governors are in operation in an IPS, the more stable the system, since primary and secondary frequency control is provided.* Therefore, tuning results comply with this principle and according to the loading of the synchronous machines the droop constants of droop speed governors tend to decrease. These results are applicable in IPSs with conventional synchronous generators exclusively or in systems with FRWEC as well. As a result, isochronous load sharing would be a best practice frequency control concept for IPSs without RESs as presented in Chapter 6 but in isolated power systems with integrated fully rated wind energy converter as well.

8. A real isolated power system – Case study of Lesbos IPS

In this chapter the results from previous chapters will be applied for a real case of IPS. Definition of steady-state scenarios as well as dynamic simulations is thought to demonstrate the effect of compared frequency control concepts as well as tuning of speed governors. The IPS of Lesbos island is presented, analysed and modelled according to real data of the power system topology and operation points that have been provided from Hellenic Electricity Distribution Network Operator (HEDNO). In the field of this thesis, Lesbos power system is modelled for the first time aiming to analyse and validate power system frequency stability.

8.1. Lesbos isolated power system topology

HEDNO has disposed all necessary data including information about power generation, distribution and consumption as well as measurement data for modelling of power system's loading conditions. It represents the operation condition of the year 2012 and it is the first time of modelling this whole power system in complete accordance to real data for frequency stability studies [70].

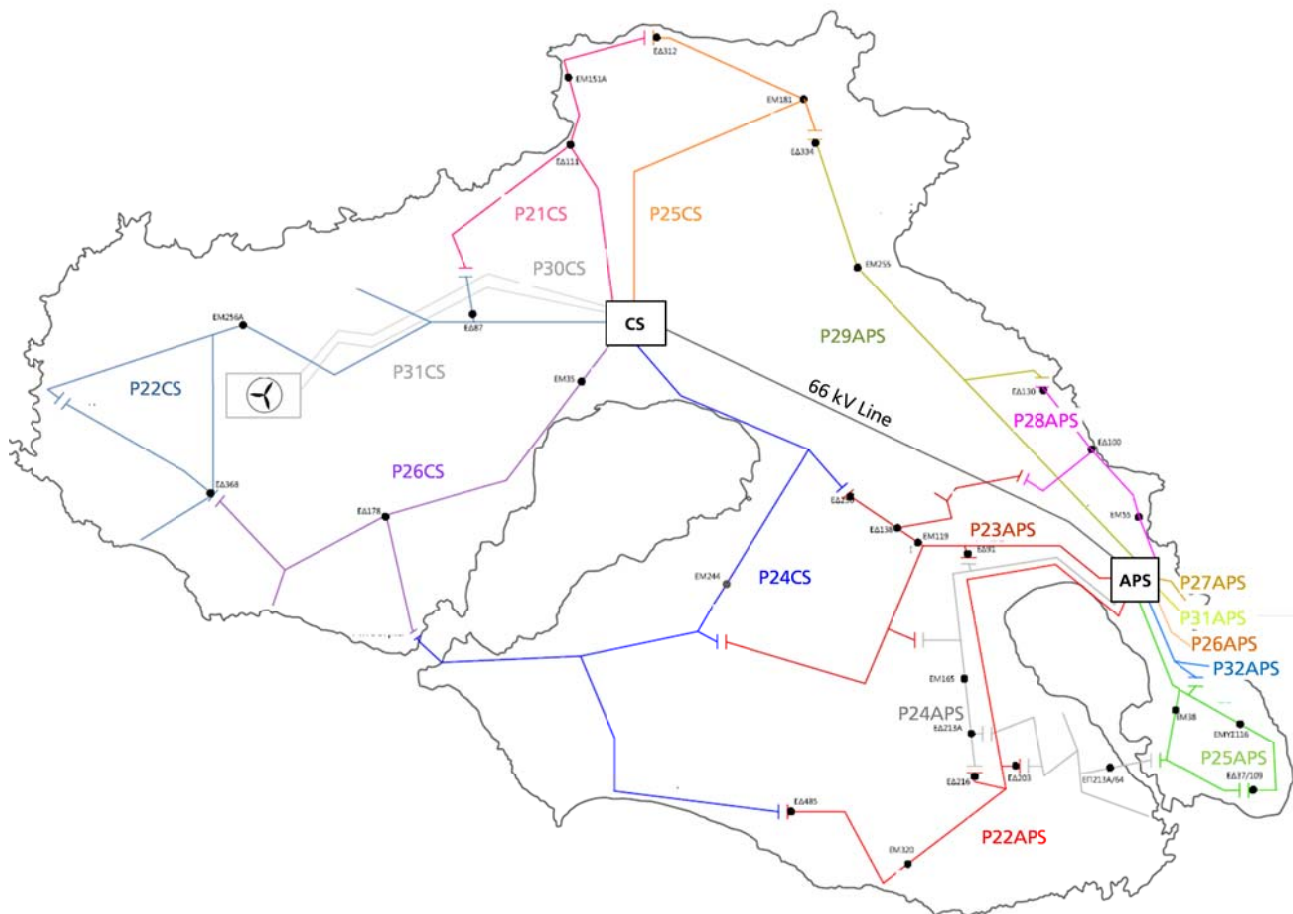


Figure 63: Lesbos isolated power system

In Figure 63 a geographical overview as well as an overview of power system topology can be seen. There is a central power station located near the main city of the island denoted as APS and is composed exclusively from DGs. All lines that are presented in Figure 63 have a nominal voltage of 20 kV except for one line connecting the APS with a second central substation (CS). The low voltage grid is not presented and has respectively not modelled in detail. A detailed power system structure is presented in Figure 64.

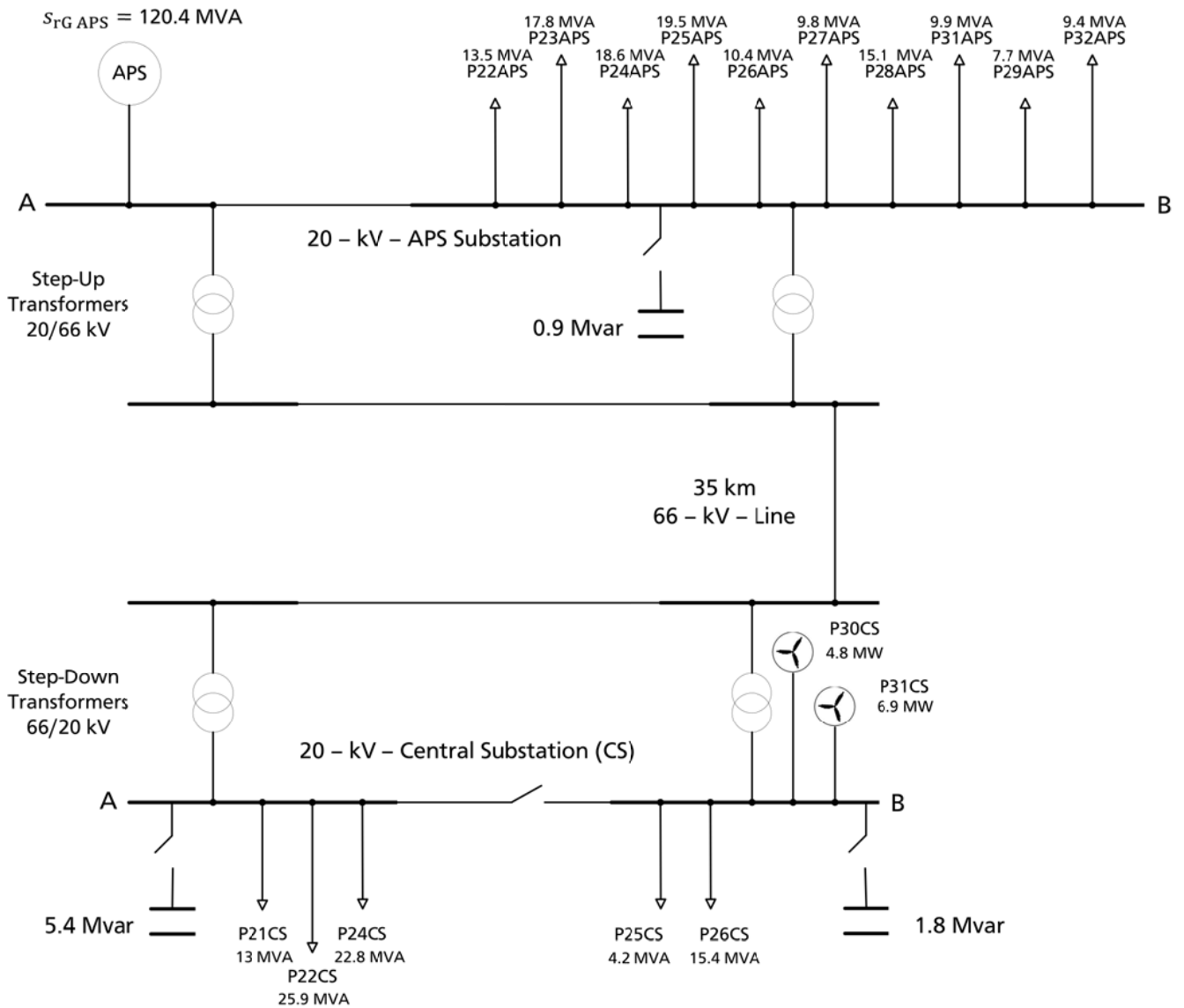


Figure 64: Simplified diagram of Lesbos island power system

Figure 64 represents a simplification of Lesbos power system to give an overview of power system's structure and components. It consists of four central double busbars of 20 kV and four central busbars of 66 kV. The 66 - kV-line serves power distribution from APS to the 20 - kV - CS and finally to the low voltage consumers. The n - 1 criterion is served through possible connection points between the 20 - kV - feeders. The model consists of the MV - grid with 20 kV and a HV - grid with the voltage level of

66 kV. The APS and all feeders belong to the MV – grid. Two step-up and two step – down transformers respectively interconnect the MV – and HV – system. The HV overhead line has a length of approximately 35 km. The 66 – kV and 20 – kV – levels are modelled completely [70].

8.1.1. Power Generation

The power generation is ensured by three types of generators in the Island of Lesbos. A set of 17 DGs with a rated power of 120.4 MVA constitute the APS of the island. A nominal power of 14.4 MW can be generated by wind power plants and around 5.7 MW installed power of photovoltaic cells. Two feeders are dedicated exclusively for the interconnection of wind farms (P30CS and P31CS). The photovoltaic cells are connected in reality to the LV-grid that has not been modelled and considered. The generation units (conventional and renewable) are modelled according to the data provided by HEDNO for the realisation of stability studies [70].

Autonomous Power Station

The APS consists of 17 DGs, which are not directly connected to the 20-kV- APS busbar. Nine of them have a rated voltage of 6.3 kV, seven of 0.4 kV and one generator of 11 kV respectively. Power transformers with tap changers have been used to enable their connection to the 20 -kV -APS, in complete accordance to the original data of the transformers installed that provided from the HEDNO [70].

One group is composed of six generators (G03, G05, G06, G07, G08 and G09) with a rated power between 13.2 MVA and 18.4 MVA. Respectively another group (G01, G02, G04 and G10) consists of generators with a rated power between 3.9 MVA and 7.3 MVA, whereas portable generators of the third group (G11 – G17) have a rated power of 1.5 MVA. Inertia time constant rated to S_{rG} is assumed to be three seconds for all synchronous generators and because no information about the real inertia constant is provided. The concept of grouping the generators enables the definition of different power-infeed scenarios taking into consideration the operation of different DGs demonstrating the influence of choice for generators in operation.

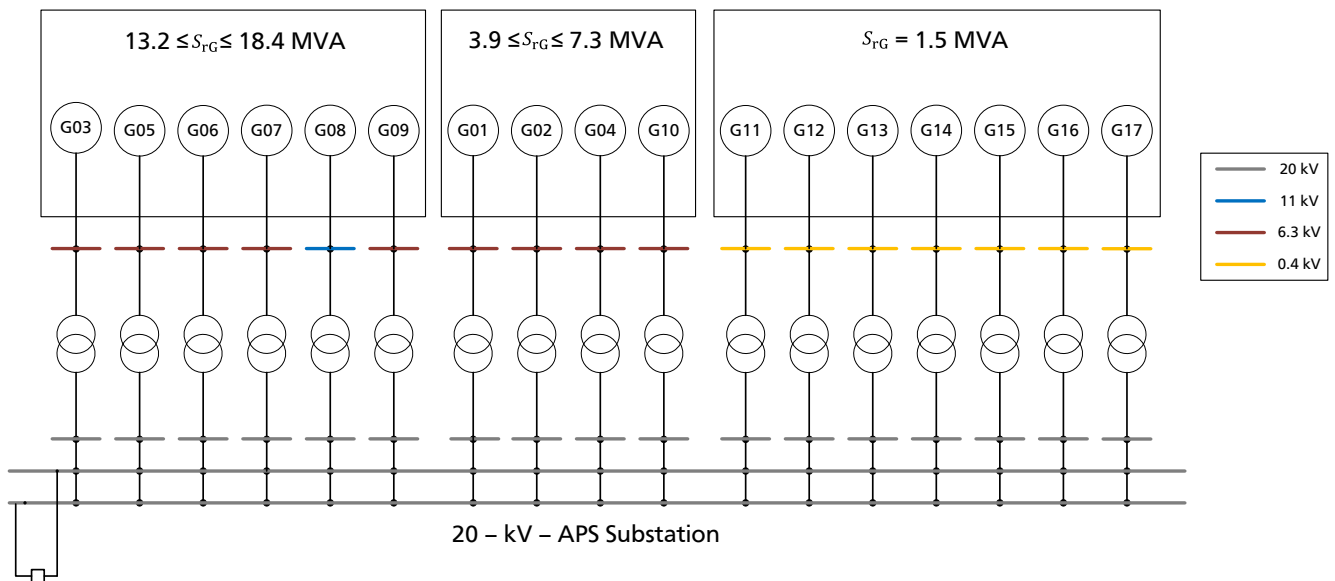


Figure 65: Detailed structure of APS

Voltage support and reactive power demand are served both from shunt capacitors installed at the feeders as well as at both central substations – APS and CS. The maximum amount of reactive power that can be provided from shunt capacitors installed at feeders is 8.1 Mvar. An amount of only 0.9 Mvar is located in APS feeders and the rest of the shunt capacitors are installed at the CS feeders, which aims to supply reactive power to the loads located far away from the APS. Additionally, at the CS 7.2 Mvar are installed. The connection or disconnection for the ones installed at the feeders depends on the loading condition of the power system.

Regarding the governors being used, HEDNO provided information concerning the selection of them for each generator. The largest DG of 18.4 MVA is used as the reference machine and uses an isochronous speed governor based on the Woodward Diesel Governor Model (DEGOV). A droop speed governor has been used for the rest of the DGs based on the Woodward Diesel Governor Model as well (DEGOV1). According to instructions and information provided on behalf of HEDNO, no modifications concerning speed governors models have been carried out, since their response to dynamic events is corresponding to the real network [70].

Furthermore, the excitation system controls the terminal voltage and the reactive power output of the generator and therefore the voltage at the connection point. The automatic voltage regulator avr_ESST1A has been used.

Fully Rated Energy Wind Converters

The wind power infeed is located in four WPPs connected to the feeders according to Figure 64 [71]. All of them are modelled according to the model as presented in Chapter 7. Data is adapted to comply with real provided data [70]. The dynamic behaviour of the model is described in detail in 7.1.2.

Wind turbines are of a rated power of 0.6 MW and 0.9 MW. However active power fed into the grid corresponds to the power coming from the power curve of the wind generators according to wind speed data provided from the Department of Geography of the University of Aegean.

8.1.2. Power Consumption

The power consumption varies dependently on the time period. Power consumption is based on the data provided by HEDNO and corresponds to a real loading situation of December 2012, which was 18.3 MW for minimum load situation including losses and for August of the same year corresponding to maximum load situation including losses, of 59.1 MW. The reason for selecting these months is that after comparing load conditions from January 2011 to December 2013 it has been established that the best match concerning load conditions and high wind speeds appeared in 2012 for these two months. These conditions enable the simulation of the highest wind power penetration. All fifteen feeders belonging to MV-grid serve for the power flow leading to LV- grid and to final consumers.

As far as the feeder is concerned, all feeders apart from the two ones dedicated to connect the wind farms to the power system have been modelled in detail and their last point representing the substation between MV- and LV-grid has been modelled as a general load of input mode S , $\cos \varphi$, using the original apparent power of the substation and a power factor $\cos \varphi$ of 0.9 inductive.

As far as the topology is concerned, the network structure is an open ring one, meaning that each one of the feeders presented in the simplified overview of the power system in Figure 63 includes a similar structure. It is also to be expected that each feeder has possible interconnections with neighbouring feeders according to their geographical distribution, which are in open position for simulation cases. As a result, feeder P24APS presented as example could be connected to feeders P22APS, P23APS and P25APS in different terminals respectively. To sum up, there are fifteen feeders representing the power consumption with a rated apparent power varying between 4.2 MVA and 25.9 MVA and two feeders for connecting of wind farms with a rated apparent power of 4.8 MW and 7.6 MW.

8.2. Power infeed scenarios of Lesbos IPS

As has been already demonstrated, the most crucial scenarios concerning dynamic simulations are the one of minimal and maximal loading with a high wind power penetration. Hence, the scenarios analysed are configured in this way to represent the real load conditions of Lesbos power system but corresponding to Scenario A and Scenario C presented until now in this thesis. The following load - flow results will be used as initial conditions for dynamic simulations.

8.2.1. Load - flow results

Scenario A corresponds to a 30 % loading for the synchronous generators in operation, as this is the case for all models in this thesis. Six from seventeen generators feed the power system with active power. This concept also reflects HEDNO operation practice, since in cases of very low loading some generators have to be shut down and some of them are considered as backup for emergency cases. The load - flow results can be seen in Table 11.

Load - flow results – Scenario A

	Bus Type	V_{base} (kV)	P_{rG} (MW)	Q_{rG} (Mvar)	V (p.u.)	V_{angle} (deg)	P (MW)	Q (Mvar)
G01	PV	6.30	5.85	4.39	1.00	-0.98	2.08	0.02
G02	PV	6.30	5.85	4.39	1.00	-0.98	2.08	0.02
G08	Swing	11.00	14.72	11.04	1.00	0.00	3.92	0.03
G15	PV	0.40	1.22	0.92	1.00	-1.51	0.44	0.00
G16	PV	0.40	1.22	0.92	1.00	-1.51	0.44	0.00
G17	PV	0.40	1.22	0.92	1.00	-1.51	0.44	0.00

Table 11: Load - flow results of Lesbos isolated power system for Scenario A

It can be also seen that the synchronous generators do not feed any reactive power and this happens because of the installed capacitors, which cover the needs of reactive power.

Load - flow results – Scenario C

	Bus Type	V_{base} (kV)	P_{rG} (MW)	Q_{rG} (Mvar)	V (p.u.)	V_{angle} (deg)	P (MW)	Q (Mvar)
G01	PV	6.30	5.85	4.39	1.00	-0.59	4.50	0.49
G02	PV	6.30	5.85	4.39	1.00	-0.59	4.50	0.49
G04	PV	6.30	4.00	3.00	1.00	0.03	2.50	0.34

G06	PV	6.30	11.00	8.25	1.00	-0.97	9.54	0.93
G07	PV	6.30	10.54	7.90	1.00	2.44	9.13	0.89
G08	Swing	11.00	14.72	11.04	1.00	0.00	12.76	1.24
G11	PV	0.40	1.22	0.92	1.00	-1.62	1.06	0.10
G12	PV	0.40	1.22	0.92	1.00	-1.62	1.06	0.10
G13	PV	0.40	1.22	0.92	1.00	-1.62	1.06	0.10
G14	PV	0.40	1.22	0.92	1.00	-1.62	1.06	0.10
G15	PV	0.40	1.22	0.92	1.00	-1.62	1.06	0.10
G16	PV	0.40	1.22	0.92	1.00	-1.62	1.06	0.10
G17	PV	0.40	1.22	0.92	1.00	-1.62	1.06	0.10

Table 12: Load - flow results of Lesbos isolated power system for Scenario C

Additionally, load - flow results concerning four WPPs are presented in Table 13. The power factor of wind generators is set to be 1.0 and therefore no reactive power is fed from wind generators as well.

Load - flow results					
	Bus Type	P_{RG} (MW)	V (p.u.)	V_{angle} (deg)	P (MW)
WPP1	PQ	2.70	1.00	-147.77	1.40
WPP2	PQ	2.70	1.03	-145.35	1.40
WPP3	PQ	4.80	1.04	-144.20	3.20
WPP4	PQ	4.20	1.05	-143.88	2.80

Table 13: Load - flow results of wind power plants of Lesbos isolated power system

The power coming from WPPs corresponds to a wind speed of 10 m/s. WPP3 is connected to P30CS and WPP1 and WPP4 to P31CS. WPP2 is connected to P22APS feeder. After evaluating wind data of the years 2011, 2012 and 2013 the highest wind speed has been selected in accordance to the time period that would represent whether a low or high loading of the network. At this way the extreme cases of wind power penetration are taken into consideration. Consequently, the active power coming from the conventional generation equals 9.4 MW for Scenario A and 50.3 MW for Scenario C and the one coming from WPPs is 8.8 MW. Wind power penetration for Scenario C equals to 48.4 % approaching a limit of

50 % wind power penetration which is with reference to experience data a high wind penetration for Lesbos isolated power system and for Scenario C equals to 14.9 % also representing real operation practice.

8.3. Outlook

After presenting the power system of Lesbos and having configured two simulation scenarios of the most crucial operating points, dynamic simulations will be presented in the next chapter. In order to evaluate the dynamic response of this power system, basic grid code requirements are presented at the beginning and dynamic simulation results verify the effect of conclusions from former chapters.

9. Frequency stability analysis of Lesbos IPS

In this chapter the real case study of Lesbos IPS is further explored concerning dynamic simulations. In the first section an overview of grid code requirements regarding IPS in Hellas is provided. According to this regulation, dynamic response can be further evaluated.

9.1. Grid code requirements

Grid code requirements referring to voltage, frequency, short circuit currents and WPPs are presented in this section.

9.1.1. Voltage

As far as voltage is concerned, every generating unit, which is connected to an IPS has to be connected using a separate transformer, in case that this is required for the interconnection in the respective nominal voltage level of the IPS in the point of connection. There are probably differences in comparison to international standards, but these values based on EN 50160 and are in accordance with the operation requirements for these IPSs [20].

The normal operating voltage has the following values:

- Low-voltage (LV nominal line voltage up to 1 kV)
230 V phase voltage
400 V line voltage
- Medium-voltage (MV line voltage between 1 kV and 35 kV)
20 kV or 15 kV or 6,6 kV
- High-voltage (HV line voltage higher than 35 kV)
150 kV or 66 kV

The acceptable limits for deviations of nominal voltage at PCC of generating units are adapted to ensure a stable operation:

- For the LV-grid: $\pm 10\%$
- For the MV-grid: $\pm 10\%$
- For the HV-grid: from -5% up to $+8\%$ under normal conditions, and from -10% up to $+13\%$ under fault conditions.

The above limits for the LV-grid and the MV-grid refer to measurements over a week period with average voltage values with 10 minutes and as long as they are valid for 95 % and 99 % of the whole time respectively. The above limits of nominal voltage are adapted for the LV-grid and the MV-grid for 100 % of the time to -15% up to $+10\%$.

9.1.2. Frequency

The system operator is responsible for frequency control of IPSs by means of the appropriate control systems of generating units and is based on EN 50160 [20].

The standard frequency is 50 Hz and the acceptable limits of the deviation are defined as follows:

- for 95 % of the time of a week, frequency has to be between 49 and 51 Hz
- for 100 % of the time of a week, frequency has to be between 42.5 and 57.5 Hz.

The above mentioned deviations refer to the average value of the principal frequency measured in time resolution of 10 seconds.

9.1.3. Short - circuit currents

HEDNO defines short - circuit current value (initial symmetric value) with reference to Standard IC 60909 for IPSs. Typical values for the network planning are the following one [20]:

- LV-grid:
 - For underground network, short - circuit current of 25 kA and exceptionally 32 kA.
 - For overhead network, short - circuit current of 8 kA and exceptionally 14 kA.
- MV-grid:
 - For 20 kV nominal voltage, a short - circuit current of 7.2 kA.
 - For 15 kV nominal voltage, a short - circuit current of 9.6 kA.
- HV-grid of 150 kV:
 - Short - circuit current of 31 kA or lower as defined according to IPS system operator.
- HV-grid of 66 kV:
 - Short - circuit current of 12 kA or lower as defined according to IPS system operator.

9.1.4. Wind power plants

As far as control of wind turbines for network faults is concerned, Hellenic grid code focuses on the *Low-Voltage-Ride-Through* (LVRT) requirements. This is the most important requirement regarding WPP operation that has been recently introduced in grid codes. It is vital for a stable and reliable operation of power supply networks, especially in regions with high penetration of wind power generation. Faults in power systems can cause large voltage dips across wide regions and some generation units without this capability can be disconnected as a consequence [72].

A main requirement of grid code is that symmetric or non-symmetric voltage dips are not allowed to lead to disconnection of WPPs, if the voltage remains above the bold green line in Figure 66. Figure 66 shows that each generating unit shall remain transiently stable and connected to the system without tripping for

a three - phase short circuit or any unbalanced short circuit in the transmission system with a fault clearing - time of up to 150 milliseconds and for a remaining voltage above 15 % of the voltage before the fault. Throughout the operating range of the generating unit, these types of faults must not result in instability or isolation from the network. Furthermore, Figure 66 shows that power units shall be capable of continuous operation down to 90 % of the voltage before the fault at PCC [20].

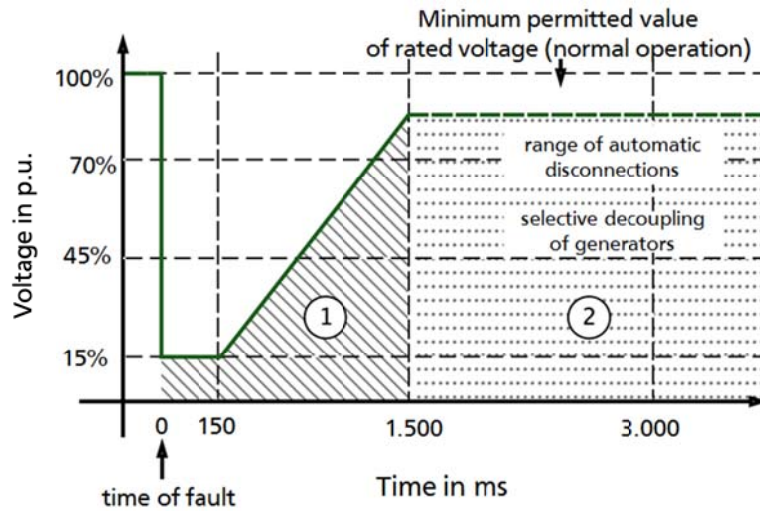


Figure 66: Voltage requirements for LVRT [20]

However, a short disconnection from the IPS is allowed in any case for voltages that correspond to Area 1 of Figure 66. The WTGs have to resynchronise in a time period shorter than two seconds with a gradient of between 10 and 20 % of the rated power per second. Resynchronisation time larger than two seconds and rate of active power smaller than 10 % of rated power are allowed exceptionally and only after approval of HEDNO.

Additionally, in case of voltage dips of a duration larger either 1.5 seconds and outside the acceptable deviation limits (the cases when voltage remains low, whether because of a permanent fault or because of other disturbance – Area 2 of Figure 66), then the automatic disconnection of WPPs is allowed for protection reasons. The disconnection has to take place in three phases [20].

1. Each phase of disconnection has to abstain from the previous 0.3 seconds and disconnection must take place within this time. In any case resynchronisation of a WPP is allowed to take place when the voltage at PCC has reverted to larger voltage values than the lowest permissible ones for the normal operation of the IPS.
2. Not disconnected WPPs from the IPS during voltage dips have to continue feeding the grid with active power after fault clearance, with a rate of active power feed between 10 and 20 % of their rated power per second.

-
3. WTGs shall provide active power in proportion to retained voltage and maximise reactive current to the transmission system without exceeding their limits during a voltage dip in the transmission system.

Activation of other means for voltage support, as for example automatic connection/ disconnection of capacitors, or system of automatic change of voltage under load for transformer etc, has to operate harmoniously in common with WPP's control system of automatic voltage/reactive power/power factor. The positive effect of additional means for voltage support has to be proved from a study performed by the owner of WPP [20].

9.2. Definition and configuration of frequency stability analysis

As far as Scenario A is concerned, the generators in operation for which load - flow results have been presented in Table 11 realise frequency control combinations at the following way: G08 has always an isochronous speed governor and is the swing machine. Respectively G15, G16 and G17 as transportable diesel engines have always a droop speed governor with a droop constant R_d of 5 % before tuning and a value of 2 % after tuning. G01, G02 realise Comb1.1 having droop speed governor with a droop constant of 5 % before tuning and a value of 2 % after tuning corresponding to their loading condition based on tuning results presented in 6.3. For realisation of Comb1.2 G01 and G02 have isochronous speed governors.

For Scenario C realisation of Com1.1 implies all generators in operation except of swing machine with isochronous speed governor G01, G02, G04, G06, G07, G11, G12, G13, G14, G15, G16, G17 with a droop constant of 5 % before tuning and a value of 3 % after tuning. The swing machine G09 has an isochronous as speed governor for both combinations. For Comb1.2 G01, G02, G04, G11, G12, G13, G14, G15, G16, G17 have a droop speed governor with the same values for the droop constant as for Comb1.1. Synchronous generators G06, G07 have isochronous speed governors.

Taking as basis the existing loading scenarios, dynamic simulations of generator tripping and short circuits are performed to analyse power system stability. Both combinations before and after tuning are presented. From now on and for this IPS, electrical frequency is presented and not the rotor speed of one generator, so as to enable a better overview of the power system's behaviour and to compare directly to the values given from HEDNO in grid code.

Table 14 presents a brief overview of the generators in operation and the used speed governors for each scenario and combination.

Generator	Comb1.1		Comb1.2	
	Scenario A	Scenario C	Scenario A	Scenario C
G01	Droop	Droop	Isochronous	Droop
G02	Droop	Droop	Isochronous	Droop
G04	not in operation	Droop	not in operation	Droop
G06	not in operation	Droop	not in operation	Isochronous
G07	not in operation	Droop	not in operation	Isochronous
G08	Isochronous	Isochronous	Isochronous	Isochronous
G11	not in operation	Droop	not in operation	Droop
G12	not in operation	Droop	not in operation	Droop
G13	not in operation	Droop	not in operation	Droop
G14	not in operation	Droop	not in operation	Droop
G15	Droop	Droop	Droop	Droop
G16	Droop	Droop	Droop	Droop
G17	Droop	Droop	Droop	Droop

Table 14: Overview of synchronous generators in operation and relevant speed governors for each scenario and combination

9.2.1. Generator tripping

As a first simulation, a generator tripping corresponding to 4.16 MW active power loss is simulated. G01 and G02 tripping at $t = 2$ seconds and dynamic response can be seen in Figure 67. Because of limited options concerning generator tripping selection, both combinations coincide. Therefore only the property of tuning can be seen.

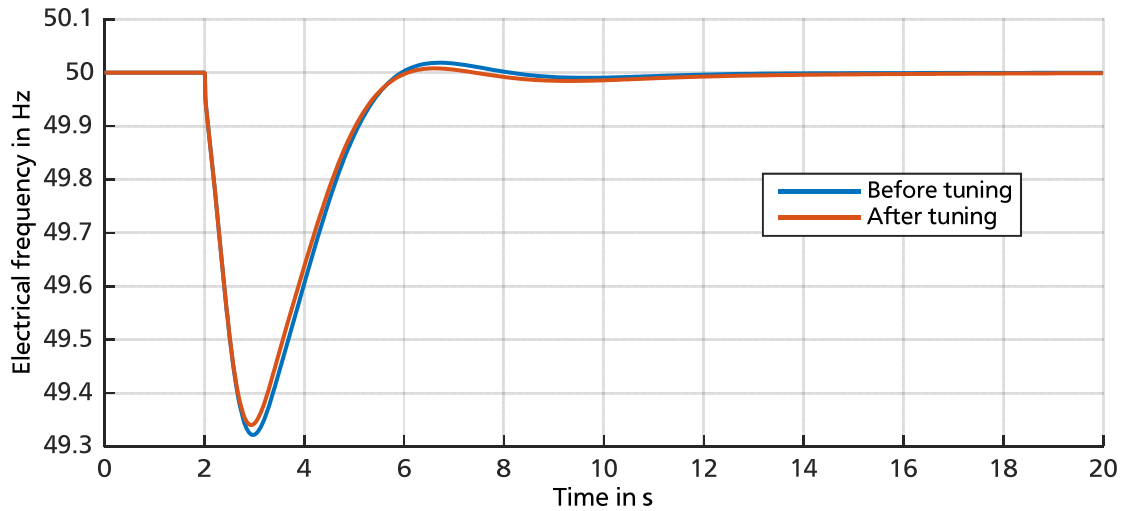


Figure 67: Electrical frequency of Lesbos IPS in case of SG tripping for Scenario A

The permissible margins concerning assessment of frequency stability presented in 9.1 are 42.5 and 57.5 Hz for abnormal conditions and 49 and 51 Hz for normal operation. As it can be seen in Figure 67, frequency remains within the acceptable margins and tuning does not play a major role in system response in such a case. Consequently, the same tripping is presented in Figure 68 concerning Scenario C. It is worth mentioning that tripping of G01 and G02 corresponds only to a 9 MW power loss for Scenario C but this is the upper limit without losing stability. A power loss above this percentage would lead to a system collapse without adding more generators in operation to feed active power, because of high loading of generators in operation.

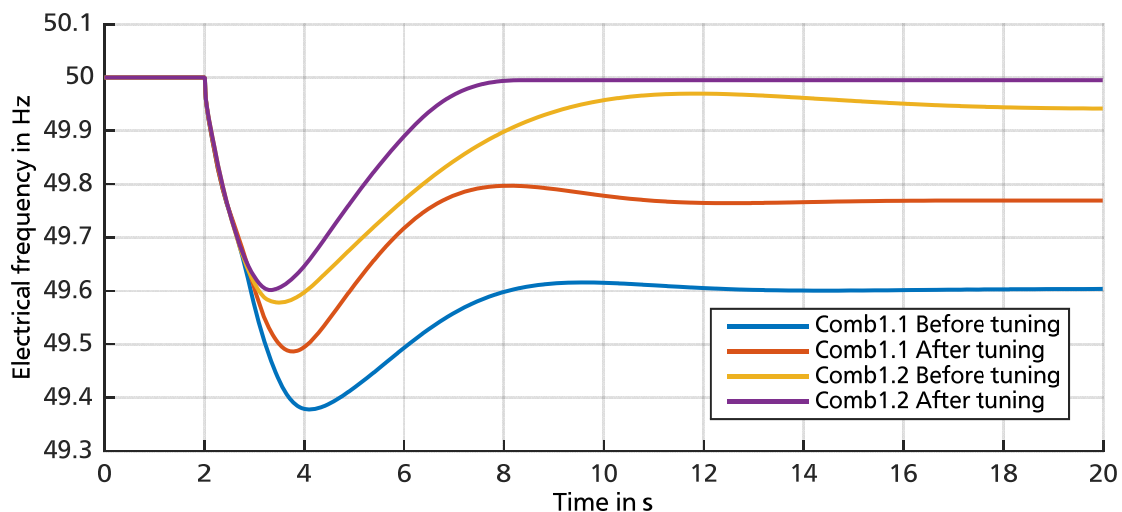


Figure 68: Electrical frequency of Lesbos IPS in case of SG tripping for Scenario C

It is also interesting that although tripping of the same generators for Scenario A could be expected to have a more severe effect, since their participation in total system active power infeed is higher than for Scenario C, it is in Scenario C that this power loss is of main importance. This is caused by higher loading

of all other generators in operation for Scenario C that cannot cover the additional power required after this loss. Therefore, in case of conventional power tripping generator's loading condition plays a major role assuming a constant wind power infeed, as in this case. Furthermore it can be seen in Figure 68 that for a high loading scenario Comb1.2 after tuning restores nominal frequency six seconds after tripping and the same combination before tuning causes a frequency deviation of 0.05 Hz. Comb1.1 on the contrary exceeds the limit of 49 Hz, which is valid for normal operation and remains within the acceptable margins causing a final frequency deviation of 0.45 Hz from nominal value. Tuning has a positive effect for Comb1.1 reducing frequency minimum value as well as final frequency deviation.

9.2.2. Wind power plant tripping

After having simulated the case for a power loss due to SGs tripping, a power loss because of WPP tripping is simulated as well. It is assumed that in $t = 2$ seconds the breaker of feeder P31KCS opens and causes tripping of two WPPs. This power loss equals to 4.2 MW and corresponds to 23 % power loss for Scenario A and to a 7.1 % for Scenario C. Frequency response can be seen for Scenario A in Figure 69 and for Scenario C in Figure 70.

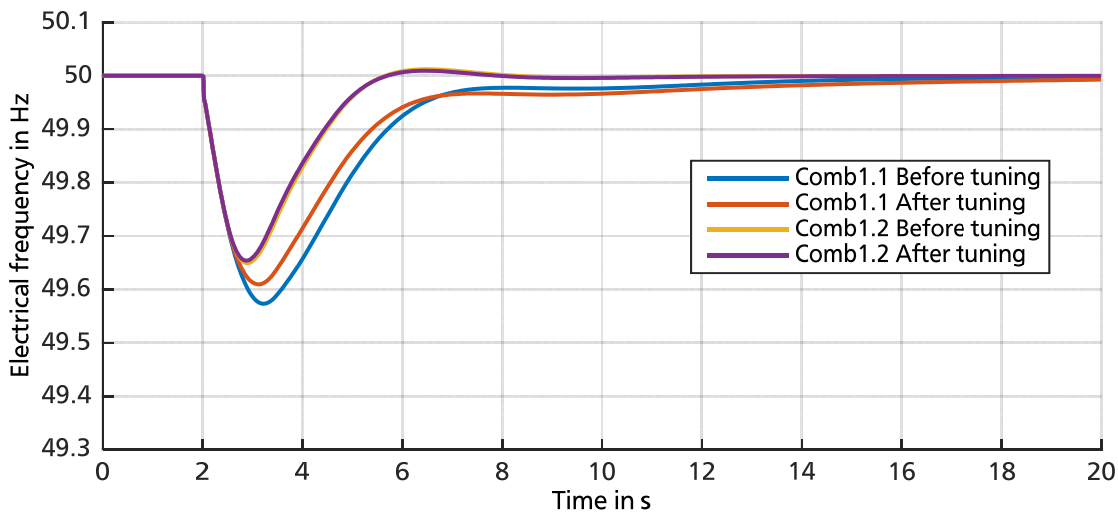


Figure 69: Electrical frequency of Lesbos IPS in case of WPP tripping - 25 % power loss for Scenario A

It is interesting to compare Figure 67 and Figure 69, since they represent approximately the same power loss in percentage with the difference that the first one is caused by SG tripping and the second one by WPP tripping. Frequency response is the one expected; meaning that in case of tripping of feeder P31KCS frequency nadir is not so low, because the DGs remain in operation and adapt their operating point to a new one providing power missing after tripping. On the contrary, FRWEC are assumed to feed the IPS with a constant power and they will not support with additional active power in case of DG tripping.

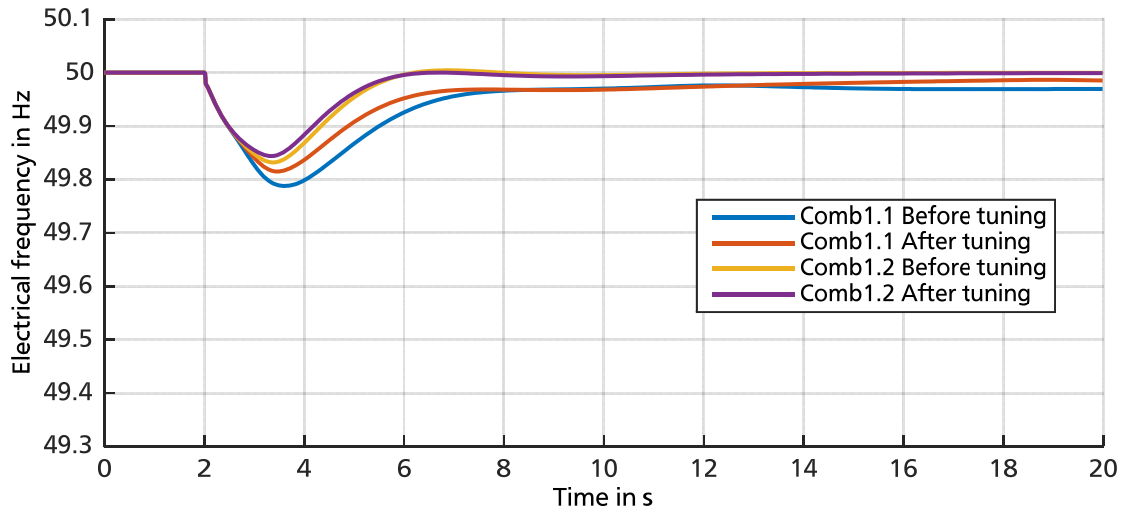


Figure 70: Electrical frequency of Lesbos IPS in case of WPP tripping - 7 % power loss for Scenario C

Figure 70 demonstrates the case of a high loading condition for the DGs and tripping of P31KCS feeder. This event would not threaten stability at all, since on the one side the amount of power loss of 7 % is relatively low and on the other side wind power penetration of 15 % is not so high to be critical.

9.2.3. Three - phase short circuit

The last phase of stability analysis is as in all models before a three - phase short circuit at the bus bar where all DGs are connected. In Lesbos power system this busbar is the APS busbar and at $t = 2$ seconds a three - phase short circuit is applied with duration of 150 ms. Figure 71 shows electrical frequency during and after this event for Scenario A.

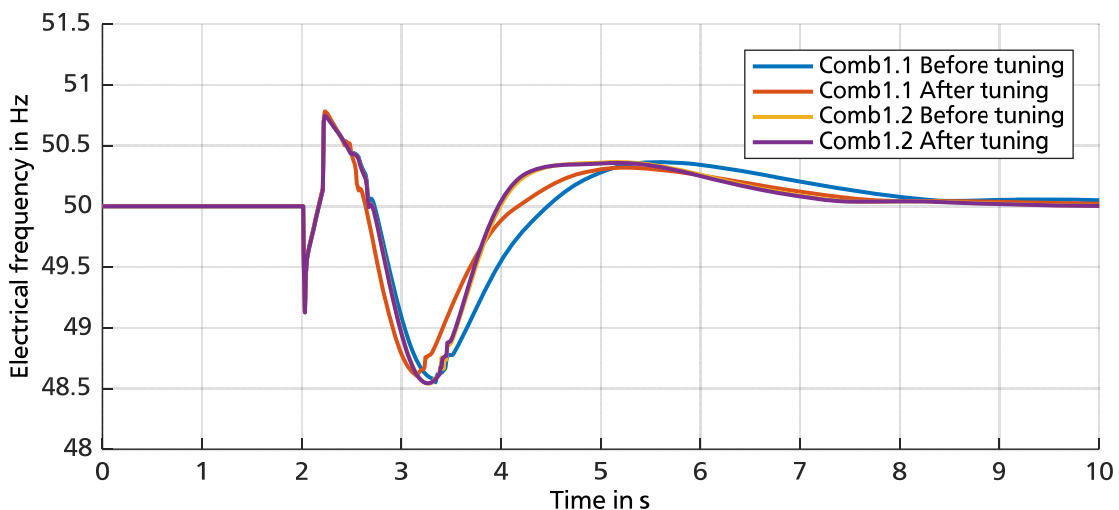


Figure 71: Electrical frequency of Lesbos IPS in case of a three - phase short circuit at APS busbar for Scenario A

The system remains stable after a three - phase short circuit and the minimum frequency value of approximately 48.5 Hz is between the acceptable limits. Comparing combinations as well as dynamic

response before and after tuning, there are hardly any differences to be seen. A slightly better dynamic behavior of Comb1.2 after tuning does not play a major role in power system operation.

The same three - phase short circuit is simulated for Scenario C, when loading of generators reaches 70 %. Electrical frequency response is presented in Figure 72. It can be seen that electrical frequency's values remain within the acceptable margins with a maximum value over 51 Hz and a minimum value of 48 Hz, which does not threaten power system stability.

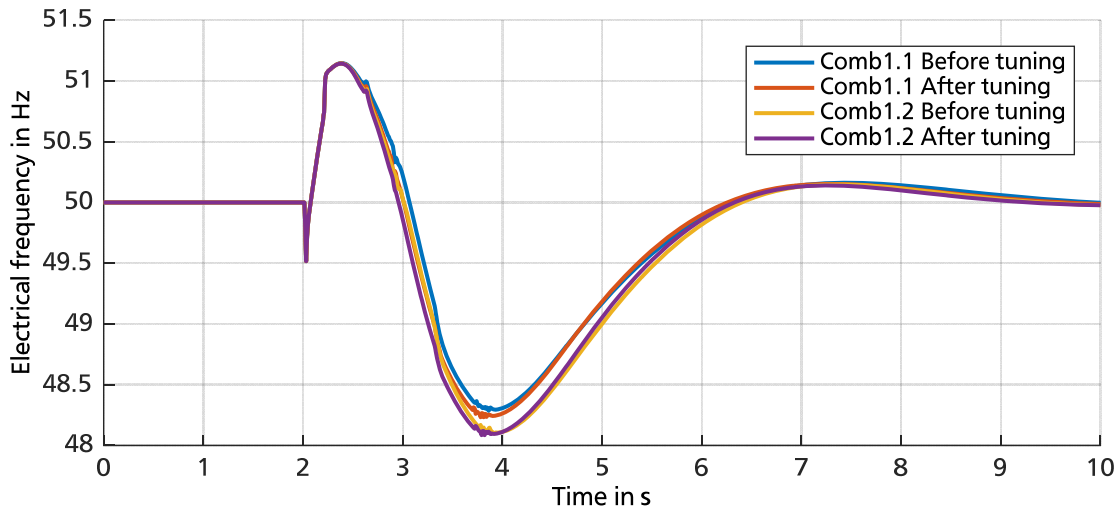


Figure 72: Electrical frequency of Lesbos IPS in case of a three - phase short circuit at APS busbar for Scenario C

It is now interesting to consider the voltage at the PCC with relation to grid code requirements presented in 9.1 as well as the dynamic response of a WPP. Voltage magnitude at the PCC of WPP4 is presented in Figure 73. This WPP is connected to feeder P31KCS.

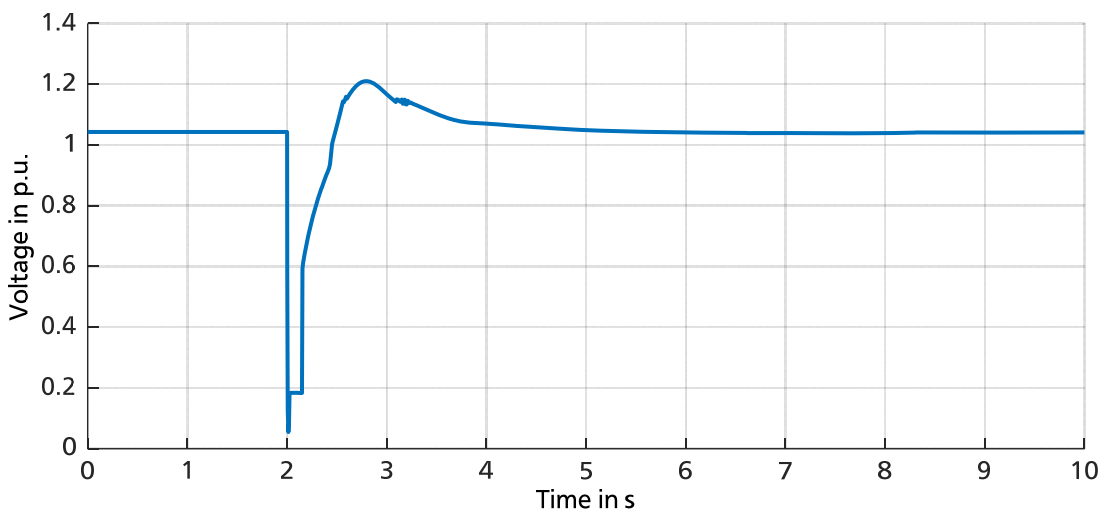


Figure 73: Voltage magnitude in p.u. at the PCC of WPP4 connected in P31KCS of Lesbos IPS

It can be seen in Figure 73 that voltage magnitude before fault is 1.05 p.u., as it has been mentioned in Table 13. At the moment of $t = 2$ seconds when short circuit happens, there is a deep voltage dip and voltage magnitude remains during the fault at a value of 0.19 p.u. and then increases trying to reach the value before the fault. As described in Figure 66, the limit of 0.15 p.u. has not been violated and therefore the WPP remains connected, as it has been required.

9.3. Conclusion and Discussion

A short summary about the frequency stability in real case study is given to enable a better understanding of conclusion concerning the isolated power system of Lesbos. In this section selected cases of dynamic events are simulated and no artificial conditions threatening stability are taken into consideration. Following statements validate former conclusion of former chapters.

1. A power loss of approximately 25 % because of synchronous generators' or wind power plant tripping for Scenario A (loading condition of 30 %) and a wind power penetration of 50 % does not threaten stability.
2. A power loss up to 15 % for Scenario C (loading condition of 70 %) and wind power penetration of 15 % does not threaten power system stability as well. Power losses above this limit would lead to system collapse without any additional active power support.
3. Wind power plant tripping does not threaten stability for a loading scenario of 70 %, since wind power penetration in this scenario reaches maximum 15 %, which is a common practice operation limit.
4. Isolated power system of Lesbos remains stable after a three - phase short circuit for a loading condition of 30 % as well as for a loading condition of 70 %.
5. Validating the conclusions of the former chapters, it can be stated that Comb1.2 (Isochronous load sharing on an isolated bus) presents a better dynamic behaviour than Comb1.1. (Droop/Isochronous load sharing on an isolated bus), as it has been expected.
6. Tuning has a positive effect for Comb1.1 (Droop/Isochronous load sharing on an isolated bus) and for Comb1.2 (Isochronous load sharing on an isolated bus) tuning would not be essential.
7. Wind power plants fulfil grid code requirements and support power system in case of faults remaining connected.

In the next and final chapter all important conclusions are summarised and discussed as well as further works are proposed that can be realised in future.

10. Final conclusion and further works

In this final chapter all important conclusions are summarised and discussed. According to these general statements it should be possible for network operators of isolated power systems to consider and select an appropriate frequency control concept with reference to usual operating condition of synchronous generators and wind power penetration limits. However, since each isolated power system is unique, the recommendations listed below could be adapted from network operators according to special grid code requirements and operating practices of the relevant isolated power systems.

10.1. Final conclusion

The most important general conclusions are listed in this section and are classified in three categories.

10.1.1. Frequency control

A secondary frequency control loop is not implemented in many small isolated power systems. Primary and secondary control is applied from speed governors of generators in operation. Therefore, these speed governors are responsible to keep frequency within the permissible limits for normal operation as well as to restore frequency's nominal value. The more isochronous speed governors are connected to an isolated power system, the more stable the dynamic system behaviour is. In this thesis it is shown that the higher the loading of synchronous generators and the more isochronous speed governors are in operation, the lower the droop constants of droop speed governors in operation. Therefore loading of generators plays a major role for the stability of a power system with and without integration of renewable energy sources. Frequency control concept of isochronous load sharing on an isolated bus including more isochronous speed governors has a better dynamic response in comparison to frequency control concept of Droop/Isochronous load sharing on an isolated bus where droop speed governors are the majority.

10.1.2. Tuning

Tuning time constants of electric control box of speed governors enables running tuning algorithm but does not influence dynamic system response because of actuator's limitation. Interaction of both speed governors is taken into consideration because tuning takes place simultaneously for isochronous and droop speed governors for the same disturbance. Tuning droop constants concerning the interaction of more than one speed governors with the defined goal of step rejection is successfully performed and proves that the resulted values are influenced from two parameters:

- a. Loading condition of synchronous generators
- b. Number of isochronous speed governors in operation in the power system.

For high loading conditions (Scenario C) tuning has a very positive effect in case of load steps. Generally, tuning has a higher importance and influence for high loading condition (Scenario C), rather than for normal operating condition (Scenario B).

Furthermore, in case of three - phase short circuits, tuning as realised in this thesis does not influence electrical frequency response in a significant way.

However, tuning has a very positive effect especially for Droop/Isochronous load sharing on an isolated bus concerning final frequency deviations, which are outside the permissible values in normal conditions before tuning. Therefore, tuning would be suggested in case of selecting frequency control concept where droop speed governors are the majority.

10.1.3. Integration of fully rated power energy converters

A wind power penetration of up to 15 % would be always possible without threatening system stability, independent of loading condition of synchronous generators for all considered dynamic events. In case of higher wind power penetration frequency behaviour is worse but without threatening power system stability as long as:

- a. Wind power converters are able to support power system with additional active power, meaning that there would be sufficient wind speed to enable such a support.
- b. Synchronous generators are able to cover the required additional active power with reference to their operating condition at the time point of a dynamic event.

Tuning values improve the dynamic response of isolated power systems with wind energy converters as well. In other words, the tendency of decreasing value of droop has a positive effect for power systems with power generation coming from renewable energy sources of this kind as well.

10.2. Further works

There are points that would be very interesting for future studies regarding IPSs and certainly belong to the challenges which isolated network operators have to confront with.

Consideration of other generation mix would be interesting. Speed governors with a similar control function (with and without droop function) interact and consider a new control loop corresponding to other types of primary energy for the synchronous generators.

Moreover, among several tuning methods, automatic tuning of control loop has been selected in this thesis. There are many other techniques that could be applied and the results could be compared with these ones from this thesis. Additionally, other goals could be applied for tuning and according to these

results a frequency control concept could be proposed combining conclusions from more than one tuning sessions.

Last but not least, except for wind power penetration, integration of photovoltaic modules could be considered and their influence on the proposed frequency control concept could be evaluated. Frequency control concepts focusing on fully rated wind energy converters could be further developed as well as considering possible techniques for tuning their control loops as well. Energy storage devices could be integrated and proposing appropriate frequency control concepts optimising their interacted operation with synchronous generators and renewable energy sources.

References

- [1] B. J. Kirby, J. Dyer, C. Martinez, Dr. Rahmat A. Shoureshi, R. Guttromson, J. Dagle, "Frequency Control Concerns In The North American Electric Power System," U. S. Department of Energy, Dec. 2002.
- [2] J. Machowski, J. W. Bialek, and J. R. Bumby, *Power system dynamics and stability*. Chichester, New York: John Wiley, 1997.
- [3] J. Lopes, C. L. Moreira, and A. G. Madureira, "Defining Control Strategies for MicroGrids Islanded Operation," *IEEE Trans. Power Syst*, vol. 21, no. 2, pp. 916–924, 2006.
- [4] W. Huang, M. Lu, and L. Zhang, "Survey on Microgrid Control Strategies," *Energy Procedia*, vol. 12, pp. 206–212, 2011.
- [5] D. Audring and E. Lerch, "Determination of islanding performance of industrial plants," in *2011 IEEE PES PowerTech - Trondheim*, pp. 1–6.
- [6] J. Kabouris, N. Zouros, G. Manos, G. Contaxis, and C. Vournas, "Computational environment to investigate wind integration into small autonomous systems," *Renewable Energy*, vol. 18, no. 1, pp. 61–75, 1999.
- [7] T. Ackermann, *Wind power in power systems*.
- [8] J. K. Kaldellis and D. Zafirakis, "Present situation and future prospects of electricity generation in Aegean Archipelago islands," *Energy Policy*, vol. 35, no. 9, pp. 4623–4639, 2007.
- [9] J. V. Milanovic and N. Soultanis, "The influence of controlled and fixed load composition on operation of autonomous wind-diesel system," in *2001 Power Tech*, p. 6.
- [10] A. Etxegarai, P. Eguia, E. Torres, and E. Fernandez, "Impact of wind power in isolated power systems," in *MELECON 2012 - 2012 16th IEEE Mediterranean Electrotechnical Conference*, pp. 63–66.
- [11] Gillian R. Lalor, "Frequency Control on an Island Power System with Evolving Plant Mix," Ph.D, School of Electrical, Electronic and Mechanical Engineering, University College Dublin, National University of Ireland, Ireland, 2005.
- [12] I. D. Margaris, S. A. Papathanassiou, N. D. Hatziargyriou, A. D. Hansen, and P. Sorensen, "Frequency Control in Autonomous Power Systems With High Wind Power Penetration," *IEEE Trans. Sustain. Energy*, vol. 3, no. 2, pp. 189–199, 2012.
- [13] Ioannis Margaris, *Power system requirements for wind penetration: Work Package 9:Electrical grid*. Part 3: Small island grid
- [14] Enemalta Cooperation, "The Network Code," 2013.
- [15] ERSE, "Manual de Procedimentos do Acesso e Operação do SEPM," 2004.
- [16] Landsnet, "Iceland grid code," 2008.
- [17] New Zealand Electricity Authority, "Electricity Industry Participation Code 2010," 2010.
- [18] National Grid Electricity Transmission, "The Grid Code: Issue 5," Revision 13, Jan. 2015.
- [19] Red Electrica De Espana, "Procedimientos de operación insulares y extrapeninsulares," 2006.

-
- [20] Regulatory Authority for Energy (R.A.E.), "Code for operating non interconnected island electrical power systems," Athens, Greece, 2014.
- [21] *EirGrid Grid Code: Version 5.0*, 2013.
- [22] R. Sebastián and J. Quesada, "Distributed control system for frequency control in a isolated wind system," *Renewable Energy*, vol. 31, no. 3, pp. 285–305, 2006.
- [23] R. Sebastián, "Smooth transition from wind only to wind diesel mode in an autonomous wind diesel system with a battery-based energy storage system," *Renewable Energy*, vol. 33, no. 3, pp. 454–466, 2008.
- [24] Kjetil Uhlen, "Modelling and Robust Control of Autonomous Hybrid Power Systems," Ph.D, The Norwegian Institute of Technology, Department of Engineering Cybernetics, The University of Trondheim, Norway, 1994.
- [25] Weisser Daniel Garcia Raquel S, "Instantaneous wind energy penetration in isolated electricity grids: concepts and review," *Renewable Energy*, vol. Volume 30, no. Issue 8, pp. 1299–1308, Jul. 2005.
- [26] P. Kundur, N. J. Balu, and M. G. Lauby, *Power system stability and control*. New York: McGraw-Hill, 1994.
- [27] H. Bevrani, *Robust power system frequency control*. New York, NY: Springer, 2009.
- [28] "Definition and Classification of Power System Stability IEEE/CIGRE Joint Task Force on Stability Terms and Definitions," *IEEE Trans. Power Syst*, vol. 19, no. 3, pp. 1387–1401, 2004.
- [29] F. Milano, *Power system modelling and scripting*. London: Springer, 2010.
- [30] "723 Digital Speed Control for Reciprocating Engines - Analog Load Share: Product Manual 02785 (Revision A)," Original Instructions, 1996.
- [31] I. Egido, F. Fernandez-Bernal, P. Centeno, and L. Rouco, "Maximum Frequency Deviation Calculation in Small Isolated Power Systems," *IEEE Trans. Power Syst*, vol. 24, no. 4, pp. 1731–1738, 2009.
- [32] Etxegarai, A, Torres, E, Eguia, P, "Frequency control in isolated power systems with wind power penetration," Department of Electrical Engenieering, University of the Basque Country UPV/EHU, Alameda Urquijo s/n, 48013 Bilbao (Spain).
- [33] Hatziargyriou, N, Pecas Lopes, J. A, Karapidakis, E, Vasconcelos, M. H, Ed, *On-Line dynamic security assessment of power systems in large islands with high wind power penetration*, 1999.
- [34] S. A. Papathanassiou and N. G. Boulaxis, "Power limitations and energy yield evaluation for wind farms operating in island systems," *Renewable Energy*, vol. 31, no. 4, pp. 457–479, 2006.
- [35] K. Uhlen, B. A. Foss, and O. B. Gjosaeter, "Robust control and analysis of a wind-diesel hybrid power plant," *IEEE Trans. On energy Conversion*, vol. 9, no. 4, pp. 701–708, 1994.
- [36] G. N. Kariniotakis and G. S. Stavrakakis, "A general simulation algorithm for the accurate assessment of isolated diesel-wind turbines systems interaction. Part II: Implementation of the algorithm and

- case-studies with induction generators," *IEEE Trans. On energy Conversion*, vol. 10, no. 3, pp. 584–590, 1995.
- [37] N. Hatziaargyriou *et al*, "Energy management and control of island power systems with increased penetration from renewable sources," in *Winter Meeting of the Power Engineering Society*, pp. 335–339.
- [38] W. He, *A simulation model for wind-diesel systems with multiple units: 17-19 November, 1993*. London: Institution of Electrical Engineers, op. 1993.
- [39] E. Nogaret *et al*, "An advanced control system for the optimal operation and management of medium size power systems with a large penetration from renewable power sources," *Renewable Energy*, vol. 12, no. 2, pp. 137–149, 1997.
- [40] S. S. Choi and R. Larkin, "Performance of an autonomous diesel-wind turbine power system," *Electric Power Systems Research*, vol. 33, no. 2, pp. 87–99, 1995.
- [41] Hatziaargyriou, N, Papadopoulos, M, Tentzerakis, S, Pecos Lopes, J. A, Vasconcelas, M. H, Monteiro, C. D. M, Kariniotakis, G, Nogaret, E, Jenkins, N, "Control Requirements for optimal operation of large isolated systems with increased wind power penetration," NTUA, INESC, ARMINES, UMIST.
- [42] E. S. Karapidakis and N. D. Hatziaargyriou, "Online preventive dynamic security of isolated power systems using decision trees," *IEEE Trans. Power Syst*, vol. 17, no. 2, pp. 297–304, 2002.
- [43] *Voltage characteristics of electricity supplied by public distribution networks*, EN 50160, 2011.
- [44] *Implementation Guideline for Network Code "Requirements for Grid Connection Applicable to all Generators"*, 2013.
- [45] R. C. Dorf and R. H. Bishop, *Modern control systems*, 12th ed. Upper Saddle River, N.J.: Pearson Prentice Hall, 2011.
- [46] K. J. Åström and T. Hägglund, *PID controllers*, 2nd ed. Research Triangle Park, N.C.: International Society for Measurement and Control, 1995.
- [47] S. Roy, O. P. Malik, and G. S. Hope, "An adaptive control scheme for speed control of diesel driven power-plants," *IEEE Trans. On energy Conversion*, vol. 6, no. 4, pp. 605–611, 1991.
- [48] B. Challen and R. Baranescu, *Diesel engine reference book*, 2nd ed. Oxford [England], Woburn, MA: Butterworth-Heinemann, 1999.
- [49] C. Cristea, J. P. Lopes, M. Eremia, and L. Toma, "The control of isolated power systems with wind generation," in *2007 IEEE Power Tech*, pp. 567–572.
- [50] A. R. Cooper, D. J. Morrow, and K. D. R. Chambers, "Development of a diesel generating set model for large voltage and frequency transients," in *Energy Society General Meeting*, pp. 1–7.
- [51] S. A. Papathanassiou and M. P. Papadopoulos, "Dynamic characteristics of autonomous wind–diesel systems," *Renewable Energy*, vol. 23, no. 2, pp. 293–311, 2001.

-
- [52] D. Das, S. K. Aditya, and D. P. Kothari, "Dynamics of diesel and wind turbine generators on an isolated power system," *International Journal of Electrical Power & Energy Systems*, vol. 21, no. 3, pp. 183–189, 1999.
- [53] Juardo, F, Saenz, R. J, "Neuro-fuzzy control in biomass-based wind-diesel systems," Department of Electrical Engineering, University of Jaén, Department of Electrical Engineering, University of the Basque Country, 23700 EUP Linares (Jaén), Spain, 48013 ESI Bilbao, Spain.
- [54] O. Lequin, M. Gevers, M. Mossberg, E. Bosmans, and L. Triest, "Iterative feedback tuning of PID parameters: comparison with classical tuning rules," *Control Engineering Practice*, vol. 11, no. 9, pp. 1023–1033, 2003.
- [55] G. Mallesham, S. Mishra, and A. N. Jha, "Ziegler-Nichols based controller parameters tuning for load frequency control in a microgrid," in *2011 International Conference on Energy, Automation, and Signal (ICEAS)*, pp. 1–8.
- [56] H. Shayeghi, H. A. Shayanfar, and A. Jalili, "Load frequency control strategies: A state-of-the-art survey for the researcher," *Energy Conversion and Management*, vol. 50, no. 2, pp. 344–353, 2009.
- [57] W. Tan, "Tuning of PID load frequency controller for power systems," *Energy Conversion and Management*, vol. 50, no. 6, pp. 1465–1472, 2009.
- [58] W. Tan and Z. Xu, "Robust analysis and design of load frequency controller for power systems," *Electric Power Systems Research*, vol. 79, no. 5, pp. 846–853, 2009.
- [59] A. E. A. Awouda and R. Bin Mamat, "Refine PID tuning rule using ITAE criteria," in *2nd International Conference on Computer and Automation Engineering (ICCAE 2010)*, pp. 171–176.
- [60] S. K. Pandey, S. R. Mohanty, and N. Kishor, "A literature survey on load–frequency control for conventional and distribution generation power systems," *Renewable and Sustainable Energy Reviews*, vol. 25, pp. 318–334, 2013.
- [61] T. S. Bhatti, Al-Ademi, A. A. F, and N. K. Bansal, "Dynamics and control of isolated wind-diesel power systems," *Int. J. Energy Res*, vol. 19, no. 8, pp. 729–740, 1995.
- [62] I. Kamwa, "Dynamic modelling and robust regulation of a no-storage wind-diesel hybrid power system," *Electric Power Systems Research*, vol. 18, no. 3, pp. 219–233, 1990.
- [63] S. R. Gampa and D. Das, "Real power and frequency control of a small isolated power system," *International Journal of Electrical Power & Energy Systems*, vol. 64, pp. 221–232, 2015.
- [64] R. W. Wies, E. Chukkapalli, and M. Mueller-Stoffels, "Improved frequency regulation in mini-grids with high wind contribution using online genetic algorithm for PID tuning," in *2014 IEEE Power & Energy Society General Meeting*, pp. 1–5.
- [65] S. Doolla and J. Priolkar, "Analysis of frequency control in isolated microgrids," in *2011 IEEE PES Innovative Smart Grid Technologies - India (ISGT India)*, pp. 167–172.

-
- [66] K. Heuck, K.-D. Dettmann, and D. Schulz, *Elektrische Energieversorgung: Erzeugung, Übertragung und Verteilung elektrischer Energie für Studium und Praxis*, 8th ed. Wiesbaden: Vieweg + Teubner, 2010.
- [67] *IEEE recommended practice for excitation system models for power system stability studies*. New York, N.Y.: Institute of Electrical and Electronics Engineers, 2006.
- [68] Technical Reference Documentation, *DIGSILENT PowerFactory 15, User Manual: Static Generator (ElmGenstat)*.
- [69] *TransmissionCode 2007 Network and System Rules of the German Transmission System Operators*, 2007.
- [70] Distribution System Operator (D.S.O.) Greece, Department of Island Grids, Jan. 2013.
- [71] G. Papaioannou, M. Fleckenstein, H. Zimmer and J. Hanson, Ed, *Dynamic Frequency Controlling for Isolated Island Power Systems*, 2014.
- [72] C. Sourkounis and P. Tourou, "Grid Code Requirements for Wind Power Integration in Europe," *Conference Papers in Energy*, vol. 2013, pp. 1–9, 2013.

Appendix

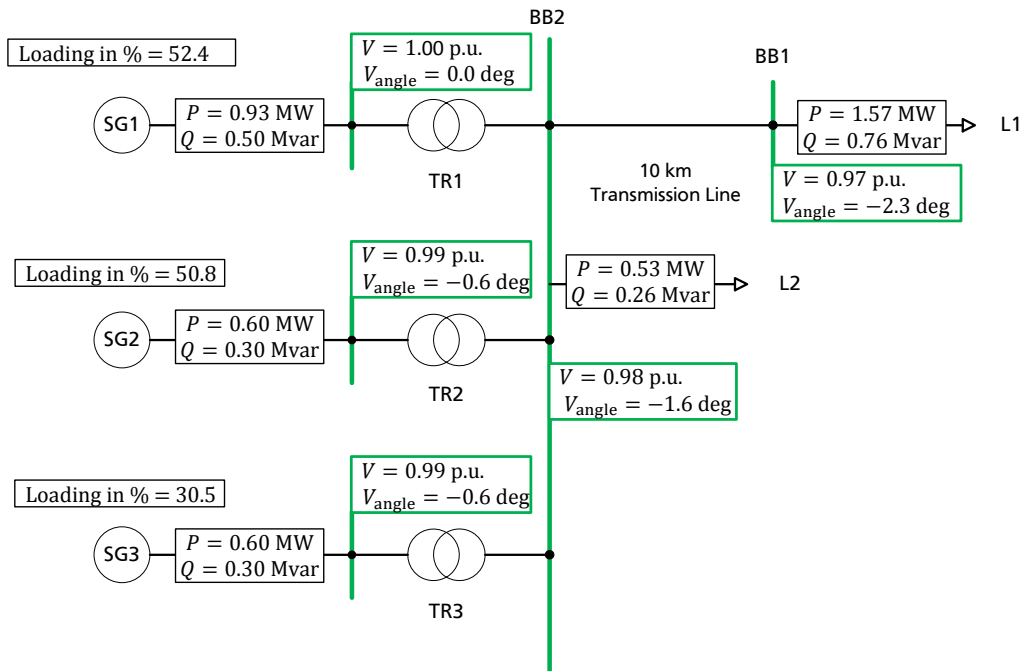


Figure 1A: Load - flow results for Scenario B of "3 DIGLO IPS" (Chapter 6.2)

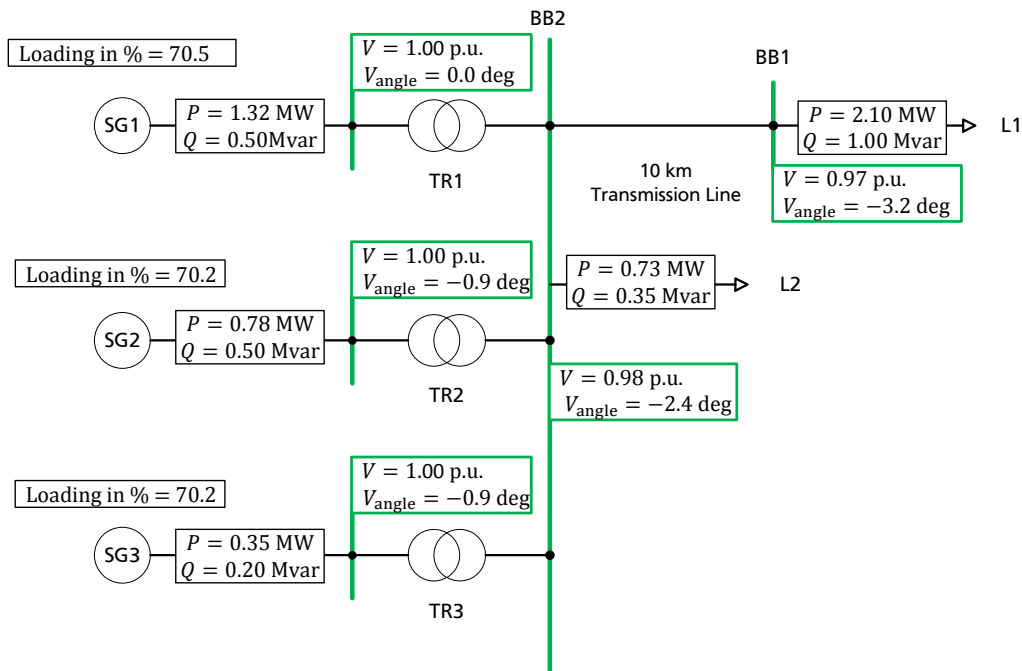


Figure 2A: Load - flow results for Scenario C of "3 DIGLO IPS" (Chapter 6.2)

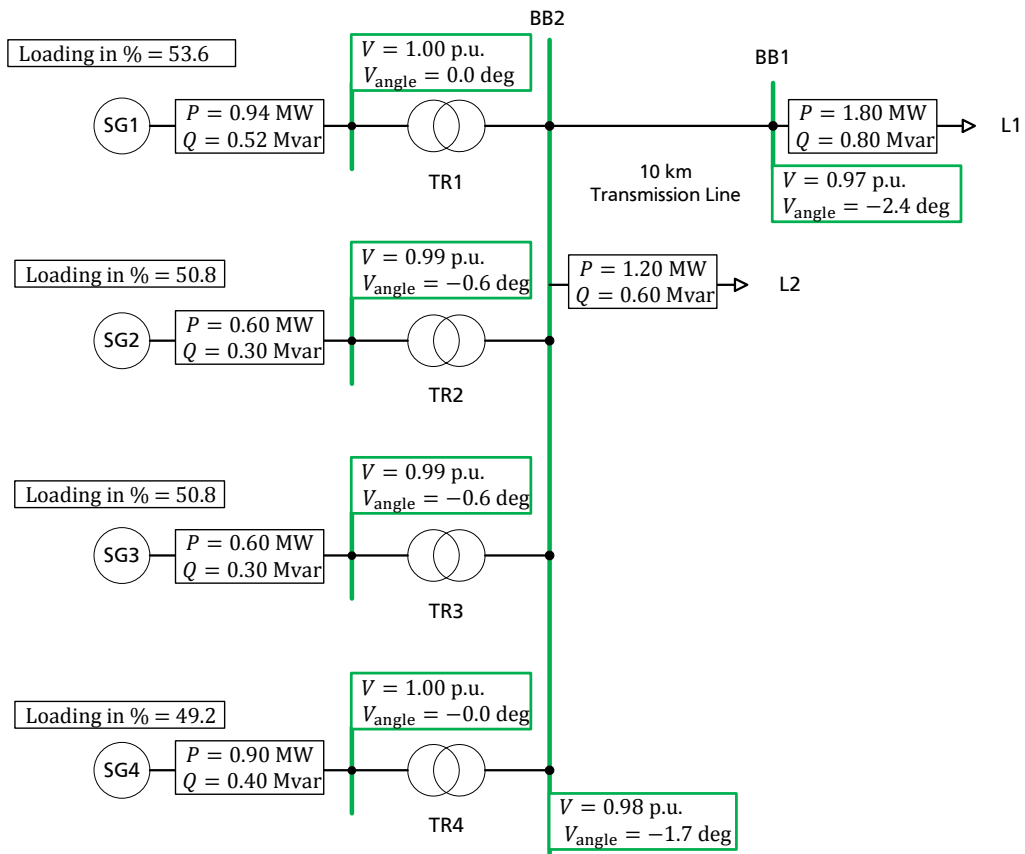


Figure 3A: Load - flow results for Scenario B of "4 DIGLO IPS" (Chapter 6.2)

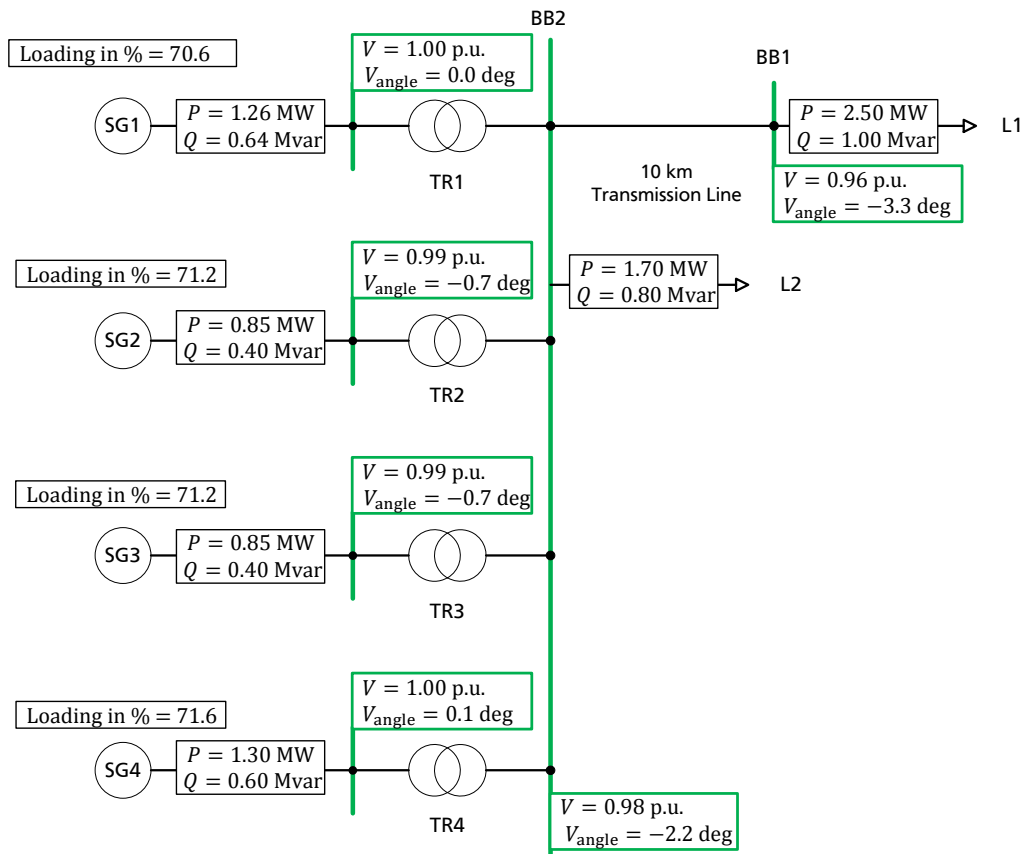


Figure 4A: Load - flow results for Scenario C of "4 DIGLO IPS" (Chapter 6.2)

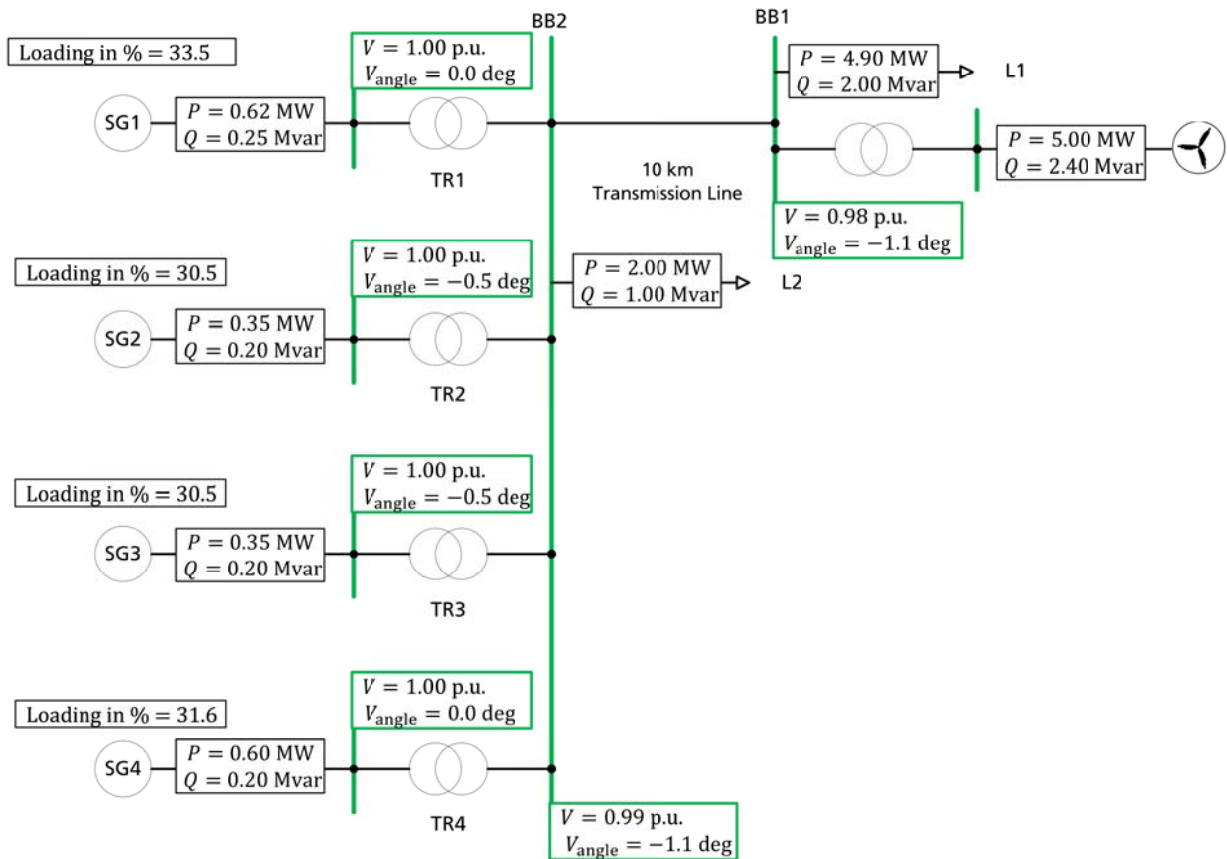


Figure 5A: Load - flow results for Scenario A_WP70 of "4 DIGLOW IPS" (Chapter 6.2)

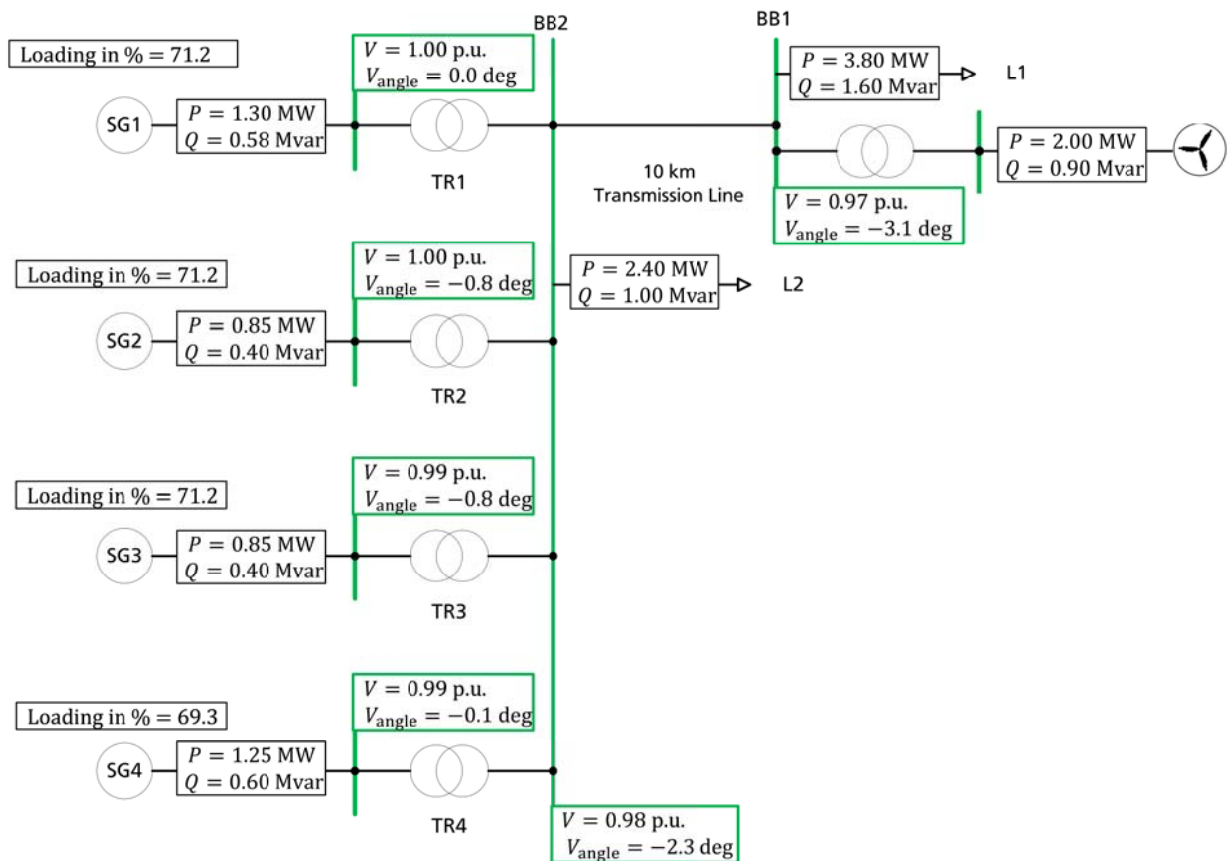


Figure 6A: Load - flow results for Scenario C_WP30 of "4 DIGLOW IPS" (Chapter 6.2)

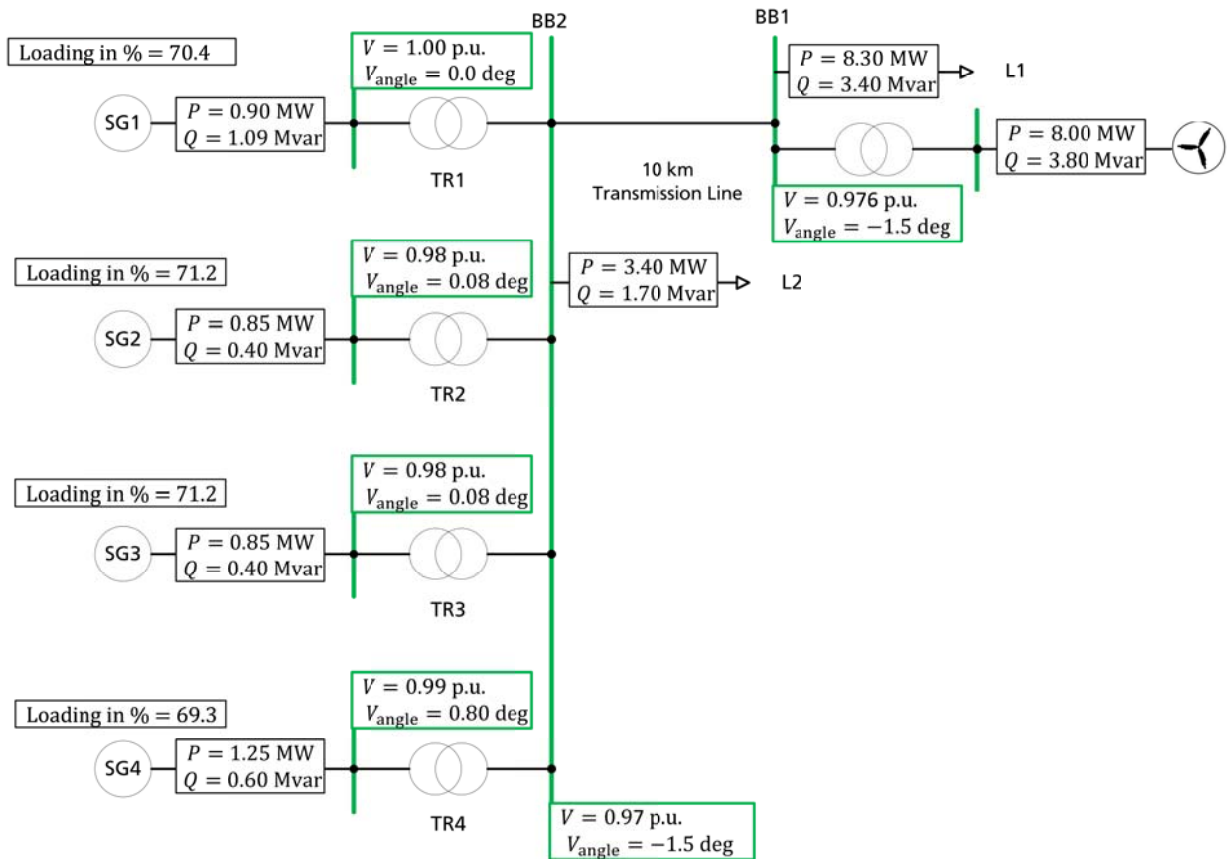


Figure 7A: Load - flow results for Scenario C_WP70 of "4 DIGLOW IPS" (Chapter 6.2)



Georgia Papaioannou

AUSBILDUNG

- 2012-2016** **Promotion am Fachbereich Elektro- und Informationstechnik**
Technische Universität Darmstadt, Deutschland
Institut für Elektrische Energiesysteme
Fachgebiet Elektrische Energieversorgung unter Einsatz Erneuerbarer Energien (E5)
- 2009-2011** **M.Sc. an der Fakultät Informations- und Kommunikationstechnik - I.S.I.C.G.**
Université de Limoges, Frankreich
Mention Sciences et Technologies de l' Information et de la Communication
- 2003-2009** **Dipl. - Ing. an der Fakultät für Elektro- und Computeringenieurwesen**
Nationale Technische Universität Metsovion, Athen, Griechenland
Vertiefung: Elektrische Energiesysteme,
Hochspannungsanwendungen und Verwaltungs- und Informationssysteme
- 2000-2003** **Schulabschluss (vgl. mit Abitur)**
Varvakios Schule, Athen, Griechenland

BERUFSERFAHRUNG

- seit 04/2017** **IT Associate Consultant, msg systems ag, Deutschland**
- Projektmanagement von IT-Projekten
 - IT Beratung im Public Sektor
- 02/2012-08/2016** **Wissenschaftliche Mitarbeiterin am Fachgebiet Elektrische Energieversorgung unter Einsatz Erneuerbarer Energien (E5), Technische Universität Darmstadt, Deutschland**
- Mitarbeit und Koordination von industriellen und Forschungsprojekten
 - Tätigkeiten in der Lehre und Betreuung von studentischen Abschlussarbeiten
 - System & Netzwerkadministrator des Fachgebiets E5
- 01/2011-12/2011** **Projektmanagerin des Projekts "Employment and Carrier Structure - Information system's development", Fachhochschule der Ionischen Inseln, Athen, Griechenland**
- Nationaler strategischer Rahmenplan der europäischen Union
 - Projektmanagement und Verwaltung von europäischen Projekten
-